The American Mineralogist

Journal of the Mineralogical Society of America

VOL. 45 JULY–AUGUST, 1960 Nos. 7 and 8

Contents

(Continued on Cover 2)

Published bi-monthly by the Society

The enlarged issues of this journal for 1960 are made possible by a grant from the Penrose Fund of the Geological Society of America.

The American Mineralogist—Journal of the Mineralogical Society of America

The journal, containing articles on mineralogy, crystallography, and allied sciences, is issued every two months. Contributions are invited.

The general conduct of the journal is in the hands of the editor, Lewis S. Ramsdell, Department of Mineralogy, University of Michigan, to whom all manuscripts should be submitted.

Second class postage paid at Menasha, Wisconsin. Acceptance for mailing at the special rate of postage provided for in section 1103, Act of Oct. 3, 1917, paragraph 4 section 429 P. L. & R. authorized March 13, 1922.

Notice of change of address, orders, and remittances should be sent to Marjorie Hooker, c/o U. S. Geological Survey, Washington 25, D. C.

Printed by the George Banta Company, Inc., Menasha, Wisconsin
Printed in the United States of America

Leitz **first in precision optics**

NEW POLARIZING MICROSCOPE SM-pol

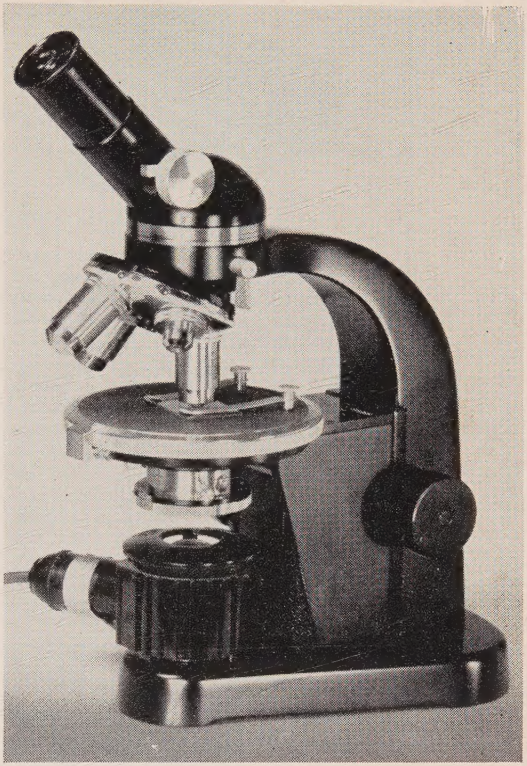

21158

Leitz sets a new standard with this student polarizing and chemical microscope of modern design, with dual, low-position focusing controls and large field of view. A reasonably priced polarizing microscope, the model SM-pol, has rugged, one-piece construction with Bertrand lens and pinhole diaphragm built into the tube. Inclined monocular tube will accommodate wide-field eyepieces and the microscope can be used faced away from the observer, permitting easy accessibility to the stage.

A reputation for integrity and a tradition of service have led thousands of scientific workers to bring their optical problems to Leitz. If you have problems in this field, why not let us help you with them?

See your Leitz dealer and examine these Leitz instruments soon. Write for information.

E. LEITZ, INC., Dept. AM-8
468 Park Avenue South, New York 16, N. Y.

Please send me the Leitz_____brochure.

NAME_____

STREET_____

CITY_____ ZONE_____ STATE_____

E. LEITZ, INC., 468 PARK AVENUE SOUTH, NEW YORK 16, N. Y.
Distributors of the world-famous products of
Ernst Leitz G. m. b. H., Wetzlar, Germany—Ernst Leitz Canada Ltd.
LEICA CAMERAS · LENSES · PROJECTORS · MICROSCOPES · BINOCULARS

FIRST: LOOK AT UNITRON'S NEW POLARIZING MICROSCOPE

Here is a precision measuring instrument for both orthoscopic and conoscopic observations, designed to meet the exacting requirements of science, education, and industry. Its many features make it ideal for work in chemistry, crystallography, mineralogy and biology as well as in the technology of paper, glass, textiles and petroleum.

CHECK THESE OPTICAL & MECHANICAL FEATURES

Note that UNITRON'S new Model MPS comes complete with optics and accessories and includes features usually associated only with much more costly models.

- **EYEPIECES:** Micro 5X providing measurements to 0.0025mm. and cross-hair 10X. The eye lenses focus to produce sharp reticle images and are keyed to prevent rotation.
- **OBJECTIVES:** 4X(N.A.0.1), 10X(N.A.0.25), 40X(N.A.0.65), achromatic, strain-free, each with centerable mount.
- **NOSEPIECE:** quick-change type for critical centering.
- **CONDENSER and POLARIZER:** three-lens condenser with upper elements on a swing-out mounting, provides either parallel or convergent light. A dovetail-slide focusing mount and iris diaphragm insure optimum illumination and resolution.
- **POLAROID POLARIZER:** rotatable through 360° and graduated every 45°. Plano-concave mirror.
- **ANALYZER:** Polaroid, in sliding metal mount.
- **BERTRAND LENS:** for the study of interference figures, fixed-focus lens is centerable and mounted in a slideway.
- **STAGE:** diameter 115mm., revolves through 360°, graduated in degrees and reads to 6' with vernier. The top is calibrated in mms. in two directions and is drilled and tapped for an accessory mechanical stage. Stage clips.
- **COMPENSATORS:** two compensators are included; a quarter-wave plate and first order red plate. These fit into a slot above the objective lens.
- **FOCUSING:** coarse and micrometric fine adjustments.
- **STAND:** heavy stand, arm inclines to horizontal position.

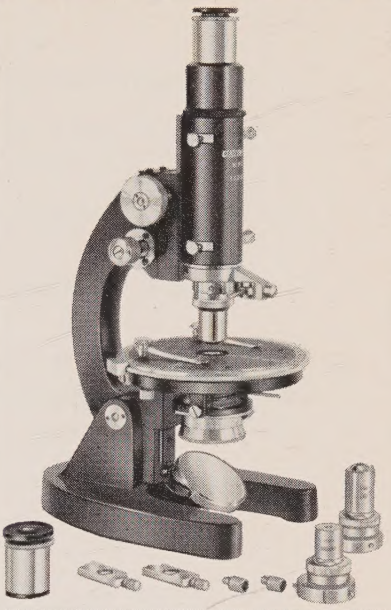

1 Iris diaphragm
2 Polarizer
3 Swing-out lever
4 Focusing lock
5 Focusing slide

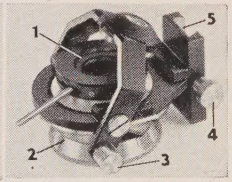

Condenser and Polarizer

THEN: LOOK AT THE PRICE!

Model MPS complete as described, in fitted cabinet . . . . . **$269 FOB BOSTON**

Quantity prices on three or more.

Accessory mechanical stage **$14.75**

AVAILABLE ON FREE 10 DAY TRIAL

Send for complete catalog on UNITRON Microscopes.

UNITRON
INSTRUMENT DIVISION OF UNITED SCIENTIFIC CO.
204-206 MILK STREET • BOSTON 9, MASSACHUSETTS

Please rush UNITRON Catalog on Microscopes.

Name_____

Company_____

Address_____

City_____ State_____

THE TREND IS TO UNITRON

THE AMERICAN MINERALOGIST
JOURNAL OF THE MINERALOGICAL SOCIETY OF AMERICA

Vol. 45 JULY–AUGUST, 1960 Nos. 7 and 8

RE-EXAMINATION OF PILINITE AND ITS IDENTIFICATION WITH BAVENITE*

GEORGE SWITZER, *U. S. National Museum, Washington, D. C.*,
AND
LAURA E. REICHEN, *U. S. Geological Survey, Washington, D. C.*

ABSTRACT

X-ray powder patterns and a new chemical analysis made on pilinite from the type locality have shown it to be the same mineral as bavenite. The strongest lines in the *x*-ray powder pattern, in order of decreasing intensity are: 3.71, 3.35, 3.22, 3.03, 2.83, 4.85 Å. The new chemical analysis shows 5.5 per cent BeO which was missed in the original analysis. The formula proposed is $(Be,Al)_4Ca_4(SiO_3)_9 \cdot xH_2O$. It is recommended that the name pilinite be dropped.

INTRODUCTION

Pilinite was described as a new mineral by von Lasaulx (1876). The mineral was described as fine feltlike masses of needles, resembling asbestos, occurring with quartz, epidote, and stilbite in cavities in granite at Striegau, Silesia. A chemical analysis gave a formula that corresponded approximately to $2CaO \cdot Al_2O_3 \cdot 5SiO_2 \cdot H_2O$.

The only additional information published about pilinite since the original very brief and incomplete description is a statement in the index of Strunz's Mineralogische Tabellen (2d ed., 1949 and 3d ed., 1957) that pilinite is an asbestiform idocrase.

Examination of the specimen in the U. S. National Museum labeled pilinite from Striegau, Silesia, has shown the mineral to be identical with bavenite. Type specimens were not available for study. However, the material in the Museum is identical in locality, appearance, and association with that described by von Lasaulx, and it seems quite certain that the two are the same.

Bavenite was described as a new mineral from Baveno, Italy, by Artini (1901), but the presence of beryllium was overlooked by him, just as it was 25 years earlier by von Lasaulx. Artini failed to recognize

* Publication authorized by the Secretary, Smithsonian Institution, and the Director, U. S. Geological Survey.

his mineral as being the same as pilinite. The presence of beryllium in bavenite was reported by Schaller and Fairchild (1932).

Chemistry

A new analysis was made of pilinite from Striegau, Silesia. Except for the separation of beryllium from aluminum and iron, the sample was analyzed by conventional procedures. Beryllium was separated from aluminum and iron by the procedure of Jilek and Kota (1931) in which tartrate is added to prevent the precipitation of aluminum and iron and the beryllium is precipitated by guanidine carbonate. Spectrographic anal-

Table 1. Analyses of Pilinite

	1			2
	Per cent	Moles	Mole ratios	Per cent
BeO	5.52	0.221	2.10	
Fe_2O_3	.60	.004		
Al_2O_3	9.62	.094	.94	18.64
CaO	23.44	.418	3.98	19.51
SiO_2	57.04	.950	9.05	55.70
H_2O^+	2.86	1.59	1.51	4.97
H_2O^-	.14			
MgO	.22			
Li_2O				[1.18]
	99.44			100.00

1. Striegau, Silesia, USNM R-7553, Laura L. Reichen, analyst.
2. Original analysis of pilinite, Bettendorf, analyst (von Lasaulx, 1876).

yses of the alumina precipitates made by Harry Bastron of the U. S. Geological Survey indicated that the separation of beryllium from aluminum was satisfactory.

The results of this analysis and of the original analysis made by Bettendorf (von Lasaulx, 1876) are given in Table 1. As the presence of beryllium was not detected in the original analysis, it can be assumed that the figure for alumina includes the beryllia also. Therefore, this incorrect alumina figure should be disregarded in making the comparison of the two analyses. The chemical analyses of bavenite from different localities have been summarized by Fleischer and Switzer (1953). They conclude that the composition of bavenite is well established. The analyses from the four locations cited in their paper are reproduced in Table 2 and the

molecular ratios have been added. The new analysis of pilinite made in the present study shows that it has the same composition as bavenite.

However, in spite of the agreement as to composition, three different formulas have been proposed for bavenite:

$Be_5Al_4Ca_8Si_{18}O_{55}\cdot 2H_2O$	Kutukova (1946), based on 9.89 per cent alumina.
$Be_4Al_2Ca_6Si_{14}O_{41}\cdot 2H_2O$	Rowledge and Hayton (1948), based on 7.00 per cent alumina.
$Be_{2.6}Al_{1.2}Ca_{3.9}Si_{8.8}O_{26}\cdot 1.2H_2O$	Fleischer and Switzer (1953), based on the oxygen content which gives best agreement between calculated and observed sp. gr. Recalculation of Rowledge and Hayton analysis.

TABLE 2. SUMMARY OF BAVENITE ANALYSIS FROM TABLE 1 OF FLEISCHER AND SWITZER (1953)

	Baveno (1)		Russia (6)		Australia (8)		California (9)	
	Per cent	Moles	Per cent	Moles	Per cent	Moles	Per cent	Moles
SiO_2	56.93	0.948	57.25	0.953	59.13	0.984	57.64	0.960
CaO	24.47	.436	24.35	.434	23.90	.426	23.96	.427
Al_2O_3	10.0*	.098	9.89	.097	7.00	.069	6.46	.063
BeO	5.4*	.216	6.33	.254	7.14	.285	7.66	.306
$BeO+Al_2O_3$		.304		.351		.354		.369
H_2O	2.49	.138	1.90	.105	2.46	.137	3.56	.198

* Fleischer and Switzer (1953) show 5.4±0.5 per cent BeO by spectrographic analysis for a sample from Baveno, Italy. Subtracting this 5.4 per cent BeO from the 15.42 per cent Al_2O_3 shown in their Table 1 for a sample from Baveno leaves 10.02 per cent Al_2O_3.

Inspection of the molecular ratios in Table 2 shows that the mole fractions of SiO_2 (0.948–0.984) and of CaO (0.426–0.436) are nearly the same for each sample. Furthermore, by comparing the sum of the mole fractions of BeO plus Al_2O_3 (0.304–0.369) instead of the weight per cents of BeO (5.4–7.66) or Al_2O_3 (6.46 10.0) we see a possibility of a relationship between beryllium and aluminum instead of only poor analytical checks. That beryllium and aluminum proxy for one another is a reasonable assumption because beryllium is known to occur in tetrahedral coordination and aluminum can occur in either tetrahedral or octahedral coordination. The atomic ratios in Table 3, therefore, have been calculated on the assumption that beryllium and aluminum proxy for each other (from the analyses given in Table 2 and pilinite copied from Table 1). We suggest $(Be,Al)_4Ca_4(SiO_3)_9\cdot xH_2O$ as a formula which fits the chemical analyses of all these samples of bavenite.

Table 3. Atomic Ratios of Components of Pilinite from Striegau and Bavenite from Various Locations

Sample	Location	Ca	Be	Al	Si	O	H_2O	Sp. gr.
Pilinite	Striegau	3.98	2.10	1.88	9.05	27	1.51	2.73
Bavenite	Australia	3.98	2.66	1.28	9.20	27	1.15	2.71
Bavenite	California	4.06	2.91	1.20	9.14	27	1.88	
Bavenite	Baveno	4.15	2.06	1.87	9.03	27	1.31	2.72
Bavenite	Russia	4.00	2.30	1.78	9.04	27	.98	2.73

One argument in favor of this formula is that the 1:3 silicon to oxygen ratio is consistent with the grouping $(SiO_3)_n^{-2n}$ known to exist in fibrous and asbestos-like material. The 9:26 ratio suggested by Fleischer and Switzer is not known to exist.

The measured specific gravity of pilinite from Striegau is 2.73 (measured by means of an Adams-Johnston fused silica pycnometer). If one assumes the unit cell of Claringbull (1940) and four formula weights per unit cell, the calculated specific gravity is 2.81. The unit cell of Claringbull, determined on bavenite from Muotta Nera, Switzerland, is $a = 19.34$, $b = 23.06$, and $c = 4.95$ kX. The fact that the calculated specific gravity (2.79) for the formula of Fleischer and Switzer agrees closely with the observed specific gravity (2.73) seems fortuitous, because it is well known that specific gravities on fibrous material can be low.

Optical Properties

Pilinite occurs in fibers or platy fibers that reach a maximum length of 2 mm., but a breadth of not more than 0.02 mm. The elongation of the fibers is negative. The indices of refraction are in close agreement with published values for bavenite, and are as follows:

$$\begin{matrix} n(\mathrm{Na}) \\ \alpha = 1.586 \\ \beta \text{ near } \gamma = 1.590 \end{matrix} \pm 0.002$$

X-Ray Powder Data

X-ray powder data for bavenite and pilinite are given in Table 4. No correction was made for film shrinkage.

Conclusion

Pilinite and bavenite are identical. Therefore, one name should be dropped. The name pilinite has priority by 25 years, and according to strict rules of nomenclature bavenite should be relegated to the syn-

TABLE 4. *X*-RAY POWDER DATA FOR BAVENITE AND PILINITE

Cu/Ni radiation; $\lambda = 1.5418$ Å

Camera diameter 114.59 mm., 2θ cut-off 6°

Bavenite Baveno, Italy USNM C-3478		Pilinite Striegau, Silesia USNM R-7553		Bavenite (Continued)		Pilinite (Continued)	
I	*d* (Å)	I	*d* (Å)	I	*d* (Å)	I	*d* (Å)
3	11.79	5	11.63	1	2.80	2	2.79
1	9.94	1	9.83	1	2.75	2	2.73
3	7.56	5	7.44	1	2.67	1	2.65
4	5.04	5	4.98	6	2.56	7	2.56
3	4.87	6	4.85	3	2.49	5	2.48
		1	4.82	3	2.42	5	2.42
1	4.48					2	2.37
1	4.35	1	4.35	2	2.33	4	2.32
5	4.19	4	4.21	2	2.29	4	2.29
4	3.87	3	3.85	2	2.25	4	2.26
10	3.74	10	3.71			3	2.23
		1	3.59	1	2.16	1	2.16
2	3.41	1	3.40	3	2.11	5	2.09
9	3.35	9	3.35	3	2.08	5	2.08
8	3.24	8	3.22	3	1.98	6	1.97
7	3.13	8	3.12	4	1.95	6	1.95
7	3.05	7	3.03	2	1.88	4	1.87
5	2.85	6	2.83	2	1.83	4	1.82

onymy. However, Dana (1892, p. xliii) states that the law of priority may be set aside, "When a name has been lost sight of and has found no one to assert its claim for a period of more than fifty years; especially if the later name adopted for the species has become intimately incorporated with the structure of the science. . . ." We suggest, therefore, that the name pilinite be dropped and bavenite retained.

REFERENCES

ARTINI, ETTORE (1901), Di una nuova specie minerale trovata nel granito di Baveno: *Atti (Rend.) reale accad. Lincei, Classe sci. fis., mat. e nat.*, **10,** 139–145.

CLARINGBULL, G. F. (1940), Occurrences of bavenite in Switzerland: *Mineralog. Mag.*, **25,** 495–497.

DANA, E. S. (1892), The system of mineralogy, 6th ed.: John Wiley and Sons, New York.

FLEISCHER, M. AND SWITZER, G. (1953), The bavenite problem: *Am. Mineral.*, **38,** 988–993.

JILEK, A. AND KOTA, J. (1931), Über die gewichtsanalytische Bestimmung des Berylliums und seine Trennung von Aluminum durch Gaunidin-carbonat: *Zeit. fur Anal. Chemie*, **87,** 422.

KUTUKOVA, E. (1946), Bavenite from the emerald mines: *Akad. Nauk S.S.S.R. Doklady*, **54,** 721–728 (in English).

ROWLEDGE, H. P. AND HAYTON, J. D. (1948), Two new beryllium minerals from Londonderry: *Royal Soc. Western Australia Jour.*, **33,** 45–52.

SCHALLER, W. T. AND FAIRCHILD, J. G. (1932), Bavenite, a beryllium mineral, pseudomorphous after beryl, from California: *Am. Mineral.*, **17,** 409–422.

STRUNZ, H. (1949), Mineralogische Tabellen, 2d ed.: Akad. Ver. Geest and Portig K.-G., Leipzig.

VON LASAULX, A. (1876), Mineralogisch-krystallographische Notizen. XII. Pilinit, ein neues Mineral: *Neues Jahrb. Mineral.*, 358–363.

Manuscript received September 25, 1959.

THE AMERICAN MINERALOGIST, VOL. 45, JULY–AUGUST, 1960

THE DESCLOIZITE-MOTTRAMITE SERIES OF VANADATES FROM MINAS DO LUECA, ANGOLA

ANTHONY P. MILLMAN, *Royal School of Mines, Imperial College of Science and Technology, London.*

ABSTRACT

The results are given of a chemical, microchemical and *x*-ray investigation of vanadium minerals from a new locality in West Africa—Minas do Lueca in Angola, together with comparative data for similar minerals from other localities. A rapid and simple technique of microchemical analysis has been devised which enables accurate discrimination to be made between different members of the descloizite $(Zn)Pb(VO_4)OH$–mottramite $(Cu)Pb(VO_4)OH$ isomorphous series. A description is given of the mode of occurrence and origin of the vanadium minerals at the Lueca Mine, and of the associated tarbuttite Zn_2PO_4OH and volborthite $Cu_3(VO_4)_2 \cdot 3H_2O$.

INTRODUCTION

In the course of a study of a new vanadium deposit at Minas do Lueca in Angola, Portuguese West Africa, it was found that there was a wide variation in color and physical properties of the "descloizite"-type minerals occurring in the deposit. Reference to literature showed that there is still some confusion in the nomenclature of these minerals and that the *x*-ray powder diffraction data have not been fully established for a representative number of members of the isomorphous series to which these vanadates belong. For paragenesis studies of the vanadium mineralization at Lueca, it was found necessary to make precise identification of members of the series present in the ore. For this purpose, complete chemical analysis was found to be too tedious in view of the large number of specimens involved, and *x*-ray powder photography too indefinite; consequently a rapid microchemical technique has been devised which enables precise discrimination to be made between members of the descloizite-mottramite series.

CHEMICAL COMPOSITION OF THE DESCLOIZITE GROUP

The "descloizite"-type minerals may be expressed by the formula $(Zn,Cu)Pb(VO_4)OH$, and a complete isomorphous series exists between the zinc and copper end-members—descloizite and mottramite respectively. The combined content of ZnO and CuO approximates 20% throughout the series, and it has been proposed that descloizite should refer to that half of the series in which the ZnO content exceeds 10%, and mottramite to the other half of the series in which the CuO content is greater than 10%. The chemical analyses of six members of the series are given in Table 1. It is suggested that members with more than 18% ZnO should be referred to as *descloizite*, those with between 10 and 18%

ZnO as *cuprian descloizite*, those with between 2 and 10% ZnO as *zincian mottramite*, and those with less than 2% ZnO as *mottramite*. Minor amounts of manganese and iron are known to substitute for (Zn,Cu), and arsenic, phosphorus and molybdenum substitute for vanadium.

Table 1. Chemical Analyses of Descloizite and Mottramite

	A*	B*	C*	D	E*	F
PbO	54.9	54.8	51.9	54.5	54.0	54.56
ZnO	19.18	15.22	10.65	5.12	3.61	2.62
CuO	0.83	4.62	8.83	13.9	15.45	16.84
V_2O_5	21.07	22.27	17.38	22.65	20.38	22.73
As_2O_5	n.d.	n.d.	trace	n.d.	n.d.	n.d.

* New analyses.

n.d. = not detected or reported.

A. *Descloizite*, Broken Hill, N. Rhodesia. Coarsely crystalline aggregate; dark-brown colour, yellowish-beige streak.

B. *Cuprian descloizite*, Oliphantsfontein, South-West Africa. Large, dark greenish-black crystals, pale lime-yellow streak.

C. *Cuprian descloizite*, Minas do Lueca, Angola. Greenish-black coarse crystal aggregates, pale brownish-yellow streak.

D. *Zincian mottramite*, Nagreib, Otavi, South-West Africa. Olive-green botryoidal, fibrous mass; olive-green streak. Bannister and Hey (1933).

E. *Zincian mottramite*, Oliphantsfontein, South-West Africa. Velvety surfaces, drusy aggregates; deep lime-green streak.

F. *Mottramite* (near end-member), Uris Mine, Tsumeb, South-West Africa. Grass-green crystals; bright green streak.

X-Ray Investigation

The published *x*-ray powder data for the descloizite series are incomplete. The first attempt to clarify the nomenclature was by Bannister and Hey (1933) and they concluded that the powder data for descloizite, cupro-descloizite, psittacinite, mottramite, chilëite, eusynchite and dechenite were identical and that they could all be expressed by the formula $(Zn,Cu)Pb(VO_4)OH$. This conclusion was modified recently by Kingsbury and Hartley (1956) who showed that although the spacings for descloizite and mottramite are similar above 1.652 Å, there were significant differences in smaller spacings. Guillemin (1956) has also shown this to be the case for the pure synthetic end-members; Guillemin has synthesized two forms of mottramite of different structure and cell-size, and has proposed the terminology of α-mottramite and β-mottramite, the β-form having slight excess of adsorbed water. He has found that naturally occurring mottramite has the α-type structure. In Table 2, new

TABLE 2. *X*-RAY POWDER DATA FOR THE DESCLOIZITE-MOTTRAMITE SERIES: 9 CM. CAMERA, CoKα, λ=1.7889 Å, CORRECTED FOR FILM SHRINKAGE (NOS. 2, 3, 4 AND 5); CuKα, λ=1.537 Å (NOS. 1 AND 6, GUILLEMIN 1956)

1. Synthetic descloizite (Guillemin, 1956).
2. Descloizite, Broken Hill, N. Rhodesia (Anal. A, Tab. 1), (Fig. 1).
3. Cuprian descloizite, Oliphantsfontein, S.W. Africa (Anal. B, Tab. 1).
4. Cuprian descloizite, Minas do Lueca, Angola (Anal. C, Tab. 1).
5. Zincian mottramite, Oliphantsfontein, S.W. Africa (Anal. E, Tab. 1), (Fig. 1).
6. Synthetic α-mottramite (Guillemin, 1956).

	d Å					
	1	2	3	4	5	6
1	5.08 m	5.03 M	5.02 M	4.96 M	4.99 W	5.04 mF
2	4.68 ff	4.68 VW	4.64 VW	4.58 VW	— —	4.61 ff
3	— —	— —	— —	— —	4.47 VW	4.39 ff
4	4.22 f	4.19 W	4.19 W	4.15 W	4.16 W	4.22 fm
5	4.02 ff	3.97 VW	3.96 VW	3.92 VW	3.94 VW	3.94 f
6	3.56 ff	— —	— —	— —	— —	3.57 fm
7	— —	3.49 W	3.50 W	3.47 W	3.50 W	3.53 ff
8	3.46 ff	— —	— —	— —	— —	3.45 f
9	— —	3.31 VW	3.30 VW	3.28 VW	3.28 VW	3.29 ff
10	3.21 F	3.20 S	3.19 S	3.13 S	3.19 S	3.22 F
11	— —	— —	— —	— —	— —	3.05 ff
12	3.01 ff	3.02 W	3.01 W	2.98 W	2.98 W	3.01 f
13	2.90 m	2.93 VW	2.96 VW	2.92 VW	—	— —
14	— —	2.87 S	2.88 S	2.86 S	2.84 S	2.84 m
15	— —	2.68 M	2.69 M	2.66 M	2.65 M	2.68 f
16	2.64 m	2.64 M	2.65 M	2.63 M	2.63 M	2.64 f
17	— —	2.59 S	2.60 S	2.58 S	2.56 M	2.57 fm
18	2.54 ff	2.54 W	2.54 W	2.51 W	2.52 W	2.51 ff
19	— —	2.46 VW	2.45 VW	2.43 VW	2.45 VW	2.47 ff
20	— —	2.42 VW	2.41 VW	2.38 VW	—	— —
21	2.30 m	2.29 M	2.29 M	2.27 M	2.28 M	2.29 ff
22	— —	2.22 W	2.22 VW	2.21 W	2.21 W	— —
23	2.10 fm	2.09 M	2.09 M	2.08 M	2.08 W	— —
24	1.96 ff	1.962 VW	1.961 VW	1.950 VW	1.952 VW	— —
25	1.88 f	1.897 VW	1.893 VW	1.885 W	1.899 VW	— —
26	— —	1.864 W	1.864 W	1.853 W	1.863 W	— —
27	1.77 f	1.777 M	1.772 W	1.767 W	1.780 W	— —
28	— —	1.750 W	1.754 VW	1.747 W	1.762 W	— —
29	1.65 f	1.647 VS	1.647 S	1.637 VS	1.642 S	— —
30	1.61 ff	1.604 M	1.604 M	1.598 M	1.609 M	— —
31	1.57 ff	1.564 S	1.560 M	1.551 M	— —	— —
32	— —	— —	— —	— —	1.538 M	— —
33	1.51 ff	1.512 W	1.508 W	1.499 W	1.504 W	— —

Lines below last spacing listed are too weak or diffuse for measurement. For Nos. 2, 3, 4 and 5, VS=very strong, S=strong, M=moderate, W=weak, VW=very weak.

TABLE 2 (*continued*)

	d Å					
	1	2	3	4	5	6
34	— —	1.496 W	1.495 W	— —	1.494 W	— —
35	— —	— —	— —	— —	1.451 W	— —
36	1.41 ff	1.409 S	1.410 M	1.400 M	1.405 W	— —
37	— —	1.393 VW	1.393 VW	1.381 VW	1.388 W	— —
38	— —	1.367 VW	1.371 VW	1.362 VW	— —	— —
39	— —	1.353 W	1.356 W	— —	— —	— —
40	— —	1.341 W	1.344 W	1.345 W	— —	— —
41	— —	1.332 W	1.334 W	1.329 M	1.335 M	— —
42	— —	1.246 VW	1.249 VW	— —	1.247 M	— —
43	— —	1.236 VW	1.241 VW	— —	— —	— —
44	— —	1.210 VW	1.210 VW	—	— —	— —
45	— —	1.198 VW	1.200 VW	—	— —	— —
46	— —	1.177 VW	1.179 VW	— —	— —	— —
47	— —	1.160 VW	1.161 VW	— —	— —	— —
48	— —	1.149 VW	1.144 VW	— —	— —	— —
49	— —	1.133 VW	1.132 VW	— —	— —	— —
50	— —	1.124 VW	1.123 VW	— —	— —	— —
51	— —	1.106 VW	1.106 VW		— —	—
52	— —	1.098 VW	1.097 VW	— —	— —	— —

x-ray powder data have been listed for four members of the series (nos. 2–5), the chemical analyses of which appear in Table 1(A, B, C and E); for comparative purposes, Guillemin's data are also listed for the pure synthetic end-members although he has not reported lines below 1.41 Å in the case of descloizite, and 2.29 Å in the case of α-mottramite. There is close agreement in the spacings and relative line intensities between 5.0 Å and 1.86 Å (lines 1–26) but substantial differences occur in the lower spacings, especially between 1.60 Å and 1.50 Å (lines 30–34), 1.41 Å and 1.33 Å (lines 36–41), and 1.25 Å to 1.09 Å (lines 42–52). The mottramite half of the series appears to have considerably fewer reflections at spacings lower than 1.38 Å (line 37). Some of these differences may be discerned in Fig. 1 which shows the powder photographs of descloizite and zincian mottramite.

Microchemical Technique for Determination of Members of the Descloizite Group

One of the most useful qualitative microchemical reagents for the identification of several ore metals is potassium mercuric thiocyanate. Details of the procedure for the preparation of this reagent are given by

Short (1948), and the characteristics of the microchemical reaction products by both Short (1948) and Guillemin (1953) for zinc, cadmium, copper, cobalt, nickel, iron and other elements. With zinc and copper the reagent forms mixed crystals, and it occurred to the writer that this might provide an elegant method for the precise identification of this group of zinc-copper vanadates in view of the speed and simplicity with which the test can be performed.

The procedure for carrying out the microchemical analysis is as follows. About 5–10 mg. of the "descloizite" sample to be tested are positioned centrally on a $3'' \times 1''$ glass slide, and one drop of 1:1 nitric acid added from a capillary. The slide is then warmed

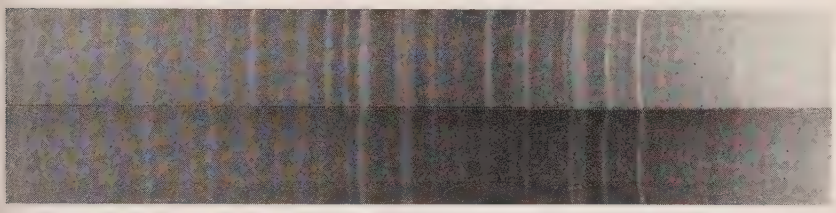

FIG. 1. *X*-ray powder photographs: CoK radiation, $\lambda = 1.7889$ Å; camera radius 9 cm. Above: Descloizite, Broken Hill, N. Rhodesia. ZnO:CuO = 19.18:0.83 (Analysis 2, Table 1). Below: Zincian mottramite, Oliphantsfontein, S.W. Africa. ZnO:CuO = 3.61:15.45 (Analysis 5, Table 1). For spacings in Å, see Table 2.

gently over a spirit-lamp or micro-burner flame to dissolve the mineral and evaporate the nitrate solution to dryness. A characteristic blood-red precipitate of vanadic oxides is produced. A drop of 1:7 nitric acid is then added with a clean capillary to the assay to take the zinc and/or copper salts into solution, and the drop is then transferred by means of a capillary to another clean glass slide. A drop of the 3% aqueous solution of potassium mercuric thiocyanate confirmatory reagent is then placed on this slide adjacent to the test drop, and the two are merged by means of a platinum wire. After about half a minute, the double-salt thiocyanate reaction products appear, and the slide is then examined under a petrological microscope and their characteristics recorded.

In the presence of zinc and absence of copper, a 3% solution of the thiocyanate reagent, $K_2Hg(CNS)_4$, in water, yields pure white feathery crystals; with copper and no zinc, green mossy clumps of fine acicular crystals. With varying amounts of copper and zinc together, a variety of mixed crystals are formed. As shown in Table 3, the descloizite members of the series yield white to purple feathery or simple crosses (for zinc) with no or few green crystals (for copper). The mottramite group give characteristic green mossy clumps of crystals (for copper) with no or very few dark violet crosses (for zinc). The only element which is sometimes present in the descloizite group of minerals and which interferes with this reaction is iron. Iron also yields purple to black crosses or

feathery crystals with zinc, but however reveals its presence by tinting the solution a pinkish brown as well. If therefore the solution does not take on this color after addition of the thiocyanate, it may be deduced that interference due to the presence of iron is negligible.

Mode of Occurrence of the Minas do Lueca Vanadium Deposit

The vanadium mineral deposits at Lueca are located in the upper parts of a range of hills, striking in a north-south direction which rise up to 70 m. above the level of the Lucunga peneplane in Northern Angola. To the south this range of hills, which is only about 500 m. in width, falls gradually to the level of the peneplane, but to the north the slopes drop

Table 3. Zinc and Copper Microchemical Reaction Products with Potassium Mercuric Thiocyanate

Percentage ZnO in descloizite-mottramite series (ZnO+CuO=c.20%)	Microscopic characteristics of thiocyanate mixed-crystal reaction products
Descloizite 20–18	Feathery crosses, white to mauve.
Cuprian descloizite 18–14	Simple crosses only, violet to black.
Cuprian descloizite 14–10	Simple crosses only, violet to black.
Zincian mottramite 10–7	Green mossy aggregates and simple violet crosses.
Zincian mottramite 7–3	Green mossy aggregates and fewer violet crosses.
Zincian mottramite 3–2	Dominant green mossy aggregates and rare violet crosses.
Mottramite 2–0	Green mossy aggregates and acicular crystals only.

sharply to the banks of the Lueca river. The main Damba Plateau is separated from the Lueca hills by a narrow valley.

The chief sedimentary formations of the area are believed to be Pre-Cambrian in age, and belong to the "Schisto-Gréseux" and "Schisto-Calcaire" systems. The former consist of Inkisi felspathic quartzites and sandstones, overlying Pioka red and grey sandstones, shales and basal conglomerate breccia. The older "Schisto-Calcaire" group is composed of a variable series of impure limestones, containing occasional algal fossils. The Damba Plateau and western flanks of the Lueca hills are composed of this limestone series; at Lueca the limestones dip 10 15° to the east, and the eastern flanks of the hills are made up of "Schisto-Gréseux" sandstones and quartzites dipping 20 50° to the west, the two series being separated by a presumed north-south fault along the axis of the Lueca range.

The surface of the Lueca hills is composed of argillaceous and siliceous

eluvium, with a maximum thickness of about 5 m., consisting of numerous hematite boulders and fragments of siliceous rocks with sporadic vanadium minerals and manganese oxides. The soil is reddish brown containing grains of pisolitic laterite and small fragments of quartz. Below this eluvial cover, the rocks are intensely altered and fragmented; pipe structures are common and contain collapse breccias of silicified rocks with argillaceous and ferruginous earths and vugs lined with chalcedonic silica, descloizite, mottramite, vanadinite and other rarer minerals.

Mineralogy of the Vanadium Ores

Primary hypogene minerals are extremely rare at Lueca, and only traces of pyrite relics were found in limonite boxworks, together with a few grains of strongly fluorescent sphalerite, the latter being very similar to the sphalerite occurring in the Tsumeb Mine in South-West Africa.

Of the secondary supergene minerals, hematite is the most common occurring in the form of ochres in solution cavities, finely dispersed material in hematitized and silicified limestones, and as large masses showing prominent colloform banding. Considerable amounts of limonite are also present. Quartz is widespread in its distribution in the ore zone, and occurs as (*a*) cross-cutting veins and lenses of crustified and comb-structured white and green quartz, (*b*) replacement disseminations of microcrystalline euhedral clear quartz in silicified limestones (see Fig. 2,A), and (*c*) vug and solution cavity fillings of colorless euhedral crystals and chalcedonic gel silica. The silica of type (*c*) occasionally contains radiating spherulites of secondary copper silicates; these are azure to sky-blue in color, with a maximum size of about 2 mm. Three different *x*-ray powder patterns have been obtained for these silicates, and none agrees with the powder patterns for planchéite, shattuckite or chrysocolla from the Tantara Prospect, near Katanga, Belgian Congo. Other rare supergene minerals have been confirmed by *x*-ray powder photography.

Tarbuttite, Zn_2PO_4OH, occurs as saddle-shaped radial aggregates of pale green crystals, up to 3 cm. across, encrusting surfaces of hematite. The presence of zinc, phosphorus and arsenic has been confirmed by microchemical and spectrographic analysis. The following optical properties were determined: $\alpha = 1.659$, $\beta = 1.685$, $\gamma = 1.702$ (for Na light, $\pm .003$), optically $(-)$, $2V = 50°$. The presence of arsenic in addition to phosphorus suggests the possibility that an isomorphous series may exist between tarbuttite and the new triclinic zinc arsenate, paradamite Zn_2AsO_4OH, described recently by Switzer (1956). *Volborthite*, $Cu_3(VO_4)_2 \cdot 3H_2O$, has also been identified, and the *x*-ray powder data agree closely with those reported recently by Guillemin (1956). It occurs as bright to

olive yellow micaceous brittle flakes, up to 1 cm. across, with high lustre and perfect cleavage. The refractive indices are >2 and <2.09 with no pleochroism; it shows high dispersion and twinning is also characteristic. The volborthite occurs as an alteration product on the surfaces of descloizite and mottramite crystals, and also as crystals lining the central cavities of geodes of green quartz.

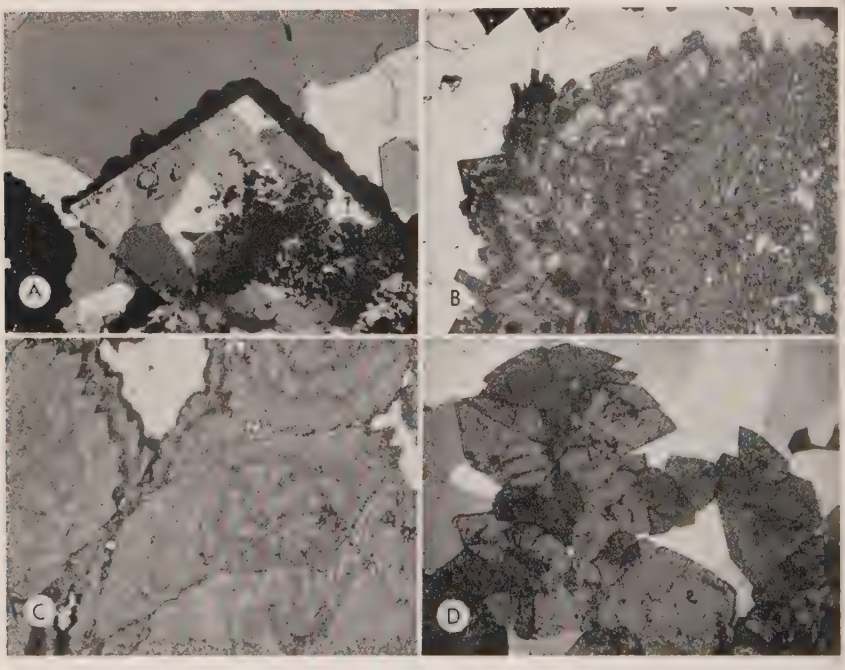

FIG. 2. Thin section photomicrographs of ore specimens from Minas do Lueca, Angola.

Upper left: Dolomite limestone totally silicified by supergene processes. Note the relic outline of original rhombic carbonate replaced by mosaic of silica, with overgrowth by colloform hematite and goethite. (Polarized light, ×55.)

Upper right: Small cavity filling of euhedral zoned mottramite and quartz. Note the diffuse boundary between the finer grained disseminated mottramite in the wallrock and the cavity lining. (Ordinary light, yellow filter, ×20.)

Lower left: Prominent color zoning and pleochroism (red to yellow) in coarsely crystallized mottramite. Interstices rimmed with manganese oxides and goethite and filled with chalcedonic silica and opal. (Ordinary light, yellow filter, ×20.)

Lower right: Aggregate of euhedral mottramite crystals enclosed in a mosaic of secondary quartz. (Polarized light, yellow filter, ×20.)

Descloizite, $(Zn,Cu)Pb(VO_4)OH$ *and mottramite,* $(Cu,Zn)Pb(VO_4)OH$

The microchemical method of analysis has shown that at Lueca mottramite members of the series are far more common than the descloizites.

The composition has been found to vary substantially and the following four main types have been discriminated:

1. Cuprian descloizite, intermediate member, CuO:ZnO 1:5
2. Zincian mottramite, intermediate member, CuO:ZnO 2:1
3. Zincian mottramite, intermediate member, CuO:ZnO 5:1
4. Mottramite, near end-member, CuO:ZnO 10:1

Other intermediate members have also been recognized (e.g. analysis C, Table 1), but do not constitute significant amounts of the ore. Qualitative spectrographic analysis has shown the presence of substantial amounts of As, Cr and Mn, and traces of Fe, Mo, Ni, Ag, Sn, Ti and P. The Cr, As, Mo, and P are probably substituting for vanadium, and the Fe and Mn for (Cu,Zn).

The descloizite at Lueca is usually dark reddish brown in color, whereas the mottramite is more inclined to a dark blackish green or more rarely a pistachio green. Both occur as crystalline sheaf-like aggregates, often with a fibrous structure and with color banding normal to the length of the fibers. Well-formed euhedral crystals (see Fig. 2,D) also occur in vugs associated with quartz, chalcedony and rare vanadinite. Very large amounts of both descloizite and mottramite however occur as minute anhedral replacement grains in the silicified limestone wallrocks (see Fig. 2,B); occasional spherulites up to 1 mm. in size are also found on the walls of joints in massive hematite. Rhythmic banding of red, yellow and green zones is conspicuous in thin-sections (Fig. 2,B and C). Relics of vanadinite crystals partially replaced by descloizite and mottramite are common, although vanadinite in places overgrows the other vanadates. Green quartz is common in the vanadium ore zone, and the green color has been found to be due to the presence of myriads of minute prisms and acicular aggregates of the descloizite-mottramite group; the size of these crystal inclusions reaches a maximum of about 15×250 microns, but most are considerably smaller than this.

Vanadinite, $Pb_5(VO_4)_3Cl$

This mineral is much less common than the other vanadates with which it is intergrown. It occurs as small orange-brown prismatic crystals up to 3 mm. in diameter, and as fine straw-like crystals and tufted fibers, pale yellow to orange in color. Deposition of the vanadinite overlaps with that of descloizite and mottramite.

Origin of the Vanadium Ore Minerals

The occurrence of the vanadium minerals at the Lueca Mine shows general geological similarities with other vanadium deposits in South-West Africa. At Grootfontein and Abenab the more common type of

deposit is usually associated with limestones and dolomites, and the ore minerals occur in vugs, interstices, collapse breccias in the form of pipes, and solution cavities, associated with considerable amounts of secondary calcite. In the Lueca area, however, the rocks are dominantly siliceous in nature and the vanadium-bearing minerals are associated with quartz and chalcedony, carbonate minerals being entirely absent. A comparable deposit is the one at Kazakstan in the Soviet Union where vein-like lenses of quartz with vanadium minerals occur at the contact of recrystallized limestones and sandstones. The Lueca-type deposit appears to be unusual in Africa.

Previous workers including Schwellnus (1946) and Taylor (1954) have concluded from spectrographic data that inadequate amounts of vanadium are present in primary sulphide minerals to account for its extensive concentration during the weathering and oxidation of base-metal deposits. However at Broken Hill, N. Rhodesia, Taylor (1954) has reported 0.0003 0.0005% V in the dolomite of the Broken Hill Series, as compared with 0.0117–0.0134% V in argillaceous members of the Series. Protracted weathering of such argillaceous rocks under tropical conditions, especially in arid regions, could account for adequate quantities of vanadium. The most likely source at Lueca is the Pioka Series containing red shales, which overlie the Schisto-Calcaire Dolomite, and which have been removed by erosion. Reprecipitation of the vanadium liberated by weathering may take place at the locus of lead, zinc and copper mineral deposits, but if the groundwaters are strongly acidic, as is frequently the case in proximity to oxidizing orebodies, the soluble lead-zinc-copper vanadates will migrate and be deposited under the optimum reducing conditions in a favorable rock or structure. It has been shown experimentally by Guillemin (1956) that mottramite is precipitated at pH 4 by the replacement of vanadinite by copper sulphate solution. He has also shown that volborthite is soluble in acid solution but will start to precipitate when the pH approaches 4.5; acid solutions will however precipitate volborthite on the surfaces of malachite and azurite, as in some Russian deposits, and in a barium or calcium rich environment, vesigneite $Cu_3Ba(VO_4)_2OH$ or tangeïte $CuCa(VO_4)(OH)$ respectively are formed.

The mineralogical assemblage at Lueca of contemporaneous descloizite-mottramite, volborthite, tarbuttite and planchéite-type copper silicates suggests therefore deposition in a moderately acidic environment together with extensive silicification of the limestone wallrocks. Some evidence is seen of the presence of rare primary sphalerite and pyrite, and the tectonic structure of the Lueca hills provided the channelway for the original deposition of the primary deposit of sulphides in the

dolomitic limestone where it is faulted against the quartzites and sandstones. It is concluded that the Lueca vanadium deposit is of residual origin, and has been formed in the area of a pre-existing Cu-Pb-Zn orebody the vanadium being derived from weathered sediments; the presence of such abundant quartz, obviously deposited under exogenic conditions in view of its intimate association with vanadates, phosphates and copper silicates and the extent of the silicification of the dolomitic limestone is unusual, and may in part at least be due to a resurgence of low temperature "hydrothermal" solutions associated with renewed movement on the Lueca fault. Contamination of these ascending solutions was then brought about by the agency of near-surface groundwaters in the region of the oxidizing orebody.

Acknowledgments

Financial assistance was kindly provided from the Central Research Fund of the University of London for chemical analyses of the vanadium minerals. I would like to thank my colleagues at Imperial College for helpful discussions and assistance, especially Dr. J. Butler for qualitative spectrographic analyses, Miss Brenda Mulligan for preparation of x-ray photographs, Miss Jill Harvey for optical determinations and J. Gee for photomicrographs. The author is also deeply indebted to the Empresa do Cobre de Angola Mining Company who invited the author to visit their properties in Angola in 1955 and 1957, and with whose permission this paper is published.

References

Bannister, F. A. and Hey, M. (1933), The identity of mottramite and psittacinite with cupriferous descloizite: *Mineral. Mag.* **23,** 376–386.

Guillemin, C. (1953), Microanalyse qualitative appliqué à la détermination des espèces minérales: Pb. 13 du Bureau des Recherches geologiques, geophysiques et minières. Paris.

——— (1956), Contribution à la minéralogie des arséniates, phosphates, et vanadates de cuivre, II phosphates et vanadates de cuivre: *Bull. soc. franç. Minér. Crist.* **79,** 219–275.

Kingsbury, A. W. G. and Hartley, J. (1956), New occurrences of vanadium minerals (mottramite, descloizite and vanadinite) in the Caldbeck area of Cumberland: *Mineral. Mag.* **31,** 289–295.

Short, M. N. (1948), Microscopic determination of the ore minerals: *U. S. Geol. Surv. Bull.* **914.**

Schwellnus, C. M. (1946), Vanadium deposits in the Otavi Mountains, South-West Africa: *Trans. Geol. Soc. S. Afr.* **48,** 49–73.

Switzer, G. (1956), Paradamite, a new zinc arsenate from Mexico: *Science* **123,** No. 3206, p. 1039.

Taylor, J. H. (1954), The lead-zinc-vanadium deposits at Broken Hill, Northern Rhodesia: *Col. Geol. Surv. Bull.* **4,** 335–365.

Manuscript received September 21, 1959.

THE AMERICAN MINERALOGIST, VOL. 45, JULY–AUGUST, 1960

DIFFERENTIATION OF A LAMPROPHYRE SILL, NORTHERN LA PLATA MOUNTAINS, COLORADO

JOHN J. W. ROGERS AND JOHN D. LONGSHORE, *Department of Geology, The Rice Institute, Houston, Texas.*

ABSTRACT

Differentiation trends in a lamprophyre sill in the northern La Plata Mountains, Colorado, indicate fractional crystallization of an originally sodic melt containing pyroxene phenocrysts and inclusions of amphibolitic rock. Injection and fairly rapid crystallization caused the abundance of pyroxene to remain approximately constant throughout the sill. Fractional crystallization, however, resulted in an increase in the amount of plagioclase toward the center of the sill and a concurrent increase in albite content of the plagioclase. Selectively greater resorption of the amphibolite inclusions toward the center of the sill caused the percentage of hornblende to decrease inward from the margins, for the hornblende in the sill has been derived entirely from digestion of the inclusions and was out of equilibrium with the melt. Extensive late-stage activity involved formation of chlorite, argillization of plagioclase, and development of minor calcite and thomsonite.

INTRODUCTION

Studies of differentiation trends have been of prime importance in igneous petrology. For example, a current major controversy concerns the question of whether or not granitic rocks have solidified from differentiates of basaltic magma, and the answer to this problem depends partly on understanding the course of basaltic differentiation. In this connection, the evolution of the large and varied group of rocks known as the lamprophyres is a problem intimately related to the question of magmatic differentiation trends. The lamprophyres, with their generally mafic phenocrysts and alkalic groundmass, are not explainable by most standard differentiation mechanisms, and their origin is uncertain. The present study of the differentiation trends within one large lamprophyre sill has been made in the hope that the data presented here will contribute to a general understanding of the origin of lamprophyres.

The sill studied is in the northeastern part of the La Plata quadrangle, La Plata Mountains, southwestern Colorado. It crops out along Indian Trail Ridge, and the lower contact is almost coincident with the 12,000 foot contour. The original extent of the sill is unknown, for the outcrop on Indian Trail Ridge is the only remnant. The sill is 130 feet thick throughout its entire present extent and is intruded conformably into flat-lying sandstones of the Morrison formation. Contact metamorphism of the sandstones is minor and appears only in a baked zone 1 to 2 feet wide. The sill had previously been studied briefly by Cross (1899) in his general survey of the La Plata quadrangle. He reported a distinct compositional and textural layering parallel to the contacts, and it was this

evidence of differentiation which attracted the writers to the present study.

Basically the sill consists of phenocrysts of pyroxene (both orthopyroxene and augite) and hornblende in a highly altered groundmass of oligoclase. Pyroxene comprises 10 to 25 per cent of the sill, hornblende ranges from 0 to 30 per cent in different portions, plagioclase constitutes from 40 to 60 per cent, and magnetite averages about 10 per cent. The plagioclase has been thoroughly altered to unidentified clays, some of the hornblende has been altered to chlorite, and calcite and zeolites form small veinlets and amygdule(?) fillings scattered throughout the sill. Amphibolitic inclusions, largely hornblende and oligoclase, are abundant near the borders of the sill but are absent toward the center. The sill is best classified as a spessartite.

The origin of lamprophyres has long aroused speculation. The literature and dominant ideas concerning them up to 1936 have been summarized by Knopf (1936), and many of the questions which he posed still remain unanswered. Differentiation in an individual lamprophyre dike has been described by Campbell and Schenk (1950), but other evidence concerning variability within single intrusions is scarce.

Procedure

A total of 31 samples was collected at intervals of 1 to 5 feet from the upper to lower contact of the sill. Owing to steepness of slopes and lack of vegetation, the sill was well exposed through its entire thickness, and the only deterrent factor in the sampling was a small amount of talus cover.

One thin section was cut from each sample, and modal compositions were determined by point counting 1000 to 1300 points. Pyroxene compositions were determined with a universal stage by measuring the optic angles of 10 grains in each of 6 slides (spanning the complete thickness of the sill); measurements were made by the Berek method (Emmons, 1943, pp. 28–32), and some were checked by stereographic plotting of the optic axes. All grains were measured more than once. Plagioclase compositions were determined in 11 slides spaced at 10 foot intervals from the base to top of the sill. Very few of the plagioclase grains in any slide could be measured owing to the intense argillization, but in each of the 11 slides determinations were made on from 3 to 6 grains which clearly showed extinction positions of albite twins. The measurements were made on the universal stage by determining the maximum extinction angle to the (010) plane and estimating the relative relief. These measurements, which showed a small range in composition within each slide, were checked by refractive index measurements made by inserting

index oils under the cover glass of the slide and into contact with an edge of the section from which the mounting medium had been removed. This method of index measurement has been described by Rogers (1960). Grain sizes of pyroxene, hornblende, and plagioclase were determined in selected slides by measuring the long axes of 10 grains of each mineral (only 3 hornblende grains in one slide) with a micrometer ocular.

Mineralogy

Pyroxene

Pyroxenes occur chiefly as phenocrysts and form large euhedral crystals throughout the entire sill (Fig. 1). Orthopyroxenes (highly magnesian) and augite are both present and appear to maintain a ratio of about 1 orthopyroxene to 1 augite throughout the sill.

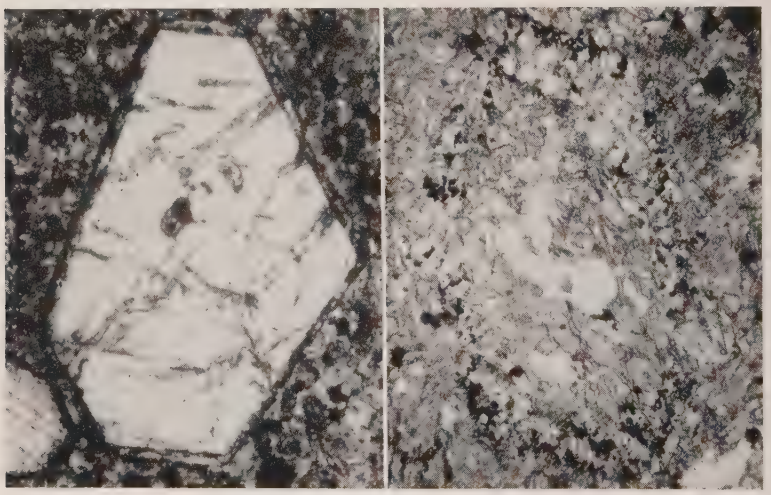

Fig. 1. (left) Euhedral orthopyroxene grain. Plain light, ×75.

Fig. 2. (right) Partially replaced hornblende grain with magnetite rim. Plain light, ×40.

The orthopyroxenes are generally optically positive, though a few grains of high 2V have a negative sign. Indices are less than 1.72, and optic angles range from about 55° to 90°. The pyroxenes, therefore, are in the high magnesian part of the series (based on data in Winchell and Winchell, 1951). Attempts to detect variation in pyroxene composition from place to place in the sill failed owing to variability of compositions in single slides; in one slide the optic angle ranged from 55° to 87° in different grains. Some of the grains are zoned, invariably with the core higher in magnesium content than the margins.

The augite grains are faintly pleochroic from colorless to pale green. They are optically positive and have average optic angles of about 62°.

Hornblende

Hornblende grains occur only as phenocrysts and generally form corroded, apparently highly altered crystals (Fig. 2). The corroded grains contrast strongly with the euhedral shape of the pyroxene and suggest that the hornblende was dissolving in the lamprophyric melt while the pyroxene was growing. The resorption of hornblende has been

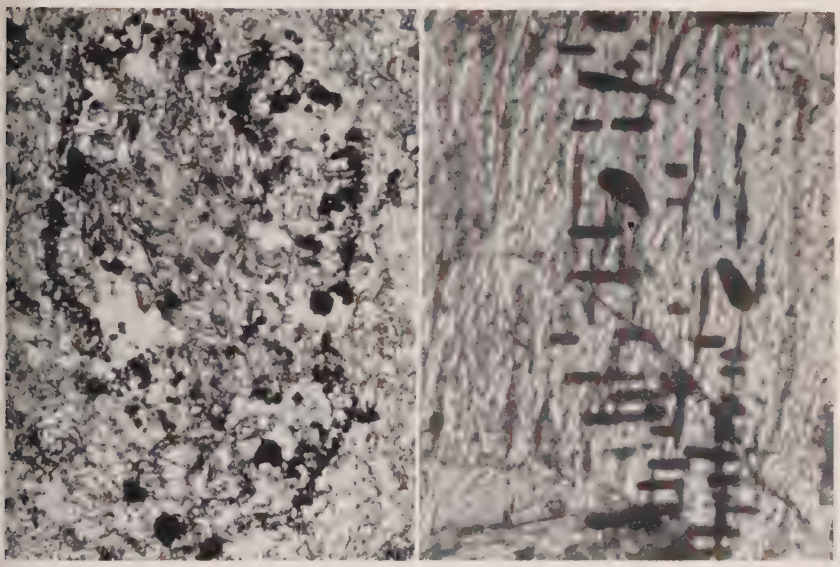

FIG. 3. (left) Magnetite grains outlining a pseudomorphously replaced hornblende grain. Plain light, ×45.

FIG. 4. (right) Schiller in hornblende. Plain light, ×195.

noted in other lavas from the general San Juan region by Larsen Jr. and Cross (1956, p. 262). Hornblende occurs only in the marginal portions of the sill, and in the center its place is occupied by amphibole-shaped pseudomorphs consisting of oligoclase, magnetite, and alteration products. Hornblende pseudomorphs are particularly marked by rims of small magnetite grains (Fig. 3). Some of the hornblende shows small-scale schiller structure (Fig. 4).

Optical properties of the hornblende are somewhat variable. The mineral is pleochroic from yellow green to greenish brown, has n_z (measured in index oils) of about 1.68, has an average extinction angle of 24° ($Z \wedge c$), and has an extremely high optic angle ($\pm 75°$–$90°$). The com-

position is apparently roughly intermediate between those of hastingsite and edenite with some iron content (based on data in Winchell and Winchell, 1951).

Plagioclase

Plagioclase forms a fine-grained groundmass of subhedral to anhedral somewhat lath-shaped grains. Almost all grains are extensively altered to clay minerals, thus preventing detection of such features as zoning, twinning, etc. A few grains in each slide were sufficiently unaltered that albite twinning could be detected, and measurement of these grains in 11 of the slides placed plagioclase in the compositional range from An_{14} to An_{24}.

Magnetite

Magnetite forms small anhedral grains either scattered throughout the slides or in clusters around altered hornblende grains. The scattered magnetite may represent primary crystallization, whereas the clusters are certainly the products of reaction and alteration. Many of the individual grains, however, are of uncertain origin, and consequently no effort was made to separate the two types in the modal analysis.

Minor minerals

Apatite forms tiny euhedral crystals in the groundmass in many samples. Quartz is very rare but occurs in a few slides as rounded, undulant grains.

Secondary and alteration minerals

Chlorite occurs both in the groundmass and as an alteration product either rimming or completely replacing hornblende. Some of the slides contain nearly 20 per cent of chlorite or similar clay mineral.

Plagioclase is almost completely altered to clay minerals, though the exact nature of the clays is unknown.

Calcite occurs in vein and cavity (amygdule ?) fillings and as an alteration product of hornblende. The zeolite thomsonite occurs in a few cavities.

Inclusions

Mafic inclusions, up to several inches in diameter, occur near the margins of the sill but are absent in the center. The rock comprising the inclusions is essentially an altered amphibolite consisting of greenish-brown hornblende (50 per cent) very similar to the hornblende grains in the sill, highly argillized oligoclase (35 per cent), and minor biotite, chlorite,

magnetite, and calcite. The hornblende, oligoclase, and biotite are probably primary constituents, whereas the magnetite, chlorite, and calcite appear to represent reaction of the inclusions with the lamprophyric magma. The alteration of the hornblende is the same as in the sill rock, and some of the grains are rimmed with magnetite in the same fashion as hornblende in the sill. The distribution of the inclusions and the similarity of the hornblende grains in the sill and inclusions indicates that the hornblende in the sill has probably been derived by digestion of the inclusions.

Differentiation of the Sill

The various components of the sill are unevenly distributed, and their variations are shown diagrammatically in Figs. 5 to 10. Except for the

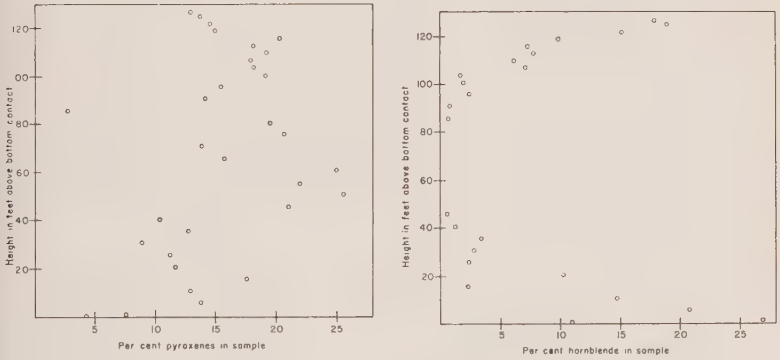

Fig. 5. Distribution of total pyroxenes in sill. The ratio of orthopyroxene to augite is about 1:1 and is roughly constant throughout the sill.

Fig. 6. Distribution of hornblende in sill.

magnetite, the distributions are symmetrical around the center of the sill and apparently indicate fractional crystallization of the lamprophyre from the edges inward.

Figure 5 shows that pyroxenes are rather uniformly distributed throughout the sill. One explanation for this uniformity, in view of the obvious variations shown by other minerals, is that the pyroxenes had nearly completed crystallization prior to injection of the magma into the sill. The pyroxene grains would then be thoroughly mixed with the melt and, having densities possibly very close to that of the residual melt, might not show appreciable gravitative settling. The failure of comparatively low-density mafic materials to settle is also indicated by the fact that amphibolitic inclusions are abundant near the upper margin of the sill as well as near the lower margin. A mixing such as proposed

above could explain the variations in composition shown by pyroxene grains within individual thin sections if it is assumed that the magma injected to form the sill was derived from a partially differentiated body at depth.

Figure 6 shows the distribution of hornblende in the sill. In view of the textural evidence for the resorption of hornblende, the distribution is best explained by assuming increasing resorption toward the center of the sill, where the magma remained fluid for a longer period of time than at the margins. Abundant digested hornblende grains (as in Fig. 3) support this conclusion. Unfortunately, many clusters of magnetite and other alteration products in the central part of the sill do not have the

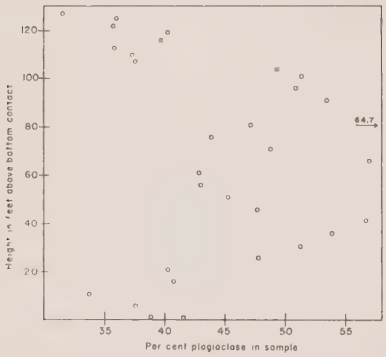

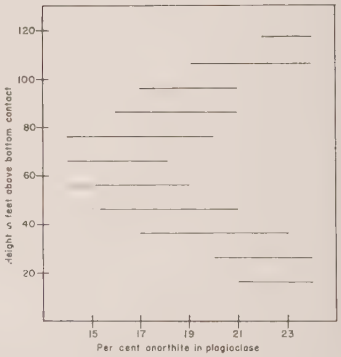

FIG. 7. Distribution of plagioclase in sill.
FIG. 8. Variation in composition of plagioclase in sill.

diagnostic hornblende outline and might be accounted for in other ways; consequently no quantitative estimate has been obtained for the abundance of completely resorbed hornblende.

The abundance of plagioclase (Fig. 7) increases inward toward the center of the sill. Presumably the variation is caused by the fact that the sodic plagioclase is a late-crystallizing component and is thus concentrated in the residual liquids toward the center of the sill. This conclusion is supported by the increase in albite content of the plagioclase toward the center of the sill (Fig. 8).

Unlike hornblende and plagioclase, the magnetite is not symmetrically distributed in the sill (Fig. 9). The greater concentration toward the base of the sill may testify to some gravitative settling of the comparatively dense magnetite. The slight decrease in abundance from the upper contact to the center, however, indicates increased viscosity of the melt near the more rapidly cooled margins, thus preventing complete settling of the relatively early-crystallizing magnetite.

Figure 10 shows the distribution of grain sizes of pyroxene, hornblende, and plagioclase. As expected, the grain size of plagioclase increases inward toward the more slowly cooled center, whereas the size of the partially resorbed hornblende grains decreases inward. Pyroxenes appear to be larger near the upper margin of the sill than near the center and base, though the explanation for this variation is uncertain.

Conclusions

The variations in the sill described in the present paper probably resulted from the differentiation and fractional solidification of an injected melt originally containing abundant solid material. The pyroxenes may

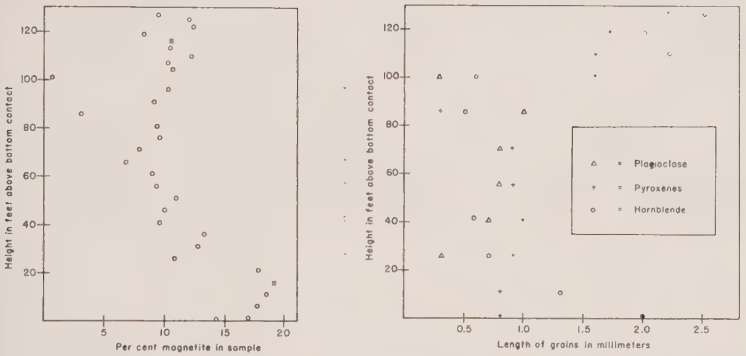

Fig. 9. Distribution of magnetite in sill.
Fig. 10. Variation in grain sizes of pyroxene, hornblende, and plagioclase in sill.

have been almost completely crystallized at the time of injection, and if the hornblende content of the sill can be attributed to digestion of amphibolite inclusions (as are found near the margins), then the total amount of solid material in the original injection was about 50 per cent. The amphibolitic rock fragments were probably part of the Archean basement and were caught in the lamprophyric magma as it was injected upward. After intrusion, the inclusions were ingested by the relatively high temperature magma, the hornblende grains were added to the melt, and the individual grains reacted with the magma and were partly pseudomorphously replaced. The plagioclase component was enriched in the residual fluids during the fractional crystallization, and both its total abundance and the percentage of albite in individual grains increased toward the center of the sill. Magnetite crystallized comparatively early and underwent minor gravitative settling. The abundance of volatiles either in the original magma or in the later phases is indicated by the chloritic alteration of the hornblende, the extreme argillization of the

plagioclase, and the presence of calcite and zeolite in veins and patches throughout the sill.

The incorporation of inclusions containing oligoclase and somewhat sodic hornblende certainly increased the sodium content of the magma. The sodic nature of the lamprophyre, however, cannot be accounted for in this manner, as shown by the fact that the rock in the margins of the sill, where digestion of the inclusions has been negligible, contains a highly sodic plagioclase. The original magma before addition of the inclusions evidently consisted of pyroxene crystals in contact with a very sodic melt. The presence of resorbed hornblende, however, is of importance in view of Bowen's (1956, p. 269–273) conclusions that resorption of hornblende and/or biotite is an important process in the development of many lamprophyres.

Acknowledgments

Field work on this project was supported by a grant from the Arthur I. Lake Fund of the Department of Geology, The Rice Institute. The writers express their thanks to Mr. Ted H. Foss, Department of Geology, Lamar State College, Beaumont, Texas, for assistance in the field work.

References

Bowen, N. L. (1956), The Evolution of the Igneous Rocks, 2nd edition, Dover, New York, 332 p.

Campbell, I. and Schenk, E. T. (1950), Camptonite dikes near Boulder Dam, Arizona: *Am. Mineral.* **35,** 671–692.

Cross, W. (1899), Description of the La Plata Quadrangle (Colorado): *U. S. Geol. Survey Folio* No. 60.

Emmons, R. C. (1943), The Universal Stage: *Geol. Soc. Am. Memoir* **8,** 205 p.

Knopf, A. (1936), Igneous geology of the Spanish Peaks region, Colorado: *Geol. Soc. Am. Bull.* **47,** 1727–1784.

Larsen, E. S., Jr. and Cross, W. (1956), Geology and Petrology of the San Juan Region, Southwestern Colorado: *U. S. Geol. Survey Prof. Paper* **258,** 303 p.

Rogers, J. J. W. (1960), Measurement of refractive indices in thin section: *Am. Mineral.* **45,** 741.

Winchell, A. N. and Winchell, H. (1951), Elements of Optical Mineralogy; Part II, Descriptions of Minerals, 4th edition, John Wiley and Sons, New York, 551 p.

Manuscript received November 4, 1959.

THE AMERICAN MINERALOGIST, VOL. 45, JULY–AUGUST, 1960

AN OCCURRENCE OF FULLY-HYDRATED HALLOYSITE AT MUSWELLBROOK, N.S.W.

F. C. Loughnan and D. C. Craig, *University of New South Wales.*

Abstract

An occurrence of halloysite($4H_2O$) in commercial quantities, at Muswellbrook, N.S.W. is described. Intrusions of slag derived from the fusion of ferruginous sediments by the underground combustion of coal seams, have partly altered the associated strata to assemblages of tridymite, cristobalite and mullite. It is considered that the halloysite originated from the rehydration of metakaolinite formed by thermal metamorphism of well crystallized kaolinite.

Occurrence and Mineralogy

A recent discovery of halloysite ($4H_2O$) by the authors, on Portion 115, Parish Brougham, County Durham, six miles south of Muswellbrook, is of interest not only because the clay is available in commercial quantities, but also the occurrence affords an opportunity to study an unusual genesis for this comparatively rare mineral.

The deposit which forms part of the Permian Lower or Greta Coal Measures (Booker, 1953) outcrops over a thickness of 20 feet on the western side of a low conical-shaped hill known locally as "The Pimple" (Fig. 1). A laminated, dark-colored microbreccia composed essentially of well-crystallized kaolinite underlies the halloysite while the ten feet or so of overlying strata consists of siliceous shales characteristic of much of the Permian Coal Measures of N.S.W. The halloysite grades laterally into a rock similar to, but coarser-grained than, the underlying material. In thin section the microbreccia displays sub-angular, equidimensional clay-aggregates ranging up to 3 mm. in diameter, with a few scattered grains of quartz and finer chalcedony, while lenticules of organic matter impart the dark coloration. The kaolinite content varies from 75% to 90% and, in addition, a trace of partly-hydrated halloysite was detected in the majority of samples examined. Elsewhere in the area occasional quartz-enriched lenses may be observed occurring within the outcrops of the clay microbreccia.

The siliceous shales overlying the halloysite are considerably brecciated in places and the voids so created are infilled by two contrasting rock types, an earlier, fine-grained, contaminated "picrite basalt" and a later, highly-vesicular, dark colored slag.

In thin section, the "picrite basalt" is sub-ophitic to intergranular with strongly-zoned, equant anhedra of diopsidic hedenbergite, up to 1 mm. in diameter, and slender plagioclase (anorthite?) laths ranging from 0.2 to 1 mm. Tridymite, cristobalite and brown glass comprise the groundmass.

On the other hand, the slag contains an abundance of cordierite mo saics, pleochroic from pale violet to colorless; fine, twinned, wedge shaped crystals of tridymite; microlitic cristobalite; magnetite grains altering to hematite, and slender mullite needles often in the form o felted masses.

Generally the slag occurs marginal to the "picrite basalt" though inter-reaction and intimate admixture of the two are common. In such cases, the feldspar of the "basalt" frequently is altered to mullite though the pyroxene remains virtually unaffected. The low viscosity of the slag is evidenced by the high degree of penetration into the bedding planes of the shales whereas the more viscous "basalt" is restricted to the larger cavities.

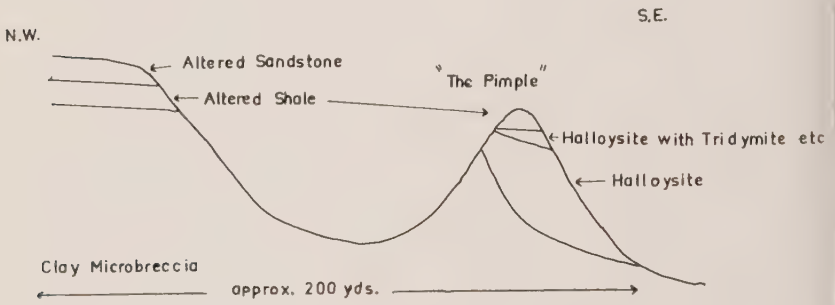

FIG. 1. Cross section of the halloysite deposit.

X-ray examination of the intruded shales revealed their almost entire alteration to an assemblage of tridymite, cristobalite and mullite. However, in thin section, a few silt-sized quartz grains were still apparent.

The bulk of the halloysite, on the other hand, consists of a dense, well-jointed, off-white clay with a texture similar to the clay-microbreccia. Examination by differential thermal, *x*-ray and chemical techniques (see Fig. 2 and Tables 1 and 2), indicated the presence of fully hydrated halloysite contaminated by a small quantity of relatively coarse quartz and a trace of kaolinite. However, electron micrographs failed to reveal any trace of the characteristic tube-like forms of halloysite.

Within a few feet of the base of the overlying shales, the halloysite assumes a platy structure which passes upward into an iron-stained zone. Though fully hydrated halloysite comprises much of both the platy and iron-stained clays, appreciable quantities of cristobalite and tridymite are also present. In addition, a few grains of quartz and possibly mullite were detected.

Approximately a hundred yards to the north of "The Pimple" the

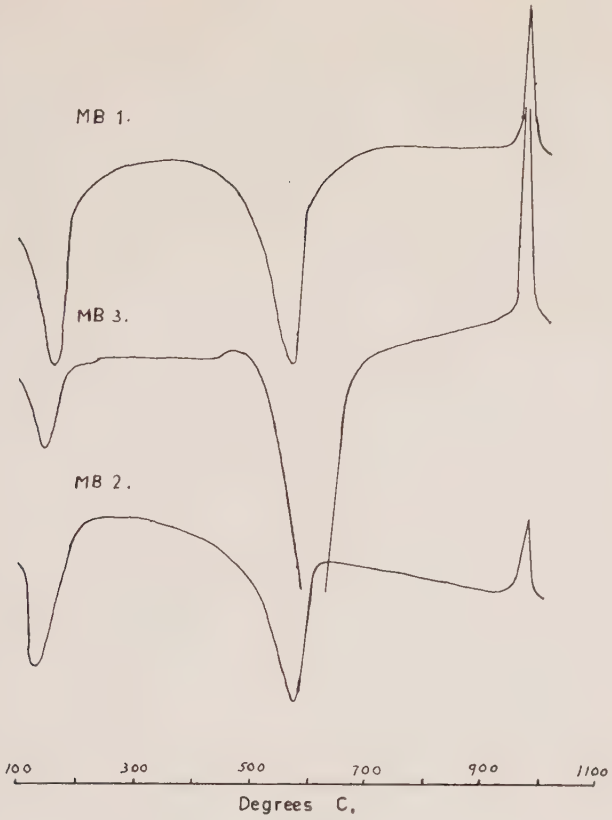

FIG. 2. DTA data. MB1—halloysite; MB2—platy halloysite near top of deposit; MB3—Clay-microbreccia.

same succession of strata outcrops on a flat-topped hill. Here, however, the brecciated shales are overlain by a few feet of sandstones which also have been metamorphosed to an assemblage of tridymite, cristobalite, mullite and interstitial glass though many of the larger quartz grains, generally rimmed with cristobalite, are still apparent in thin section.

On a ridge a few hundred yards south of "The Pimple," the succession is repeated, though with a greater thickness of the overlying sandstones, of which only the basal portion has been affected by metamorphism.

ORIGIN OF THE CLAY-MICROBRECCIA

The term "clay-microbreccia" is used in this paper to describe a type of sediment which, though relatively rare, has been recognized in many

Table 1. *X*-Ray Data

MB1		MB1 (*a*)		MB2 (*a*)		MB3		MB4		MB5		MB6	
d	I	*d*	I	*d*	I	*d*	I	*d*	I	*d*	I	*d*	I
10.0	10	11.1	10	11.0	10	8–9	2 (b)					8.30	3
7.20	1	7.20	1			7.10	10	7.20	1	7.15	2		
		5.72	1					5.38	2	5.4	3		
4.84	1	4.84	1					4.80	1	4.80	3		
4.45	7	4.45	7			4.42	8						
				4.30	6			4.30	10	4.30	10	4.30	10
4.22	2	4.22	2										
						4.14	8						
				4.05	10			4.05	10	4.05	7	4.05	10
		3.75	4	3.81	3	3.84	2	3.81	7	3.81	7	3.81	6
3.52	2	3.52	2			3.56	10					3.66	1
								3.40	5	3.40	4	3.40	4
3.35	4	3.35	4	3.35	2	3.35	4	3.35	2	3.35	5		
												3.30	4
				3.14	1								
				2.98	1			2.98	3	2.98	4	3.00	6
				2.84	2			2.84	1	2.84	2		
				2.69	1			2.70	3	2.70	2	2.69	7
2.55	2	2.58	2	2.53	1	2.55	5	2.54	3	2.54	3	2.54	10
2.50	1	2.50	1	2.49	4	2.50	5	2.50	3	2.49	4		
						2.34	7						
				2.29	1	2.29	5	2.30	3	2.30	3	2.30	3
				2.20	1			2.21	4	2.20	3	2.20	3
				2.11	1			2.11	1	2.11	2	2.10	4
				2.09	1			2.08	1	2.08	2		

(*a*) Glycerol Treated.
(*b*) Broad and Diffuse.
MB1 Halloysite.
MB2 Platy halloysite near top of deposit.
MB3 Clay-microbreccia
MB4 Metamorphosed shales capping "The Pimple."
MB5 Metamorphosed sandstones overlying the shales.
MB6 Slag.

of the fresh-water deposits of N.S.W., including the Permian (both Lower and Upper Coal Measures), Triassic (Narrabeen Group) and Jurassic. Though only a few of these occurrences have been examined in detail (Loughnan, 1958), it would appear that the significant features are (*a*) a high kaolinite or metahalloysite content, (*b*) coarse subangular quartz rarely in excess of 10%, (*c*) a relatively high titania content, and (*d*) remnant volcanic textures in some of the clay aggregates. A rock with

these characteristics could have resulted from the extensive leaching of an intermediate or basic tuff, a parent material which under non-leaching conditions would have yielded bentonite. Significant in this respect are the occurrences of bentonite in both the Permian and Jurassic freshwater sediments of N.S.W. (Loughnan and See, 1959). It is considered that the quartz represents contamination of the volcanic debris.

Closely related to the clay-microbreccias in occurrence and mineralogy are the chocolate shales of the Triassic and Jurassic of N.S.W. and probably these have had a somewhat similar origin.

Table 2. Chemical Data

	MB1	MB3	MB4	MB5	MB6	MB7	MB8
SiO_2	42.3	50.1	65.7	80.7	58.4	64.7	62.6
Al_2O_3	30.4	31.8	23.4	13.2	14.4	11.9	11.5
Fe_2O_3	2.3	0.7	5.8	1.4	15.7	3.9	3.6
FeO	0.1	0.6	0.3	0.1	6.4	1.5	2.2
TiO_2	1.7	2.1	1.4	0.5	—	0.6	0.5
CaO	0.0	0.1	0.2	1.4	0.5	8.6	10.7
MgO	0.1	0.1	0.1	0.3	1.7	2.4	3.6
Na_2O	0.0	0.6	0.2	0.2	0.3	0.1	0.1
K_2O	0.0	0.2	0.8	0.1	0.0	1.0	1.1
H_2O^+	11.5	12.0	2.1	0.7	0.3	2.1	1.9
H_2O^-	11.0	1.6	0.6	0.3	1.0	1.9	1.7
CO_2	0.0	—	0.1	0.2	—	0.9	0.2
P_2O_5	0.5	—	0.1	0.2	—	0.9	0.2
MnO	0.0	—	0.0	0.0	—	0.1	0.1
	99.9	99.9	100.8	99.3	98.7	100.6	100.0

MB1—Halloysite, MB3—Clay-microbreccia, MB4—Shale, MB5—Sandstone, MB6—Slag, MB7 and MB8—"picrite basalt."

Origin of the Intrusive Rocks

It was difficult to ascertain the relationship between the "picrite basalt" and the slag since in places each appears to have intruded the other. However, perhaps the most significant feature is that where the two are in contact, the "basalt" has been modified with much of its feldspar transformed to mullite whereas the slag is unaffected.

In the vicinity of the Savoy Trigonometrical Station, a few miles to the south of "The Pimple" and still within the Lower Coal Measures, Raggatt and Whitworth (1932) described analcite dolerite and syenite intrusions of sill-like character to which they assigned a Tertiary age. The analcite dolerite, which comprises the bulk of these extensive masses,

was correlated with the Older Basalts of N.S.W. and the syenite with the younger Alkaline Extrusives. Igneous rocks later than the Tertiary are unknown in the area.

In contrast to the above rock types, the "picrite basalt" (see chemical analyses, Table 2) is particularly calcic and notably deficient in the alkalies even after consideration is made for the high degree of silica contamination. Possibly the rock represents a particularly basic differentiate of the Tertiary intrusives or, alternatively, contamination by lime in addition to silica occurred, with a simultaneous release of alkalies to the country rock. In either case, the typical igneous texture of the rock indicates an essentially magmatic origin.

On the other hand, the slag closely resembles a furnace product and is dissimilar, in both composition and texture, to any igneous rock yet encountered. In a recent paper, Whitworth (1959) described similar slag like intrusions from the Upper Coal Measures in the vicinity of Liddell some ten miles or so in an east-south-east direction from "The Pimple," and reached the conclusion that the material represented highly-ferruginous sediments fused by burning coal seams *in situ*. Moreover, he considered that "the isolated outcrops of slag may be remnants (of a burnt out seam) left by the erosion of a large area, or may represent 'chimneys' or fissures through which flames and hot gases escaped from an underlying fire and about which intense heating was localized."

The occurrence of slags from the burning of coal seams *in situ* had been recorded previously from the Lower Coal Measures at Cessnock (David, 1907) and Muswellbrook Open Cut (Booker, 1953).

Detailed examination revealed no trace of a coal seam in the strata between the clay-microbreccia and the uppermost sandstones in the vicinity of "The Pimple." However, it was ascertained from bores put down in the area during the immediate post-war years that a considerable amount of the coal underlying "The Pimple" is cindered.

From a consideration of these points it would appear that:

(*a*) the slag was derived from the fusion of associated iron-rich sediments by burning of coal seams underground and has risen through vents and/or fissures to intrude the overlying sediments.

(*b*) the vents or fissures were created by the earlier intrusions of "basalt" which brecciated and intruded the shales preferentially.

(*c*) the shales and sandstones were intruded under low cover, as evidenced by the brecciation, and hence erosion in the area since the Late Tertiary has not been great.

(*d*) the "basalt" intrusions pre-dated the injection of the slag though the time interval probably was small (in fact it is possible that the "basalt" magma actually fired the coal).

(*e*) the metamorphic effects in the shales and sandstones were caused by the slag.

Origin of the Halloysite

To account for the origin of the halloysite, two factors must be considered: the parent material and the mechanism of formation.

With respect to the former, there can be little doubt that the clay-microbreccia comprised the parent material for not only does a close similarity in chemical composition and micro-texture exist between the two, but every gradation both lateral and vertical may be observed in the field.

On the other hand, the mechanism by which the kaolinite was converted to a fully-hydrated halloysite is problematical. According to Bates (1952), the kaolinite-halloysite transition can be achieved only after the destruction of the initial kaolinite structure and a water saturated atmosphere is necessary for the genesis of fully-hydrated halloysite. Though halloysite ($4H_2O$) readily loses water to form metahalloysite ($2H_2O$), the process is irreversible, at least at atmospheric temperatures and pressures.

Roy and Osborn (1952 and 1954), working with pressures up to 30,000 psi, were unable to synthesize halloysite from the system Al_2O_3-SiO_2-H_2O. However, from a study of the dehydration characteristics of this mineral, they concluded that the stability curve rises sharply with small increments of pressure to a temperature of 175° C. where the pressure is 5,000 psi. Beyond that temperature, irrespective of the pressure, halloysite is no longer stable.

As shown earlier, erosion in the vicinity of "The Pimple" since the Late Tertiary has been small, and hence the alteration of the clay-microbreccia to the halloysite was accomplished under low pressure, probably no more than 10 atmospheres. This would indicate a formation temperature for the halloysite of not much in excess of 100° C., insufficient to cause the break-down of the parent kaolinite structure and permit the development of tridymite and cristobalite in the upper portion of the halloysite deposit.

In consequence, it is considered that there were two stages in the kaolinite-halloysite transition:

(*a*) A period of thermal metamorphism during which a maximum temperature of 850°–900° C. was reached in the upper part of the deposit, facilitating the quartz inversion to tridymite and cristobalite but insufficient to cause the destruction of the metakaolinite structure. The lower extent of the halloysite corresponded to the 500° C. isotherm, beyond which dehydroxylation did not occur.

(*b*) A later, low-temperature period of hydrothermal activity, in which water, driven from the adjacent and underlying sediments as the burning section of the coal seam became more distant, permeated and reacted with the metakaolinite forming fully hydrated halloysite.

From the examination by infra-red absorption spectroscopy, of various metakaolins, preheated to 600°–850° C., Stubican found that those derived from well-crystallized kaolinite retained their initial atomic arrangement whereas poorly crystallized varieties readily rearranged to yield gamma-alumina in the gibbsite layers. Since it is doubtful that gamma-alumina or mullite, once formed, would recombine with silica and water to yield halloysite at a low temperature, it would follow that the development of the halloysite at "The Pimple" must have been considerably influenced by the high degree of crystallinity of the parent kaolinite. The failure of the tube-like form of halloysite to develop could be related to the retention of the initial kaolinite stacking of the layers.

Though the postulated origin appears the only one in accord with the data, it should be noted that Roy and Brindley (1956) studied the progressive rehydration of thermally decomposed members of the kaolin group, including kaolinite, disordered kaolinite, dickite, nacrite and halloysite, under varying conditions of time, temperature and water vapor pressure and were unable to synthesize halloysite from any of the products.

Acknowledgment

The authors are indebted to Mr. J. Pyle of the N.S.W. Dept. of Mines Laboratory for the majority of the chemical analyses.

References

Bates, T. F. (1952), Problems of clay and laterite genesis: *A.I.M.M.E.* (New York), 144–153.

Booker, F. W. (1953), Ph.D. Thesis, Sydney University (unpublished).

David, T. W. E., Sir. (1907), The geology of the Hunter River Coal Measures, N.S.W.: *Mem. Geol. Surv. N.S.W., No.* **4.**

Loughnan, F. C. (1958), Ph.D. Thesis, University of N.S.W. (unpublished).

Loughnan, F. C. and See, G. T. (1959), The bentonite and fuller's earth deposits of N.S.W., Pt. 1: *Aust. Inst. Min. Met.* No. 190, 85–104.

Raggatt, H. G. and Whitworth, H. F. (1932), Igneous rocks of the Muswellbrook-Singleton Area: *Roy. Soc. N.S.W.*, **66,** 194–232.

Roy, R. and Brindley, G. W. (1956), A study of the hydrothermal reconstitution of the kaolin minerals: *Clays and Clay Minerals, 4th Nat. Conf.* 125–132.

Roy, R. and Osborn, E. F. (1952), Problems of clay and laterite genesis: *A.I.M.M.E.* (New York) 76–80.

Roy, R. and Osborn, E. F. (1954), The system Al_2O_3-SiO_2-H_2O: *Am. Mineral.*, **39,** 853–885.

Stubican, V. (1959), Residual hydroxyl groups in the Metakaolin range: *Min. Mag.*, **32,** 38–52.

Whitworth, H. F. (1959), Some fused sedimentary rocks in the Ravensworth District, N.S.W.: *Roy. Soc. N.S.W.* (in press).

Manuscript received November 19, 1959.

THE AMERICAN MINERALOGIST, VOL. 45, JULY–AUGUST, 1960

THE MINERALOGY AND PETROLOGY OF A RODINGITE DIKE, HINDUBAGH, PAKISTAN

S. A. Bilgrami* and R. A. Howie, *Geology Department, The University, Manchester, England.*

Abstract

A rodingite dike is described from Pastoki, 15 miles south of Hindubagh, Pakistan, and chemical analyses are given of the serpentinite country rock as represented by a xenolith in the dike, of four specimens of rodingite, and of a typical unaltered dolerite dike and a peridotite of the area. The mineralogy of the rodingite includes the extensive development of calcium-rich minerals such as prehnite and hydrogrossular and the dike is traversed by numerous veins of xonotlite. Analyses and optical properties are given for hornblende, prehnite, sphene, chlorite (pycnochlorite), diopside, and xonotlite from the rodingite and for lizardite from the serpentinite xenolith. The chemistry and mineralogy of the rodingite indicate the introduction of calcium, carbon dioxide and water and the removal of sodium and potassium. The calcium-rich hydrothermal solutions involved may be related to the serpentinization of the peridotite country rocks.

Introduction

An area of about 90 square miles around Hindubagh, a small town 74 miles north-east of Quetta, in the former Baluchistan, Pakistan, has been mapped on a scale of 4 inches to a mile. The igneous complex of which the Hindubagh area forms a part occupies over 2000 square miles and consists of dunites, chromitites, serpentinites, harzburgites, and peridotites all cut by later dolerite dikes. It is proposed to discuss here the mineralogy and petrology of a rodingite or garnetized doleritic dike near Pastoki, about 300 yards north-east of hill 8083 which lies approximately 15 miles south of Hindubagh.

The term rodingite was first used by Marshall (1911) to describe certain dike rocks from Roding River, Dun Mountain area, Nelson, New Zealand, consisting of grossular, and diallage, and sometimes also prehnite. Since then the name rodingite has been applied to garnetized gabbros and dolerites by various authors. Grange (1927), Miles (1950), and Bloxam (1954) have described garnetized gabbros from different parts of the world applying the name rodingite to these rocks. It is in this extended sense that the term is here applied to a Hindubagh dike rock.

Field Occurrence (S.A.B.)

Only one dike of rodingite composition has been proved in the area but recent field work has yielded specimens from other dikes which suggests that in a few cases partial or incipient garnetization has occurred. The Pastoki rodingite dike is Y-shaped and varies in thickness from 14

* Present address, 196 P.I.B. Colony, Karachi 5, Pakistan.

to 19 feet. It has been intruded into serpentinite which here forms the country rock. Several varieties of the dike can be distinguished in the field. On the outermost margin the rock is fine-grained, buff-colored, and very tough: no minerals can be separately distinguished in hand specimen. Nearer the center of the dike the rock is white, speckled with green patches, though again no individual minerals can be recognized and the rock is remarkably compact. In places the marginal rock is pale green in color and is traversed by numerous veins of a white mineral, and inwards from this is a part of the dike consisting mainly of brown hornblende in a white or light green matrix. In some places this zone is represented by a dark chocolate-brown rock composed entirely of brown hornblende. In the core of the dike numerous xenoliths of serpentinite occur. All these rock types are traversed at varying intervals by veins of a very fine-grained white material which follow no definite direction. At several places patches of a dark colored medium-grained doleritic rock traversed by white veins occur: this, as far as can be judged, appears to represent the original dike rock which has escaped complete alteration

Petrography (S.A.B.)

Under the microscope the marginal rock is seen to be composed of a dense brown isotropic material showing good flow structure. It is traversed by veins of fibrous material which has been identified from its *x*-ray powder pattern as the hydrated calc-silicate xonotlite. Other marginal specimens show weak anisotropism and varying amounts of xonotlite veining. The latter veins pinch, swell and branch, and do not follow any definite pattern: their general appearance suggests a replacement origin. The xonotlite is colorless, and its cleavage is poor or absent. Under crossed polarizers it appears as sheaves and tufts with first-order gray polarization colors in radiating fibers. Detailed optical properties of the mineral together with a chemical analysis are given in Table 4.

In some sections of the marginal rock colorless grossular and xonotlite can be identified, but the bulk of the rock consists of dirty brown amorphous material. In some instances the xonotlite veins are as much as 1 cm. in thickness. Calcite is present in veins and patches and is considered to be a secondary mineral.

In the next zone brown hornblende in large crystals is the dominant mineral: crystals measuring up to $2\frac{1}{2}''$ by $2''$ are common. In hand specimens the hornblendes are black to chocolate-brown in color with an almost pearly lustre on cleavage faces. Under the microscope this hornblende is dark brown, strongly pleochroic, with 2V 81°, $\gamma = 1.671$ and $\gamma : c = 2°$. Faint zoning and single twins are observed in some crystals and the mineral is traversed by veins of prehnite. An analysis of this

hornblende is given in Table 3. The prehnite veins are very variable in thickness and the mineral also occurs as discrete patches in the rock (167). It is optically positive with 2V 68°, and γ 1.638: its chemical analysis also is given in Table 3. A small amount of almost colorless epidote is also present in aggregates of small crystals. Pale green chlorite is present in all the specimens, and varies in abundance from rare grains to being second in importance only to the brown hornblende.

The specimens from the Y junction of the dike show well-developed schistosity in thin section and are seen to be composed of pale green chlorite, euhedral sphene and colorless diopside (e.g. 177). The chlorite is in large anhedral crystals with prominent cleavage, distinct pleochroism from pale green to colorless, and brush polarization colors. It is mostly in clean grains, but where surrounded by sphene it has inclusions of minute needles of a brownish material throughout the crystal. The chlorite has $2V_\alpha$ 14°, γ 1.625. A chemical analysis is given in Table 2, as also is an analysis of the sphene from the same rock. The sphene is euhedral in form, brownish-pink in color and fairly strongly pleochroic from brownish-pink to very pale pink; $2V_\alpha$ is 39°. The crystals are often elongated and sub-parallel to each other giving a definite schistosity to the rock. The associated diopside is in clear or clouded crystals which are often bent or broken. An intricate intergrowth between diopside and chlorite is also observed, and inclusions of sphene in diopside are common. The diopside has $2V_\alpha$ 62°, γ 1.707, and $\gamma:c = 39°$.

The white vein rock is microcrystalline and microporphyritic in thin section, showing anhedral and rounded crystals of colorless diopside set in a matrix of dirty pale brown or colorless grossular. The diopside has a moderate 2V and $\gamma:c = 43°$: it shows a marked tendency to twinning, and simple twins are common. The garnet forms shapeless patches, and well developed crystals are not observed: in some sections the mineral is entirely clear, whereas in others it has a dirty brown appearance. It has not proved possible to separate an entirely pure sample for chemical analysis, but its cell edge of 11.920 Å indicates that it is hydrogrossular. In some thin sections of this rock a few grains of brown spinel occur which are associated with a dense brown alteration product appearing golden-brown in reflected light. A small amount of a brown serpentinous material is also present, and veins of pectolite and prehnite also occur.

The rock thought to be the nearest representative of the original doleritic dike rock is composed of almost colorless pyroxene in a matrix of green and brown serpentine, sericite, and leucoxene, penetrated by numerous veins of xonotlite.

The serpentinite xenoliths are olive-green and are very fine-grained, and sparse crystals of chromite can be recognized in a hand specimen. In

thin section the rock is seen to be composed of pale green serpentine traversed by numerous magnetite veins, probably developed as an alteration product of olivine: a small amount of chromite is also present, in anhedral grains. The pale green serpentine mineral appears to be optically positive in aggregate and an *x*-ray examination has shown it to be lizardite; chemical analyses of a serpentinite xenolith and of the lizardite are given in Tables 1 and 4.

Chemistry of the Rodingite (R.A.H.)

Four chemical analyses of the Hindubagh rodingite and an analysis of a serpentinite xenolith from the dike are given in Table 1, together with those of rodingites from other localities. The analysis of the type rodingite from Roding River (anal. B) shows higher alumina and lime and lower silica than any of the Hindubagh specimens though analyses 2, 3 and 5 show the same general trend, with relatively high CaO, low MgO and low SiO_2 unlike those of normal dike rocks of the area. An analysis of a typical normal dolerite of the area is also given (anal. 5), and analyses of five other Hindubagh dolerites show that in all of them CaO is around 10%. Thus the overall change in composition from a rock of doleritic composition to a rodingite can be seen to involve a considerable increase in calcium with a correspondingly proportional decrease in most of the other constituents except alumina, which remains approximately the same. The rock of analysis 4 has markedly different chemistry from the other rodingites and this is reflected in its very unusual mineral composition: it is composed almost entirely of chlorite, diopside, and sphene which account for its high water, magnesia and titania content. In general the analysis (D) of a prehnite-zoisite aggregate from a New Zealand gabbro shows close similarities with that of the marginal rock (anal. 5) whereas that of the rodingite from Ayrshire (anal. A) is comparable with the analysis for the altered doleritic rock from Hindubagh (anal. 2).

Chemical Mineralogy of the Rodingite (R.A.H.)

Seven minerals have been separated from the rocks of the Pastoki dike and purified by means of an isodynamic magnetic separator, followed by treatment with heavy liquids. The results of the chemical analyses of these minerals together with their optical and other properties are given in Tables 2, 3 and 4.

Analyses of diopside, sphene, and chlorite from the same rock (177) are given together with that of the rock itself in Table 2. The diopside is relatively low in the $FeSiO_3$ molecule, it is also low in Al_2O_3 and in the structural balance all the Al has been included with Si in the *Z* group. The sphene is seen to belong to the grothite variety, being relatively rich

TABLE 1. CHEMICAL ANALYSES OF THE HINDUBAGH RODINGITES AND ASSOCIATED ROCKS

	1	2	3	4	5	6	7	A	B	C	D
SiO_2	37.04	38.58	44.23	34.43	49.54	41.22	39.33	38.04	33.95	45.31	43.04
TiO_2	0.58	1.21	0.73	2.91	0.92	0.41	tr.	0.82	0.42	0.46	0.43
Al_2O_3	15.15	17.81	14.02	12.37	15.61	4.47	1.31	15.07	19.91	7.49	15.61
Fe_2O_3	1.81	1.41	1.14	2.76	4.93	4.58	5.65	1.78	1.28	1.02	0.67
FeO	6.98	5.64	6.48	9.67	8.12	5.62	1.31	3.02	6.98	5.12	4.99
MnO	0.13	0.11	0.14	0.10	0:09	0.05	0.08	0.21	0.28	0.31	0.32
MgO	6.70	8.28	7.47	18.96	5.79	34.69	38.46	9.62	5.23	14.66	9.14
CaO	27.35	19.75	16.67	10.91	9.65	2.84	0.04	25.84	26.95	22.70	19.99
Na_2O	0.18	1.17	2.43	0.06	2.32	0.32	0.01	0.18	0.15	0.04	0.17
K_2O	0.02	0.06	0.04	0.00	0.54	tr.	tr.	0.04		0.04	0.00
H_2O^+	4.04	5.39	3.75	7.57	2.56	5.47	12.39	4.19	4.85	2.65	4.70
H_2O^-	0.21	0.19	0.21	0.13	0.04	0.32	0.93	1.15		0.24	0.45
Cr_2O_3	—	—	—	—	—	0.10	0.41	—	0.00	0.26	0.00
P_2O_5	0.09	0.02	0.11	0.05	0.17	0.11	0.02	0.24	0.00	0.08	0.00
CO_2	—	0.28	2.69	0.28	—	—	—	nil	—	0.06	0.20
Total	100.28	99.90	100.11	100.20	100.28	100.20	99.94	100.20	100.00	100.47	99.76

Analyst: 1, 2, 3, 4 & 7 R. A. Howie; 5 & 6 S. A. Bilgrami.

1. Fine-grained rodingite (20),* Pastoki.
2. Brown hornblende-prehnite rock (167), Pastoki.
3. Fine-grained rodingite (173), Pastoki.
4. Chlorite-diopside-sphene rock (177), Pastoki.
5. Normal dolerite of the Hindubagh area.
6. Typical peridotite of the Hindubagh area.
7. Serpentinite xenolith in rodingite dyke (170), Pastoki.

* Numbers in parentheses refer to collection in Department of Geology, University of Manchester.

A. Rodingite, Byne Hill, Ayrshire, Scotland (Bloxam, 1954). Anal.: W. H. Herdsman.

B. Rodingite, Roding River, Nelson, New Zealand (Marshall, 1911).

C. Garnetized gabbro, Eulaminna, Western Australia (Miles, 1950). Anal.: J. D. Hayton (also includes NiO 0.03).

D. Prehnite-zoisite aggregate in altered gabbro, Macquarie Island, New Zealand (Grange, 1927). Anal.: F. T. Seelye (also includes NiO 0.04, S 0.01%).

TABLE 2. CHEMICAL ANALYSES, STRUCTURAL FORMULA AND OPTICAL PROPERTIES OF DIOPSIDE, SPHENE, AND CHLORITE FROM ROCK 177, PASTOKI, HINDUBAGH

	1	2	3	4		1A		2A		3A	
SiO_2	53.20	28.45	28.32	34.43	Si	1.955	1.99	1.850	2.00	1.415	2.00
TiO_2	0.12	36.30	0.09	2.91	Al	.032		.150		.585	
Al_2O_3	0.75	3.14	19.03	12.37	Al	—		.091		.530	
Fe_2O_3	0.76	2.70	1.19	2.76	Fe^{+3}	.021		.132		.048	
FeO	2.92	0.70	14.85	9.67	Mg	.948		.072	2.11	1.769	
MnO	0.21	0.03	0.09	0.10	Ti	.003		1.775		.003	
MgO	17.32	0.75	23.72	18.96	Fe^{+2}	.088	2.03	.038		.621	3.01
CaO	24.41	27.20	0.62	10.91	Mn	.007		.002		.003	
Na_2O	0.07	0.02	0.01	0.06	Na	.003		.002	1.91	—	
K_2O	tr.	0.07	0.00	tr.	Ca	.959		1.895		.033	
P_2O_5	—	—	—	0.05	K	—		.006		—	
CO_2	—	—	—	0.28	OH	—		.360		3.985	
H_2O^+	0.05	0.83	11.95	7.57							
H_2O^-	0.06	0.03	0.06	0.13							
Total	99.87	100.22	99.93	100.20							
α	1.680	—	1.620								
β	1.693	—	1.621								
γ	1.707	—	1.625								
2V	62°	39°	14°								
$\gamma:c$	39°	—	—								
Sp. Gr.	3.266	3.488	2.82								

Analyst: R. A. Howie.

1. Pale greenish white diopside (atomic % Ca 47.4, Mg 47.0, Fe 5.6).
   1A. Number of ions on the basis of 6 (O).
2. Brown sphene (grothite). Analysis also includes F nil.
   2A. Numbers of ions on the basis of 10 (O, OH).
3. Green chlorite (pycnochlorite), Fe total/Fe+Mg=0.273.
   3A. Numbers of ions on the basis of 9 (O, OH).
4. Rock (quoted from Table 1).

Table 3. Chemical Analyses, Structural Formulas and Properties of Hornblende and Prehnite from Rock 167, Pastoki, Hindubagh

	1	2	3		1A		2A	
SiO_2	42.28	42.86	38.58	Si	6.162	8.00	5.930	6.00
TiO_2	2.36	0.01	1.21	Al	1.838		.070	
Al_2O_3	12.46	24.41	17.81	Al	.304		3.900	
Fe_2O_3	2.42	0.52	1.41	Fe^{+3}	.262		.050	
FeO	9.48	0.28	5.64	Mg	3.113	5.09	.006	3.99
MnO	0.15	0.06	0.11	Ti	.258		.001	
MgO	14.38	0.03	8.28	Fe^{+2}	1.154		.033	
CaO	12.01	26.89	19.75	Mn	.017		.008	
Na_2O	2.14	0.32	1.17	Na	.594	2.52	.081	4.06
K_2O	0.20	0.01	0.06	Ca	1.871		3.973	
H_2O^+	2.21	4.45	5.39	K	.034		.002	
H_2O^-	0.04	0.08	0.19	OH	2.150		4.096	
P_2O_5	—	—	0.02					
CO_2	—	—	0.28					
Total	100.13	99.92	99.90					
α	1.650	1.613						
β	1.664	1.624						
γ	1.671	1.638						
2V	81°	68°						
$\gamma:c$	2°	—						
Sp. gr.	3.153	2.936						

Analyst: R. A. Howie.

1. Chocolate-brown hornblende.
   1A. Numbers of ions on the basis of 24 (O, OH).
2. White prehnite.
   2A. Numbers of ions on the basis of 24 (O, OH).
3. Rock (quoted from Table 1).

in both Al_2O_3 and Fe_2O_3. It has been recalculated on the basis of 10(O, OH, F) and again considerable Al has to be included in the Z group: the Fe^{+3} probably replaces some Ti. Although the rock contains 18.96% MgO, the sphene has only 0.75%, probably indicating that the Mg ion does not readily substitute for tetravalent Ti of similar ionic radius, and is equally out of place in any possible replacement of the considerably larger Ca ion in this structure. In view of the substitution reported in many sphenes of appreciable F for OH, F was looked for spectrographically, but this element, if present, was below the level of sensitivity (100 p.p.m.). The co-existing chlorite occurs in fairly large pale green crystals and shows the typical anomalous interference colors. Its analysis shows

it to be fairly rich in Mg and Al, and following the classification of Hey (1954) it may be termed a pycnochlorite, with Fe (total):(Fe+Mg) =0.273 and Si 2.83, on the basis of 14 oxygens (anhydrous): the basal spacing $d_{100}=14.22$ Å. No comparable analyses have been found in the literature, those given by Wiseman (1934) and Macgregor (1941) being considerably richer in Al and Fe^{+2}.

The rather coarse-grained dike rock (167), with chocolate-brown hornblende crystals 1 inch or more in length in the hand specimen, has also been studied mineralogically. The analysis of this hornblende is given in Table 3 together with that of its associated prehnite and of the rock itself. The hornblende is relatively rich in magnesium and its calcium content is slightly higher than that of many hornblendes, in line with the overall high calcium content of the rodingites. The prehnite although essentially colorless contains small amounts of both ferrous and ferric iron, and a minor amount of sodium substitutes for calcium. The structural formula approximates closely to the theoretical $Ca_4Al_4Si_6O_{20}(OH)_4$ and

Table 4. Chemical Analyses, Structural Formulae and Properties of Xonotlite and Lizardite

	1	2		1A		2A	
SiO_2	49.53	41.42	Si	4.964	5.00	3.895	3.98
TiO_2	0.01	tr.	Al	.036		.083	
Al_2O_3	0.75	0.74	Al	.052		—	
Fe_2O_3	0.47	3.62	Fe^{+3}	.034		.259	
FeO	0.12	1.12	Mg	.003		5.614	
MnO	0.03	0.08	Fe^{+2}	.010	5.09	.088	5.97
MgO	0.02	40.12	Mn	.004		.006	
CaO	46.48	tr.	Na	.005		—	
Na_2O	0.04	nil	Ca	4.980		—	
K_2O	nil	nil	OH	1.787		7.988	
H_2O^+	2.68	12.74					
H_2O^-	0.04	0.32					
Total	100.17	100.16					
α	1.582	1.568					
β	—	1.569					
γ	1.592	1.581					
Sp. gr.	2.710	2.581					

Analyst: R. A. Howie.

1. White to flesh-pink, fibrous xonotlite, veins in rodingite, Pastoki, Hindubagh.
   1A. Numbers of ions on the basis of 16 (O, OH).
2. Green, fine-grained lizardite, serpentinite xenolith in rodingite, Pastoki, Hindubagh.
   2A. Numbers of ions on the basis of 18 (O, OH).

optical properties are not far removed from those for pure prehnite. This rock also contains fine-grained turbid material in the groundmass which is isotropic or weakly anistropic. It has not proved possible to separate a completely pure fraction for analysis, but the mineral grains are yellowish-white and give the x-ray powder pattern of garnet, with $a = 11.920 \pm 0.005$ Å. It is thus tentatively identified as hydrogrossular, a mineral first recognized in rodingite from the type area in New Zealand (Hutton, 1943).

Xonotlite occurs as veins and stringers of varying thickness throughout the rodingite itself. In hand specimen the mineral is chalky-white to light flesh-pink in color and forms a close, compact, extremely tough fibrous mass. Under the microscope it is seen as a mesh of fibers giving straight extinction and fairly low polarization colors. Its analysis is given in Table 4, where it has been recalculated on the basis of 16 (O, OH) to the formula $5CaSiO_3 \cdot H_2O$. If the infra-red absorption spectra (Kalousek and Roy, 1957) are interpreted as indicating unbonded hydroxyl groups this should perhaps be written as $Ca_5Si_5O_{14}(OH)_2$. Various formulas have been assigned to this mineral particularly with respect to the ratio of calcium silicate to water: Berman (1937) considered it to be close to $3CaSiO_3 \cdot H_2O$, Taylor (1954) gave the formula as $5CaSiO_3 \cdot H_2O$, while Mamedov and Belov (1955) on structural grounds preferred the formula $Ca_6Si_6O_{17}(OH)_2$. The analysis of the Hindubagh xonotlite confirms the 1:1 ratio of Si:Ca and shows relatively small amounts of other cations replacing these. The (OH) group at 1.787 is slightly less than the theoretical 2.0 but shows evidence that the older formula of $3CaSiO_3 \cdot H_2O$ had considerably too much water. A detailed investigation of xonotlites from other localities is now being carried out particularly with regard to their water content: most of the new analyses report H_2O+ around 2.65 to 2.85% which would indicate a formula approaching $11CaSiO_3 \cdot 2H_2O$. Although it might be expected that, like wollastonite, xonotlite may contain appreciable iron replacing calcium, for the Hindubagh xonotlite the iron content is low.

The serpentine mineral in the xenotlith of serpentinite occurring in the center of the dike has been separated and its analysis is given in Table 4. The x-ray powder diffraction pattern of this serpentine showed it to have the single-layer orthohexagonal structure of the lizardite serpentine subgroup (Whittaker and Zussman, 1956), and some details of this Hindubagh specimen were given in the original description of the mineral lizardite (Whittaker and Zussman, 1956, p. 118, and p. 125, No. 18). The analysis shows that the mineral is fairly close to the ideal formula $Mg_6Si_4O_{10}(OH)_8$, but with an appreciable amount of both ferric and ferrous iron. That this iron is present in the structure of the mineral, prob-

ably replacing magnesium, is indicated both by the lack of any visible grains of magnetite or other ore in the analyzed specimen and also by the slight increase in the refractive indices of this material above those for pure $Mg_6Si_4O_{20}(OH)_8$.

Petrogenesis

Various hypotheses have been advanced for the origin of rodingites. Marshall (1911) considered that the grossular-bearing rocks originally described from Roding River resulted from magmatic differentiation. Benson (1926), Grange (1927) and Turner (1934) suggested that the rodingites have been formed by the garnetization of gabbroic rocks by concentrated magmatic waters acting at high pressures, whereas Arshinov and Merenkov (1930) demonstrated that garnet-pyroxene, garnet-chlorite and garnet-vesuvianite dikes had been formed by the garnetization of micro-diorite and the alteration of pyroxenite schlieren by calcium metasilicate solutions, liberated in the process of serpentinization. Miles (1951) has described dike-like outcrops of garnetized gabbro from the Eulamina district, Western Australia, and concluded that they were garnetized by hot solutions also responsible for the serpentinization of the surrounding peridotite. The breakdown of monoclinic pyroxene and calcic plagioclase feldspars is assumed to have supplied the calcium required for the formation of grossular and other lime-bearing silicates. Bloxam (1954) has suggested that the rodingites of the Girvan-Ballantrae complex, Ayrshire, were formed by lime-rich hydrothermal solutions and CO_2 which immediately post-dated serpentinization, and which were responsible for the alteration of the gabbro to rodingite and also produced local carbonatization of the serpentinite.

In all the occurrences of rodingites and garnetized gabbros whose descriptions are known to the present authors two facts are pre-eminent. Firstly the occurrence of these rocks typically as dike-like bodies apparently of original gabbroic or doleritic composition; and secondly the association in the area, either immediately adjacent to the rodingite or within a short distance of its outcrop of an ultrabasic peridotite or serpentinite mass (e.g. Graham, 1917; Grange, 1927; Turner, 1930; Arshinov and Merenkov, 1930; Watson, 1942, 1953; Miles, 1951; Bloxam, 1954). It must thus be considered probable that the ultrabasic rocks are in some way related to these altered basic rocks, and, as has been noted above, Grange (1927) and Arshinov and Merenkov (1930) suggested that the breakdown of pyroxene in the serpentinization process could have yielded the necessary calcium involved in the metasomatism of the dolerite or gabbro. Although Bloxam (1954) considered this hypothesis, in the Girvan-Ballantrae district the ultrabasics are dominantly harz-

burgites (olivine and bronzite) and are unlikely to have yielded much calcium. In the Hindubagh area at present under consideration, however, the ultrabasic rocks include both peridotites and hornblende-peridotites. An analysis of a typical peridotite of the area is given in Table 1 (anal. 6) showing it to contain 2.84% CaO while the hornblende-peridotite although less abundant in the area has up to 7.7% CaO. In contrast the serpentinite xenolith in the rodingite has only 0.04% CaO. The probability of serpentinization having occurred after the intrusion of the dike is demonstrated by the fact that elsewhere in the area dikes cut through fresh peridotite and there is no development of rodingites at such contacts. It therefore seems not unreasonable to suggest that the serpentinization of the peridotites of the Pastoki, Hindubagh, area could have brought about the breakdown of the pyroxene (and the small amounts of calcic plagioclase sometimes present) releasing calcium in a reaction of the general form:

$$3CaMgSi_2O_6+2H_2O\rightarrow Mg_3Si_2O_5(OH)_4+3CaO+4SiO_2$$

This CaO then being added to the dolerite body by percolating hydrothermal solutions rich in CO_2, giving rise to new calcium aluminum silicates and minor calcite, the aluminum coming from the original plagioclase of the dolerite.

Acknowledgments

The authors are indebted to Prof. D. S. Coombs, of Otago University, for providing a specimen of rodingite from the type area, and to Dr. J. Zussman for *x*-ray work on the lizardite (serpentine) mineral. Part of this work was done by one of the authors (S.A.B.) in part fulfilment of Ph.D. requirements and he is indebted to Prof. W. A. Deer for encouragement and advice and to the University of Manchester for a Research Studentship.

Two papers have been published recently dealing with an occurrence of grossular-chlorite-vesuvianite rodingite in the ultrabasic complex of Anderson's Creek, Beaconsfield district, northern Tasmania. Baker (1958) concludes that the rodingite was derived from hornblende gabbro by a process of lime metasomatism which antedated the intrusion of serpentine, whereas Green (1959) considers that the dike-like gabbros were intruded into the ultrabasic rocks before the latter were serpentinized.

References

Arshinov, V. V. and Merenkov, B. J. (1930), Petrology of the chrysotile asbestos deposits of the Krasnouralky Mine in the Ural Mountains: *Trans. Inst. Econ. Miner.*, No. **45**, Moscow.

Baker, G. (1958), Rodingite in nickeliferous serpentinite, near Beaconsfield, northern Tasmania. *Journ. Geol. Soc. Australia*, **6**, 21–35.

Benson, W. N. (1926), The tectonic conditions acompanying the intrusion of basic and ultrabasic igneous rocks: *Mem. Nat. Acad. Sci., Washington*, **19**, No. 1.

Berman, H. (1937), Constitution and classification of the natural silicates: *Am. Mineral.*, **22**, 342–408.

Bloxam, T. W. (1954), Rodingite from the Girvan-Ballantrae Complex, Ayrshire: *Mineralog. Mag.*, **30**, 525–528.

Graham, R. P. D. (1917), Origin of massive serpentine and chrysotile-asbestos, Black Lake-Thetford area, Quebec: *Econ. Geol.*, **12**, 154–202.

Grange, L. I. (1927), On the "rodingite" of Nelson: *Trans. New Zealand Inst.*, **58**, 160–166.

Green, D. H. (1959), Geology of the Beaconsfield district, including the Anderson's Creek ultrabasic complex. *Rec. Queen Victoria Mus., Launceston (Tasmania)*, New Ser., No. 10.

Hey, M. H. (1954), A new review of the chlorites: *Mineralog. Mag.*, **30**, 277–292.

Hutton, C. O. (1943), Hydrogrossular, a new mineral of the garnet-hydrogarnet series: *Trans. Roy. Soc. New Zealand*, **73**, 174–180.

Kalousek, G. L. and Roy, Rustum (1957), Crystal chemistry of hydrous calcium silicates: II, characterization of interlayer water: *Journ. Amer. Ceram. Soc.*, **40**, 236–239.

Macgregor, A. M. (1941), Native gold and silver with other minerals from the Old West mine, Penhalonga, Southern Rhodesia: *Mineralog. Mag.*, **26**, 97–104.

Mamedov, Kh. S. and Belov, N. V. (1955), The crystalline structure of xonotlite: *Doklady Acad. Sci. USSR*, **104**, 615–618.

Marshall, P. (1911), The geology of the Dun Mountain subdivision, Nelson: *New Zealand Geol. Surv.*, Bull. **12**, 31–35.

Miles, K. R. (1951), Garnetised gabbros from the Eulamina district, Mt. Margaret Goldfield: *Geol. Surv. Western Australia*, Bull. **103**, part 2.

Taylor, H. F. W. (1954), The identity of jurapaite and xonotlite: *Mineralog. Mag.*, **30**, 338–341.

Turner, F. J. (1934), The metamorphic and intrusive rocks of southern Westland; *Trans. New Zealand Inst.*, **63**, 178–284.

Watson, K. P. (1942), Zoisite-prehnite alteration of gabbro: *Am. Mineral.*, **27**, 638–645.

——— (1953), Prehnitization of albite: *Am. Mineral.*, **38**, 197–206.

Whittaker, E. J. W. and Zussman, J. (1956), The characterization of serpentine minerals by *x*-ray diffraction: *Mineralog. Mag.*, **31**, 107–126.

Wiseman, J. D. H. (1934), The central and south-west Highland epidiorites: a study in progressive metamorphism: *Quart. Journ. Geol. Soc. London*, **90**, 354–417.

Manuscript received September 5, 1959.

THE AMERICAN MINERALOGIST, VOL. 45, JULY–AUGUST, 1960

SECOND OCCURRENCE OF TODOROKITE

A. A. Levinson, *The Dow Chemical Company, Freeport, Texas.*

Abstract

Todorokite, a hydrated manganese oxide mineral previously reported only from Japan, is described from an occurrence in Cuba. A chemical analysis, *x*-ray powder spacings, data on various physical properties and occurrence are presented and compared with those of the type todorokite from Japan.

Introduction

During the course of a routine mineralogical study of approximately twenty commercially available manganese ores from various parts of the world, as expected, many different mineral species were encountered. The "manganese ores," as they were designated, were found by *x*-ray diffraction to contain pyrolusite, ramsdellite, braunite, cryptomelane, hausmannite, psilomelane, psilomelane-like minerals, lithiophorite (from South Africa) and todorokite from a Cuban locality. Inasmuch as todorokite has only been reported from the type locality at the Todoroki Mine, Hokkaido, Japan (Yoshimura, 1934), a description is presented of this second occurrence.

The todorokite was first identified as the only manganese mineral in a shipment of ten pounds of "manganese ore" from E. J. Lavino and Company, Philadelphia, Pennsylvania. A second shipment of 500 pounds of what was supposed to be identical ore turned out to be predominantly todorokite with small amounts of pyrolusite.

Representative samples of Cuban todorokite have been deposited with the Smithsonian Institution, U. S. National Museum, Washington, D. C., where they have been given the numbers 113966 and 113967.

Montenegro Mine—Location, Description, Mineralization

The todorokite described in this paper is found at the Montenegro Mine which is located on the northern flank of the Sierra Maestre Mountains twenty kilometers south of Baire, Oriente Province, Cuba. Manganese mineralization at the Montenegro Mine is apparently typical of that in the region. The geology of the area and a description of the Montenegro Mine may be found in Simons and Straczek (1958).

Mr. F. R. Dykstra of the E. J. Lavino Company, from whom the ore was obtained, has supplied the writer with details of the locality, geology and mineralization. His observations and conclusions, which are similar to those of Simons and Straczek (1958), are quoted below:

"Mineralization is confined to the contact between the massive Charco Redondo limestone and underlying volcanic tuffs. The contact is well defined by fault breccia and gouge.

Mineralization is unquestionably related to this interformational movement and to the minor accessory faults in both the limestone and tuff members. This is indicated by the fact that the major ore bodies are typically found at fault intersections.

Unlike most manganese deposits, these would seem to be secondary in nature with the manganese derived from some unknown source but probably related to the regional volcanics. The fact that the most extensive degree of mineralization is found down dip indicates emplacement by ascending solutions.

The mineralized fault zone outcrops at the toe of prominent cliffs formed by the limestone. At the surface the contact dips at about 15° steepening to nearly vertical within four or five hundred feet down dip. Mining has so far proceeded no deeper than six hundred feet down dip. On the up dip extension of the mineralization, the ore bodies tended to be relatively thin, rarely exceeding four or five feet. A good deal of disseminated manganese in the breccia and in the tuff is found here. At depth the ore bodies become much more massive frequently reaching a width of three or four meters. Lateral extension of ore is haphazard particularly up dip where the ore frequently pinches out all together. Down dip this pinching is much less evident and the individual ore bodies are proportionately larger.

In appearance the ore in places varies from a massive kidney form, although relatively soft ore, to a brown ore with a rather unusual fibrous texture."

The todorokite from Cuba is found in an entirely different geological setting from the Japanese material and is of different origin. The Cuban todorokite appears to be a fissure or breccia filling of hypogene origin. Yoshimura (1934) reported todorokite at the type locality to be a hydrothermal alteration product of inesite. Other minerals found in the Todoroki Mine (Syûetu vein) include quartz, rhodochrosite, pyrite, sphalerite and galena as well as several alteration products. The Todoroki Mine consists of workings on gold-bearing quartz veins in Tertiary volcanics.

Physical and Optical Properties of Cuban Todorokite

The todorokite is black with earthy to submetallic luster. It is found predominantly in massive form but fibrous aggregates are abundant and botryoidal structures are occasionally observed. All types may be porous but particularly the massive variety which disintegrates with evolution of air bubbles when placed in water. The mineral is readily soluble in warm concentrated HCl.

Todorokite is soft ($H = 1\frac{1}{2}$ to $2\frac{1}{2}$) and soils the fingers. The hardness will vary slightly with the fibrous aggregates apparently slightly harder.

As far as could be determined, the Cuban todorokite is opaque in crushed fragments. This is distinctly different from the Japanese material which Yoshimura (1934) found to be transparent, pleochroic, show extinction, etc., and on which he was able to measure some optical properties. However, he does report the mineral to be black with metallic luster.

On the bulk sample the specific gravity was measured twice by the pycnometer using n-heptane and found to be 3.24 at 25° C. When this value is corrected for 12.1 per cent $CaCO_3$ and 5.7 per cent acid (HCl) insolubles, assuming an arbitrary average specific gravity of 2.7, the corrected specific gravity of Cuban todorokite is approximately 3.36 which is considerably lower than the 3.67 at 15° C. reported by Yoshimura (1934). Because of the impurities, the value of 3.36 for Cuban todorokite can be considered no more than an order of magnitude.

A polished section was made in an attempt to study todorokite in reflected light. Because the material did not polish well, only a poor section was obtained. Nevertheless, it could be determined that the color in reflected light is various shades of dark gray.

Table I. *X*-Ray Powder Spacing Data for Cuban Todorokite

d(Å)	I	*d*(Å)	I
9.6	10	2.16	1
7.1	½	2.04	½
4.77	8	1.98	2
4.45	2 broad	1.74	2
4.2		1.68	½ broad
3.19	2	1.64	
2.46	3	1.53	2
2.40	5	1.42	5
2.35	3 broad	1.38	2
2.22	4		

Fe radiation, Mn filter. Composite pattern from several films obtained on camera of 143.2 mm. diameter and also from several Norelco spectrometer scans.

X-ray Diffraction

The todorokite from Cuba was first identified by its *x*-ray diffraction pattern the *d*-spacings of which are presented in Table I. The spacings compare favorably with those reported by both Frondel (1953) and Ramdohr (1956) for Japanese todorokite. (These previously published powder *x*-ray spacings show slight variations for presumably identical material.) Good *x*-ray patterns were obtained from examples of the fibrous, botryoidal, and massive types. However, some specimens gave diffuse patterns indicating differences in perfection of crystallization in Cuban todorokite.

The first spacing reported in Table 1 showed some variation from specimen to specimen ranging from 9.50 Å to 9.65 Å. The reflection at 7.1 Å was found on two patterns only and may conceivably represent an

impurity, possibly kaolinite from the alteration of the acid insolubles most of which are orthoclase and quartz. Frondel (1953) reports a very weak line for Japanese todorokite at 7.2 Å whereas Ramdohr (1956) does not. Another possibility could be birnessite (delta-MnO_2) which Jones and Milne (1956) found has its strongest line in the range 6.9 Å–7.4 Å.

In addition to calcite, orthoclase and quartz, a very small amount of magnetite may possibly be present in the first (chemically analyzed) todorokite sample. In the second shipment of 500 pounds, pyrolusite and and goethite were identified as additional impurities.

Cuban todorokite was heated at several temperatures in air for an hour and then studied by *x*-ray diffraction. It was found that at approximately 550° C. todorokite inverts to a phase which gives an *x*-ray powder pattern identical to hausmannite. Worthy of note is the fact that hausmannite typically occurs in high-temperature veins.

Little can be said about the crystal structure of todorokite. Yoshimura (1934) suggested monoclinic symmetry on the basis of morphology. Wadsley (1950) has indexed various synthetic hydrated manganese materials on the basis of a hexagonal cell; some of these synthetic materials have *x*-ray spacings and intensities very similar to those of todorokite. Unfortunately, it has been found that even fine fibers of Cuban todorokite are aggregates, and are not amenable to single crystal *x*-ray diffraction studies.

Chemical analysis

A chemical analysis of the Cuban todorokite is presented in Table II along with the analysis of the type Japanese material. The composition of the todorokite has been recalculated from an analysis of a bulk ore sample (dried at 110° C.) containing 12.1 per cent calcite and 5.7 per cent insolubles from HCl leach; the insolubles are chiefly potash feldspar (orthoclase) and quartz. No pyrolusite was detected on *x*-ray powder patterns of long exposure. Calcium, strontium, barium and magnesium were determined by the emission spectrograph. Mr. J. A. Greear, the wet analyst, has indicated that the H_2O figure may be slightly inaccurate owing to the hydroscopic nature of the todorokite. Furthermore, there seems to be evidence that composition of the todorokite from this Cuban locality is slightly variable.

The original analysis by Yoshimura (1934) reported total Mn as MnO (65.89%) and oxygen (12.07%). The actual valence is not known and the analysis given in Table II reports Mn and O recalculated as MnO and MnO_2 using the figures of Frondel (1953). The weight per cent of the manganese oxides reported in the analysis of Cuban todorokite are calculated in a similar manner.

TABLE II. CHEMICAL ANALYSES OF TODOROKITE

	1. Japan (Yoshimura, 1934)	2. Cuba
Na_2O	0.21	1.3
K_2O	0.54	0.7
CaO	3.28	0.4
BaO	2.05	0.9
SrO	—	1.2
MgO	1.01	2.7
CuO	—	0.5
MnO	12.38	9.2
MnO_2	65.58	70.6
Fe_2O_3	0.20	2.2
Al_2O_3	0.28	1.2
H_2O^+	9.72	8.2
H_2O^-	1.56	Not determined
P_2O_5	0.42	0.2
SiO_2	0.45	Not determined
SO_3	0.28	Not detected
Insol.	1.28	—
	99.24	99.3

Notes on analysis of Cuban todorokite:

1. Wet analyst: J. A. Greear.
2. Emission spectrograph analyst: H. Holt; determined Ca, Ba, Sr, Mg.
3. Material dried at 110° C. before analysis. H_2O^- not determined by J. A. Greear. Another analyst on another portion determined $H_2O^- = 1.58$ per cent.
4. Analysis recalculated on basis of 5.7% HCl insolubles and 12.1% $CaCO_3$.

The ratios of the analysis of the Cuban todorokite are close to the formula:

$$(Mn^2, Na, K, Mg, Ba, Sr, Ca, Cu)\ (Mn^4, Fe, Al)_3O_7 \cdot 2H_2O$$

if the H_2O- (see Note 3, Table II) is included as being essential. Frondel (1953) has shown that the Japanese todorokite has ratios that are between the above formula and $(Mn^2, \text{etc.})_2Mn^4{}_5O_{12} \cdot 4H_2O$. Inasmuch as no other manganese oxide or mineral could be detected in the analyzed material, the high MnO_2 value for Cuban todorokite must be used in the calculation although it is likely that 4–5 per cent of many manganese minerals would not be detected by x-ray techniques.

Frondel (1953) has posed the question of whether or not woodruffite and todorokite are isostructural. On the basis of this new analysis it would appear that they are not. However, because of the uncertainties mentioned above, the problem cannot be unquestionably resolved on the basis of the new analysis.

Acknowledgment

Mr. F. R. Dykstra, Assistant Vice-President, E. J. Lavino and Company, kindly supplied the writer with information on the occurrence of the todorokite and also gave permission to publish. His assistance and cooperation are greatly appreciated.

References

Frondel, C. (1953), New manganese oxides: hydrohausmannite and woodruffite: *Am. Mineral.*, **38,** 761–769.

Jones, L. H. P. and Milne, A. A. (1956), Birnessite, a new manganese oxide mineral from Aberdeenshire, Scotland: *Min. Mag.*, **31,** 283–288.

Ramdohr, P. (1956), Die Manganerze: Symposium sobre yacimientos de manganeso. *Tomo I. XX Internat. Geol. Congress, Mexico,* 19–73.

Simons, F. A. and Straczek, J. A. (1958), Geology of the manganese deposits of Cuba: *U. S. Geol. Survey, Bull.* **1057.**

Wadsley, A. D. (1950), Synthesis of some hydrated manganese minerals: *Am. Mineral.*, **35,** 485–499.

Yoshimura, T. (1934), "Todorokite," a new manganese mineral from the Todoroki Mine, Hokkaido, Japan: *Journ. Fac. Sci. Hokkaido University, Ser. 4,* **2,** 289–297.

Manuscript received October 11, 1959.

TRACE ELEMENTS IN KYANITE, SILLIMANITE AND ANDALUSITE

G. R. Pearson* and D. M. Shaw.†

Abstract

12 Kyanites, 3 sillimanites and 7 andalusites were analysed spectrographically for various minor and trace-elements. Ga, Cr, Mg, Ti, Li, Cu, V, Zr and Mn could be measured in most samples; B, Be and Ba were found in several; Ni, Co, Mo, Sn, Ag, Y, Sc, Sr and Pb were usually below detection limit. No indisputable differences in trace-element contents were found, but andalusite probably contains less Cr, whereas B, Be and Ba may be concentrated in sillimanite. It is unlikely that trace elements are factors in the polymorphic relations between these minerals.

The trace element distribution in aluminum silicates can in general be explained by crystal chemical considerations, but V is rather more abundant than might be expected. Li and B are unexpectedly rich in many samples, suggesting origin under pneumatolytic or greisen conditions: both Li and B could however have come from the parent sediments.

One of each of the minerals was analysed chemically. Slight deficiencies of Al with respect to Si can be explained by substitution of minor and trace-elements for Al. Alkali metals are present in small amounts but Jakob's hypothesis that they are essential constituents is untenable.

Introduction

The polymorphic minerals kyanite, sillimanite and andalusite present a problem in the interpretation of their stability-fields and the bearing this has on general questions of metamorphism. All three have been synthesised during the last few years but much remains to be learned of their manner of formation. It appeared worth while to examine their content of some minor and trace-elements, to enquire whether there might be any systematic differences of crystal chemical significance.

Samples

The samples are listed in Table 1: precise localities were not available for many. In two cases the specimens were visibly pure gem-quality crystals, but most of the other samples were coarse-grained aggregates, rich in the principal mineral but containing abundant impurities. In several at least two of the aluminum silicates were present.

Hand-specimens were crushed and sieved, retaining the fraction between 100 and 200-mesh stainless steel sieves. Magnetic and heavy liquid separation followed. The greatest difficulty was experienced in separating the aluminum silicates from each other, but repeated fractionation in diluted liquids gave nearly pure concentrates. Purity was checked continually by grain mounts in immersion oils, and in the final samples the grains were counted to estimate impurities and contamination.

* Present address: Research Council of Alberta, Edmonton, Alberta, Canada.
† Department of Geology, McMaster University, Hamilton, Ontario, Canada.

TABLE 1. SAMPLE LOCALITIES, DESCRIPTIONS AND PURITY

Sample	Locality	Description	Mineral extracted	Impure grains %	Foreign grains %	Comments on mineral extracts
E 1	S. Dakota	Pink A with a little white mica.	A	4.2	*	S and mica inclusions
E 2	Spain	Pink A with veinlets of S and muscovite.	A S	3.5 6.5	*	S inclusions A inclusions
E 3	Switzerland	Massive A with gray K and a little muscovite.	A	2.5	2.6	Limonite stain, K and mica inclusions
			K	—	—	Quite clean
E 4	California	Pale blue bladed K with muscovite and magnetic oxides.	K	9.0	*	A, muscovite and quartz inclusions
E 5	Germany	Blue bladed K in limonitic quartz-muscovite aggregate.	K	0.5	*	Quartz and muscovite inclusions
E 7	Wyoming	Blue gray bladed kyanite in schist also containing staurolite and micas.	K	8.4	*	Biotite, staurolite inclusions
E 9	S. Dakota	Coarse pink A with quartz and muscovite.	A	5.3	5.0	S, mica grains and inclusions
E 10	Brazil	Blue gem crystal of K with limonite stain.	K	5.0	*	Limonite stain
E 11	Brazil	Green gem crystal of A.	A	*	*	Quite clean
E 12	N. Carolina	Coarse blue K in two-mica schist.	K	20.0	*	Mica inclusions
E 13	White River Jct., Vermont	Coarse blue K with limonite stain in two-mica garnet gneiss.	K	2.0	0.1	Limonite stain
E 14	Clarkesville, Georgia	Large blue-gray crystal of limonite-stained K.	K	8.0	0.5	Limonite stain, mica inclusions
E 15	Dillon, Montana	Fibrolite with two micas, quartz and microcline.	S	*	1.7	Limonitic A grains present
E 16	White Mts., Mono Co., Calif.	Massive A with diaspore and muscovite	A	3.8	*	K and mica inclusions
E 17	Salamanca, Spain	Coarse pink-green A with muscovite and chlorite	A	12.0	3.1	Mica, chlorite grains and inclusions
E 18	Broken Hill, N.S.W.	Fibrolite-muscovite-quartz-iron oxide schist.	S	10.0	*	Muscovite inclusions
E 19	Big Joco River, 25 miles NW of Mattawa, Ont.	Kyanite-biotite gneiss.	K	14.0	*	Quartz, mica, graphite inclusions
E 20	Kake Kippawa, near Timiskaming, Ont.	Kyanite-biotite gneiss	K	7.1	*	Quartz, mica inclusions
E 21	Near E 19	Green K, green mica and pyrite	K	7.0	*	Mica, pyrite inclusions
L 73	1 mile SSE of North Thetford, N. H.	Coarse blue K in biotite gneiss	K	9.1	*	Quartz inclusions

About 350 grains counted in each case.
* Not detected.
— = No information.

Table 2. Determinations of Cr by Different Methods

Sample	Analysts		Sample	Analysts	
	Shaw	Pearson		Shaw	Pearson
E 3	6 ppm	12 ppm	E 2A	* ppm	17 ppm
E 4	27	35	E 15	83	43
E 5	39	46	E 18	140	95
E 7	180	210			
E 10	50	67	E 1	*	10
E 12	11	19	E 2B	*	11
E 13	33	43	E 3A	*	14
E 14	9	8	E 9	8	7
E 19	—	105	E 11	78	62
E 20	11	21	E 16	14	17
E 21	170	200	E 17	14	11
L 73	35	72			

Analytical Methods

The following elements were determined, using quantitative spectrographic methods: B, Be, Ga, Cr, Ti, Li, Mg, V, Cu, Zr, Mn, Ba, Sr. In addition the following were sought but were usually absent: Ge, Y, Pb, Mo, Ag, Ni, Co, Sc, Sn.

The methods have already been described (Pearson, 1955; Shaw, 1959). The latter reference describes a general method for silicates, which was modified in this instance by using standards made from a pure silica-alumina matrix. Precision was from 5–15% of amount present for most elements. Some elements (Ga, Cr, Ti, V, Cu, Zr, Mn) were determined several years apart by different analysts using different methods: the agreement was generally satisfactory, as may be seen from the example in Table 2, which gives the two sets of analyses for Cr (averages of triplicate determinations). The two sets of data were averaged in each case to give the values in Table 3. The results on Be, Mg and Ti were obtained by averaging the results on two different spectral lines.

Discussion

The significance of contamination must first be discussed. The data in Table 1 showed that most of the samples were free of foreign grains, but usually contained intergrowths. In no case did the admixed mineral, whether an inclusion or alteration, constitute more than 1/20 of the host grain, as estimated under the microscope: the volume of the contamination would thus be about $(1/20)^{3/2}$ or about 1%.[1] If 10% of all grains in-

[1] This assumes a spherical particle embedded in a larger sphere.

clude such intergrowths the total impurity amounts to about 0.1% by volume or 0.2–0.3% by weight. Thus the total contribution of the impurity to the analysis of the host mineral would be 2000–3000 ppm, including both major and minor elements.

One might therefore expect that the less pure samples, as counted with the microscope, should in fact show no clear evidence of contamination, when compared with the apparently quite clean samples. This is seen to be the case, if specimens E 3B and E 11, both of which appeared quite pure, are compared with E 12 and E 17, which contain respectively 20 and 12% of intergrowths. The trace-element suite of the latter pair show no marked differences from the previous pair, even for Mg, Ti and Li, which might be expected from mica contamination. It may perhaps be concluded that contamination is not as serious as first inspection of Table 1 would suggest, but it must nevertheless be borne in mind throughout the following discussion.

The average trace-element contents of the three minerals are presented in Table 4, which includes abundances in the crust and in pelitic rocks (the latter from Shaw, 1954, 1956). The distribution of some elements in individual mineral groups is rather erratic (e.g. Ti in kyanite, Table 3), and the significance of the averages is therefore uncertain. In addition

TABLE 3. TRACE-ELEMENT ANALYSES OF 12 KYANITES, 3 SILLIMANITES AND 7 ANDALUSITES

Sample Number	.23	.35	.62	.63	.66	.68	.68	.72	.74	.79	.80	1.12	1.34	r Å
	10	.5	2	5	30	5	30	.5	10	5	5	10	5	Sensitivity (ppm)
	B	Be	Ga	Cr	Mg	Ti	Li	Cu	V	Zr	Mn	Sr	Ba	
E 3B	*	tr.	55	9	250	240	94	6.2	36	tr.	20	*	58	
E 4	tr.	tr.	54	31	280	2,500	190	1.3	23	85	6	130	tr.	
E 5	*	*	25	43	65	420	43	1.0	40	7	8	*	5	
E 7	*	*	34	190	1,600	580	*	1.5	100	20	29	*	14	
E 10	*	tr.	28	59	70	42	38	.2	83	tr.	7	*	tr.	
E 12	tr.	*	29	38	60	250	tr.	.1	25	92	49	*	3	
E 13	*	tr.	34	15	63	100	120	1.2	93	tr.	6	*	tr.	
E 14	*	tr.	29	9	43	58	110	8.4	31	tr.	6	*	5	
E 19	*	—	24	105	—	450	*	4.2	54	tr.	11	—	—	
E 20	*	tr.	66	16	45	150	*	.2	5	26	5	*	tr.	
E 21	*	*	61	180	170	44	*	3.1	100	22	4	*	tr.	
L 73	*	*	12	54	46	33	tr.	1.5	90	tr.	20	*	5	
E 2A	170	25	95	17	100	51	150	7.9	110	tr.	17	*	6	
E 15	20	tr.	70	63	1,900	280	140	4.1	90	11	13	tr.	77	
E 18	30	2	33	120	35	830	*	2.9	150	180	12	*	31	
E 1	25	*	210	10	130	280	250	4.5	8	tr.	11	*	tr.	
E 2B	16	2	58	11	150	81	220	1.9	45	tr.	12	*	tr.	
E 3A	—	—	61	14	—	160	190	13	56	tr.	30	—	—	
E 9	*	*	62	8	170	86	96	2.5	36	tr.	5	*	*	
E 11	*	*	75	70	160	140	tr.	3.0	46	8	5	*	tr.	
E 16	tr.	*	45	16	tr.	3,200	71	8.3	51	280	10	tr.	5	
E 17	10	*	69	13	300	110	580	2.9	35	tr.	34	54	33	

Triplicate analyses, expressed in ppm.
* Below detection limit.
— = no data.
tr. = trace.

Table 4. Average Trace-Element Content of Kyanite, Sillimanite and Andalusite Compared with the Crust and Pelitic Rocks

Element	Ky	Sill	Andal	C	Reference	Pelite
B	*	73	10	3	Goldschmidt (1937)	3–300
Be	tr.	9	*	2	Sandell (1952)	4
Ga	38	66	83	19	Shaw (1957)	19
Mg	220	680	160	12,500	Goldschmidt (1937)	15,120
Cr	62	67	20	100	Shaw (1954)	110
Ti	410	390	580	4,400	Goldschmidt (1937)	4,900
Li	55	110	210	29	Horstmann (1957)	55
Ni	tr.	tr.	tr.	80	Sandell & Goldich (1943)	64
Co	*	*	*	23	Sandell & Goldich (1943)	18
Mo	*	*	*	1	Kuroda & Sandell (1954)	—
Sn	*	*	*	2	Onishi & Sandell (1957)	—
Cu	2.6	5.0	5.2	70	Sandell & Goldich (1943)	18
V	57	120	40	100	Shaw (1954)	120
Zr	24	65	45	156	Degenhardt (1957)	200
Mn	14	14	15	1,000	Green (1953)	540
Sc	tr.	tr.	tr.	15	Shaw (1954)	14
Ag	*	*	*	0.1	Goldschmidt (1937)	—
Y	tr.	tr.	tr.	40	Fleischer (1955)	—
Sr	tr.	tr.	tr.	450	Turekian & Kulp (1956)	710
Pb	tr.	tr.	tr.	15	Wedepohl (1956)	16
Ba	10	38	9	250	Green (1953)	570

it seems unwise to use statistical methods to test apparent differences between species, both on this account and also because of the small number of sillimanite specimens.

Looking first at differences between the three minerals, the data of Tables 3 and 4 show that the elements Ga, Ti, Cu, Zr and Mn are clearly at about the same concentration-level in each. However B, Be, Cr, Li, Mg, V and Ba appear to show differences. In calculating the averages in Table 4 all analyses were used, including those where the element in question was below the detection limit (*tr* was assigned a figure equal to the sensitivity limit). This procedure appears reasonable where an element is distributed in a fairly regular manner, but in the case of Li, for example, the range in concentration in kyanite is so great that the average calculated in this manner (55 ppm) differs considerably from that obtained from averaging only the analyses where Li was detected (99 ppm). In consequence, the averages for B, Be, Li and Ba have little real value. Inspection of the individual analyses does however suggest that sillimanite might be richer in B, Be and Ba than either kyanite or andalusite, but that is the most that can be said.

Every analysis however showed presence of Cr, Mg and V. Andalusite

definitely contains less Cr than either of the other two. The three sillimanite analyses suggest that the mineral may be somewhat enriched in V, but that the Mg-average is unduly affected by one high value.

It must be concluded that the results show no indisputable differences in trace-element values between the three minerals, but there is a possible concentration of B, Be and Ba in sillimanite and a probable paucity of Cr in andalusite. These results suggest that minor and trace-elements can not be considered as factors influencing the polymorphic behaviour of the minerals.

Comparing the minerals with the crust of the earth, the elements studied fall into three groups:

Ga, B, Li are distinctly enriched in the aluminum silicates,

Be, Cr, V show about the same abundance in both,

Mg, Ti, Ni, Co, Mo, Sn, Cu, Zr, Mn, Sc, Y, Sr, Ba are more abundant in the crust.

Comparing with the average pelitic sediment, the position is the same, except for B and Li which have passed into the category of elements with no clear enrichment either way. In addition, if the Al_2O_3 contents of aluminum silicate, the crust and pelitic rocks are taken as 62.2, 15.34 and 16.95% respectively, then the Ga/Al ratios are 1.7, 2.3 and 2.1×10^{-4}.

In part these results are what would be expected. Thus the larger ions Sc, Y, Sr, Ba, would not be expected to find lattice sites in these minerals, where the largest major metal is Al, and whose coordination numbers are 6 and 6 in kyanite, 6 and 5 in andalusite, and 6 and 4 in sillimanite.

Mn occurs in only small amounts in the minerals analysed and does not exceed 50 ppm. It should be noted however that manganandalusite containing 3.63% MnO_2 has been reported by Odman (1950), from a manganese-rich environment. Other occurrences of manganandalusite are also known, but the writers know of no occurrences of Mn-kyanite or Mn-sillimanite. It is probable that Mn^{+2} cannot substitute for Al^{+3} to any notable extent and that extensive Mn-Al substitution requires the smaller ion Mn^{+4} which forms only in strongly oxidising environments.

The elements Mg, Ti, Ni, Co, Mo, Sn, Cu, Zr, Li and V customarily occupy 6-coordinated positions in ferromagnesian minerals, and might therefore be expected to substitute for Al. All except the last two however show concentrations much lower than the parent pelitic rocks from which these minerals usually form. This must be attributed to a greater attraction to the micas and garnets, which generally form at the same time. Al^{+3} is a smaller ion than Mg^{+2}, and even in 6-fold coordination the lattice sites must be "smaller" than in most ferromagnesian minerals. This also accounts for the fact that Cr^{+3} and Ga^{+3} (both small ions) show average and high concentration in the aluminum silicates. The usual close co-

herence of Ga and Al however does not explain why Ga concentrates less than Al in these minerals (see Ga/Al ratios).

The data are not adequate to discuss Be with profit. The remaining elements are Li, V and B. The concentration of Li may in part be attributed to a prior concentration in pelitic rocks with respect to the crust. The figures in Table 4 however suggest that there is in many cases a further concentration into the aluminum silicates formed during recrystallisation of shales, etc. It may be that the source rocks of the silicates with high Li-values were themselves richer than normal, but in any case one would again expect Li to be preferentially concentrated in the accompanying micas. It should be added that the quantities of Li involved are much too great to be explained by mica contamination, even if the mica were lepidolite. The radii of Li^{+1} and Al^{+3} are .68 and .51 Å respectively and mutual substitution would hardly be expected on crystal chemical grounds. The overall Li average is 110 ppm if all samples are included and 170 ppm if the samples with undetectable Li are discarded.

V would not be expected to substitute for Al any more than would Li if in its usual valence state V^{+3} (radius .74 Å): its radius however changes to .63 and .59 Å for V^{+4} and V^{+5}, respectively. These smaller ions are closer to the size of Al^{+3}, but there is no evidence that V is in an oxidised state except in supergene and sedimentary minerals. In any case the concentration of V in the minerals is less than in the crust, and is noticeable only by contrast with such an element as Ni, which is completely excluded.

The data is rather equivocal for B, but six samples showed values well in excess of the crust. These almost certainly reflect formation from marine shales, which are well-known to be rich in B, but the location of the B-atoms, ions or radicles in the minerals is uncertain. Minute tourmaline inclusions could readily be the explanation, but although tourmaline occurs very commonly with sillimanite none was observed under the microscope in these samples.

The concentration of both Li and B in several samples suggests crystallisation in the presence of fluids similar to those which form greisen or pneumatolytic deposits (the same effect is more prominently displayed by scapolite, which also is rich in B and Li).

It may be concluded that all the elements examined, with the exception of B, Be and Ba, probably occur at Al lattice sites: Be might alternatively replace Si, while the significance of B and Ba is uncertain.

Two kyanites and one andalusite were analysed for Ba, Cr, Cu, Ga and V by Hietanen (1956). She found similar amounts of Ba and Cu, but lesser amounts of Cr, Ga and V, by comparison with the writer.

Major element analyses of three samples are given in Table 5. The only

noteworthy constituents in addition to SiO_2 and Al_2O_3 are Fe oxides and H_2O+: the sillimanite (E 18) also contained a little CaO, K_2O and TiO_2 (the last is greater than the amount determined spectrographically). Densities were determined using a pycnometer: refractive indices were measured by immersion methods, using sodium light.

Table 5. Chemical Analyses

	Sillimanite E 18	Andalusite E 9	Kyanite E 14
SiO_2	36.61	37.25	36.85
Al_2O_3	61.54	61.90	62.26
Fe_2O_3	.22	.29	.21
FeO	.14	.04	.03
MgO	.04	.06	.03
CaO	.40	.08	.08
Na_2O	.06	.08	.07
K_2O	.25	.08	.11
H_2O^+	.33	.39	.41
H_2O^-	.11	.09	.05
TiO_2	.22	.05	.04
F	.02	.01	.01
Less 0=F	.01		
Sum	99.93	100.27	100.15
Al_2O_3/SiO_2	1.68	1.66	1.69
G	—	3.02	3.69
α	1.655	1.629	1.710
β	—	—	—
γ	1.673	1.641	1.725
$\gamma-x$	.018	.012	.015

Analyzed at the Rock Analysis Laboratory, University of Minnesota: Director, Dr. S. S. Goldich: Analysts, D. Thaemlitz, (E 18) and E. H. Oslund (E 9, E 14).
Other data by G. R. Pearson.

The theoretical value of the ratio Al_2O_3/SiO_2 is 1.70. In all three of the analysed specimens the ratio is a little less than this figure. This suggests a deficiency of Al with respect to Si (analytical error can be disregarded, in the opinion of the writers), which is entirely reasonable if the substitution of small amounts of Fe, Ti, Mg and trace-elements for Al be allowed. Such substitution can hardly be extended to the much larger elements Na and K, however, and the significance of alkalies in aluminum silicates has

been discussed by many authors (in particular—Jakob, 1937, 1940, 1941; Henriques, 1957; Eigenfeld & Machatski, 1957). Jakob believed the alkali metal and water content of these minerals to be essential constituents, in the sense that one or two molecules of each were combined with 40 SiO_2 and 40 $(Al_2O_3+Fe_2O_3)$. With the present three samples, however, the proportions are as follows:

	SiO_2	$(Al_2O_3+Fe_2O_3)$	(Na_2O+K_2O)	H_2O
Sillimanite	100	100	1	3
Andalusite	160	160	1	6
Kyanite	160	160	1	6

It is most unlikely that these large figures represent a formula in the accepted sense, and Jakob's hypothesis appears untenable. The problem of the significance of Na and K however remains, and the quantities appear too great to be explained by mica contamination. Some kind of concealment in lattice voids seems the best explanation at present.

Acknowledgments

The study reported here has been carried out intermittently from 1954–59. Part has already been written up as a thesis (Pearson, 1955). The authors wish to express their indebtedness for research grants to the National Research Council of Canada and the Geological Survey of Canada, and to the Penrose Fund of the Geological Society of America for defrayment of costs of the gravimetric analyses. The first author was a recipient of an Ontario Research Foundation Scholarship while working on this research. C. Yip, J. N. Weber and J. Capel gave valuable assistance.

Bibliography

Degenhardt, H. (1957), Untersuchungen zur geochemischen Verteilung des Zirkoniums in der Lithophäre. *Geo. et Cosmochim. Acta*, **11**, 279–309.

Eigenfeld, I. and Machatski, F. (1957), The supposed alkali content of kyanite. *Österr. Akad. Wiss. Math.-naturv. Kl. Anz.* **94**, 151–152. *C.A.*, 5984d (1959).

Fleischer, M. (1955), Estimates of the abundances of some chemical elements and their reliability. *Geol. Soc. Amer., Spec. Paper No.* **62**, 145–154.

Goldschmidt, V. M. (1937), Geochemische Verteilungsgesetze der Elements. IX. Die Mengenverbältnisse der Elemente und der Atom-Arten. *Skr. Norske Vid.-Akad. Oslo, I. Math.-naturv. Kl.*, No. 4.

Green, J. (1953), Geochemical table of the elements for 1953. *Geol. Soc. Amer., Bull.*, **64**, 1001–1012.

Henriques, Å. (1957), The alkali content of kyanite. *Ark. för Min. och Geol.*, **2**, 271–274.

Hietanen, A. (1956), Kyanite, andalusite and sillimanite in the schist in Boehls Butte Quadrangle, Idaho. *Am. Mineral.*, **41**, 1–27.

Horstman, E. L. (1957), The distribution of lithium, rubidium and cesium in igneous and sedimentary rocks. *Geo. et Cosmochim. Acta*, **12**, 1–28.

Jakob, J. (1937), Über den Alkaligehalte der Disthene. *Schweitz Min. Petr. Mitt.*, **17**, 214–219.

——— (1940), Über den Chemismus des Andalusites. *Schweitz Min. Petr. Milt.*, **20,** 8–10.
——— (1941), Chemische und strukturelle Untersuchungen am Disthene. *Schweitz Min. Petr. Milt.*, **21,** 131–135.
Kuroda, P. K. and Sandell, E. B. (1954), Geochemistry of molybdenum, *Geo. et Cosmochim. Acta*, **6,** 35–63.
Odman, O. F. (1950), Manganese mineralisation in the Ultevis district, Jokkmokk. Part 2: Mineralogical notes. *Sver. Geol. Undersok., Arsbok*, **44,** No. 2.
Onishi, H. and Sandell, E. B. (1957), Meteoritic and terrestrial abundance of tin. *Geo. et Cosmochim. Acta*, **12,** 262–270.
Pearson, G. R. (1955), A geochemical study of sillimanite, andalusite and kyanite. M.Sc. thesis (unpublished), McMaster University.
Sandell, E. B. (1952), The beryllium content of igneous rocks. *Geo. et Cosmochim. Acta*, **2,** 211–216.
——— and Goldich, S. S. (1943), The rarer metallic constituents of some American igneous rocks. *Jour. Geol.*, **51,** 99–115 and 167–189.
Shaw, D. M. (1954), Trace elements in pelitic rocks. Part I: Variation during metamorphism. *Geol. Soc. Amer., Bull.*, **65,** 1151–1166.
——— (1956), Geochemistry of Pelitic Rocks. Part III: major elements and general geochemistry. *Geol. Soc. Am., Bull.* **67,** 919–934.
——— (1957), The geochemistry of gallium, indium, thallium—a review. Physics and Chemistry of the Earth, Vol. 2. Pergamon Press.
— — (1959), Spectrochemical analysis of silicates using the Stallwood jet. *Can. Mineral.* (in press).
Turekian, K. K. and Kulp, J. L. (1956), The geochemistry of strontium. *Geo. et Cosmochim. Acta*, **10,** 245–296.
Wedepohl, K. H. (1956), Untersuchungen zur Geochemie des Bleis. *Geo. et Cosmochim. Acta*, **10,** 69–148.

Manuscript received September 9, 1959.

THE AMERICAN MINERALOGIST, VOL. 45, JULY–AUGUST, 1960

SOME REACTIONS PRODUCED IN CARBONATES BY GRINDING

JOHN C. JAMIESON AND JULIAN R. GOLDSMITH, *University of Chicago, Chicago 37, Illinois.*

ABSTRACT

Samples of carbonates were ground in a mechanical mortar for periods up to three days, and *x*-ray powder diffraction patterns were taken at intervals. Calcite was partially converted to aragonite as had been reported by Burns and Bredig. The effect of Mg-substitution in the calcite structure gives an estimate of the local pressures involved in mortar grinding of $CaCO_3$ to be the order of 20,000 bars. Several mixtures of pure carbonates reacted to form heterogeneous solid solutions which could be roughly related to their phase diagrams. Several pure carbonates decomposed, and in the case of $MnCO_3$ at least two oxidation states were attained after loss of CO_2.

INTRODUCTION

Recently, Burns and Bredig (1956) have reported the conversion of aragonite to calcite by prolonged grinding in a laboratory mortar. Acampora *et al.* (1956) have reported formation of heterogeneous solid solutions by grinding a mixture of KCl and KBr, a result similar to that of Vegard and Hauge (1927), who reported that heterogeneous solid solutions of HgCl and HgBr also formed in this manner. Bradley *et al.* (1935) studied the effects of prolonged grinding on dolomite and others have examined the effects produced by grinding clay minerals (Keller, 1955, also see Eitel, 1954, for a partial bibliography). Lea (1893) observed color changes in various salts upon grinding. A ball mill has been described by Roy and Osborn (1952) for grinding at high temperatures and moderate water pressures which is essentially a modified Morey bomb. Its use to date has been to speed up hydrothermal reactions (Roy and Roy, 1955).

We have conducted further experiments of this nature with the thought that prolonged grinding might in a crude sense be related to direct high pressure-high temperature studies on mineral systems. It was determined that an ordinary laboratory power mortar can be roughly "calibrated" in terms of the quasi-hydrostatic pressures and temperatures developed.

EXPERIMENTS

All grinding was done in an ordinary laboratory power mortar, with mullite parts. For quick *x*-ray analysis of results powder pictures were taken with a North American Philips 57.3 mm. camera using Co or Fe filtered radiation. A 114.59 mm. camera was used when greater resolution was desired.

Since the grinding motion of the mortar is complex, the results ob-

tained as far as quantity and time of appearance of a new phase is concerned are a function of amount of sample and the alignment of the pestle with respect to the mortar. It was soon found that when the pestle was carelessly aligned a large amount of mullite would appear in the mixture early in the grind. This is apparently a danger in using this type of mortar in any work. Careful alignment minimized this as no mullite was apparent in the x-ray patterns in many cases even after 48 hours of grinding. The summary of results appears in Tables 1 and 2.

A. The Calcite-Aragonite Transition

Other than in the length of time required before detection of aragonite our results on the grinding of dry Iceland Spar duplicate those of Burns and Breding (1956). These authors stated that while the stability of aragonite at high pressures (Jamieson 1953, MacDonald 1956, Clark 1957) may account for its formation during grinding, they felt that more than hydrostatic pressure was involved and postulated that their results could only be accounted for by assuming the presence of a shearing force in addition to the high hydrostatic pressure. This is partially verified by results of Bridgman (1936, 1937). He found that the density of calcite after being sheared at pressures up to 50,000 bars at room temperature was increased to somewhat less than 2.84, presumably due to the formation of aragonite. His samples however were not examined by x-ray diffraction and the identification is uncertain since a portion of this density increase could have been due to material from his pistons being extruded in the sample.

MacDonald (1956) was able to form aragonite from calcite at temperatures as low as 250° C. ($\sim$8000 bars) using the "simple squeezer," but again in this device shear is a factor. However shear appears not to be absolutely necessary for the transformation since Clark (1957) using truly hydrostatic pressure definitely formed aragonite from calcite at 575° C. and 12,700 bars.

With the assumptions of ideal mixing, of no Mg in the aragonite structure, and using various thermodynamic data (cf. Jamieson, 1953), it is possible to show that the calcite-aragonite equilibrium point (about 16,000 bars) is raised about 3000 bars at 1000 ° K. by the addition of 7% Mg to the calcite structure and about 6000 bars by the addition of 13% Mg. The (P, T) extension of these curves parallels that of the pure calcite-aragonite curve (Clark 1957, Jamieson 1953). It should be mentioned in passing that an extension of this type of calculation gives excellent agreement with unpublished data of one of the authors (J.R.G.) on the (P, T) equilibrium curve for the triple point calcite-aragonite-dolomite.

The pressures (stresses) and temperatures developed in a grinding ex-

TABLE 1. SINGLE SUBSTANCES GROUND

Sample Number	Initial Material	Time	*Observations from x-Ray Pattern
1	Iceland Spar	6 hr.	No significant change
		24 hr.	Some aragonite formed
		48 hr.	More aragonite formed
2	Iceland Spar ground under distilled H_2O	22 hr.	Some aragonite formed
		46 hr.	No significant further alteration
3	Iceland Spar ground under ethyl alcohol	15 hr.	Little aragonite present
		22 hr.	More aragonite present
5	Natural aragonite crystals	18 hr.	No significant change
		39 hr.	No significant change
24	Synthetic $CdCO_3$	5 hr.	No significant change
		22 hr.	Sample yellow, some CdO present
13	Siderite (Roxbury)	$\frac{1}{4}$ hr.	Sample began to darken. No change (x-ray)
		3 hr.	Sample darker, no change (x-ray)
		6 hr.	Sample darker, trace Fe_2O_3 present
		24 hr.	All Fe_2O_3, no $FeCO_3$ visible on pattern
		46 hr.	All Fe_2O_3, no $FeCO_3$ visible on pattern
11	Synthetic $MgCO_3$	67 hr.	General structural degradation but no formation of MgO
19	"$MgCO_3$," Mallinkrodt's An. Reag.†	23 hr.	No trace of anything other than mullite (amorphous to x-rays)
12	Brucite (natural)	25 hr.	Very badly degraded x-ray patterns—still $Mg(OH)_2$
		48 hr.	No trace $Mg(OH)_2$ (amorphous to x-rays), trace of mullite
10	Rhodochrosite	19 hr.	Large amount of hausmanite (Mn_3O_4)
		42 hr.	Only bixbyite (Mn_2O_3)
		88 hr.	Bixbyite
9	Synthetic $MnCO_3$	17 hr.	Largely bixbyite
8	Smithsonite (Saurium, Greece)	23 hr.	Largely ZnO
16	$BaCO_3$—An. Reagent	21 hr.	No significant change
6	Calcareous Algae‡ 13% Mg	19 hr.	Mullite appears, no aragonite
		40 hr.	Mostly mullite, no aragonite
7	Coral Spicules‡ 17% Mg	43 hr.	No significant change, no aragonite
21	Echinoid plates‡ 6% Mg	70 hr.	Some aragonite formed
		90 hr.	
23	Dolomite, Lee Mass.	24 hr.	Significant structural degradation

* The general pattern degradation, characteristic of ground materials is only reported when it seems somewhat excessive for a given substance.

† Basic magnesium carbonate.

‡ Metastable magnesian-calcites.

periment of this nature are actually spectrums of values over the area of grinding action at any instant. With this in mind the data from organically produced carbonates as seen in Table 1 would seem to indicate that the quasihydrostatic pressures and temperatures developed with $CaCO_3$ lie along a (P, T) curve given roughly by a band passing though 1000° K. and 19,000–22,000 bars parallel to the calcite-aragonite equilibrium curve. However the lack of aragonite formation in calcites containing

Table 2. Mixtures Ground

Sample Number	Initial Material	Time	*Observations from x-Ray Pattern
14	Synthetic $MgCO_3$ and $MnCO_3$	17 hr.	Uninterrupted Solid Solution Bands Tr. Mn_3O_4
		35 hr.	Mostly Mn_3O_4 plus $MgCO_3$
15	Synthetic $MnCO_3$ and Iceland Spar	4 hr.	No significant change
		21 hr., 44 hr., and 64 hr.	Heterogeneous solid solution bands. Line broadening of CaCO greater than that of $MnCO_3$. Bands increase width with time. No oxidation apparent
18	Synthetic $MgCO_3$ and Iceland Spar	21 hr.	Aragonite formed, possible dolomite or protodolomite
		45 hr.	Pattern more degraded. Possible dolomite reflection no longer visible. No solid solution effects
25	Synthetic $MgCO_3$ and Synthetic $CdCO_3$	6 hr.	$CdCO_3$ reflection broadened toward $MgCO_3$
		23 hr.	$CdCO_3$ reflections broadened toward $MgCO_3$ and displaced
		41 hr.	No further significant alteration

* The general pattern degradation, characteristic of ground materials is only reported when it seems somewhat excessive for a given substance.

more than 7% Mg may be due only to the rate of the required processes of forming a calcite richer in Mg than the starting materials along with the pure Ca-aragonite. The failure to develop calcite in grinds of aragonite as the starting material would indicate that local temperatures in excess of ~700° K. were only reached (in any significant amount of material) when the pressures were above those for the pure calcite-aragonite equilibrium. If this were not true some calcite should have formed from aragonite, for the conversion is well known to take place rapidly at temperatures above 425° C.

The actual local physical conditions in the present set of experiments must be regarded as ill-defined; it is however of some interest to discuss them qualitatively. That stresses in the tens of kilobars range are available seems obvious since even one gram of force applied to a square micron of area (10^{-8} cm^2) gives a pressure of 10^5 kilograms/cm^2. The principal unknown factors are the number (and area) of particles supporting the stress, whether the particles themselves are supported by neighbors, or whether they are generally free to roll or move about. If it is assumed that at least a few particles are trapped in such high stress environments by the moving pestle, then the stress developed depends on their ability to undergo plastic flow (Bowden and Tabor (1950)). If the onset of plastic flow in the material is instantaneous then the limiting "pressures" and hence temperatures are given by the yield pressure of the material. The yield pressure is a fairly strong function of the total confining pressure, and indeed, King and Tabor (1954) have found a factor of seven between the bulk shear strength and the specific shear strength of NaCl calculated from sliding experiments. A factor of twenty-four was found for sapphire. It does not seem unreasonable to assume that CaCO possesses a "frictional" shear strength in the 10,000 bar range and thus can maintain higher stresses for short periods of time. In the presence of such stresses, frictional heating to several hundred degrees centigrade occurs (see for example Bowden and Thomas (1954)). In the case of calcite-aragonite another temperature factor enters in, namely, the change in temperature due to inversion. If the inversion takes place throughout the whole of a small particle, at constant pressure, in an adiabatic fashion we have $\Delta T = T\Delta S/C_p$ where ΔS is the molal entropy change in calcite transforming to aragonite and C_p is the average molal specific heat of the two phases. This gives $\Delta T \cong .04T$ or $\Delta T \cong 40°$ at 1000° K. for the rough values of the thermodynamic parameters of $CaCO_3$ in this range. The adiabatic assumption makes this a maximum estimate of the temperature effect from this source. (It should be noted that this is a temperature decrease for calcite→aragonite at constant stress). In any case, the local temperatures from ordinary frictional heating should dominate the latent heat effect. However, it is probable that the presence of a polymorphic transition in a substance undergoing frictional heating will limit the temperature rise, since the coefficient of friction may become very low for a surface which is in a process of change. A possible analogue has been described by Bowden and Tabor (1950), who report that the rise in temperature of a sliding metal is limited by its melting point. Bowden and Thomas (1954) have also described the converse effect, namely the much greater temperature increase obtained in

local hot spots when an easily oxidizable metal is heated by friction to the point where it reacts readily with air.

Aragonite ordinarily occurs in nature only as a metastable form, and it might be supposed that in the grinding experiments it is also produced metastably, perhaps due to precipitation from a solution. In the dry grinds the only solution phase available for aragonite "precipitation" is the water (and gas) absorbed on the grain surfaces. It is felt that this mechanism does not operate in this case since all experiments with calcite, whether ground dry, or with distilled water or alcohol covering the sample, produced aragonite. It is known that (1) precipitation of $CaCO_3$ from a saturated solution by release of high pressure at room temperature gives both aragonite and vaterite (Jamieson, 1953), and (2) alcohol inhibits the formation of aragonite in precipitation from chemical reactions (Faivre, 1946). However since the conditions for the metastable formation of aragonite are not known at present this argument can not be deemed conclusive.

B. Carbonate Solid Solutions

A mixture of $CaCO_3$ and $MgCO_3$ (synthetic) after 21 hours of grinding was found to contain much aragonite in addition to a calcite phase. A very faint line on the *x*-ray pattern could conceivably be the strongest reflection from dolomite, or more likely, a protodolomite-like material. 19 hour exposures in the 114.59 mm. camera using filtered Cu radiation verified the existence of this line. The amount of solid solution to be expected in this system is very small for the apparent working conditions of the mortar. For example, the solubility of Mg in $CaCO_3$ is $\sim 8\%$ at 900° K. (Graf and Goldsmith, 1958). Unreported work of one of the authors (J.R.G.) shows the effect of pressure on this solubility to be small.

In grinding $CaCO_3$ and synthetic $MnCO_3$ the diffraction lines became "bands," $CaCO_3$ lines progressively widening toward the corresponding $MnCO_3$ lines and vice-versa. This indicates that heterogeneous solid solutions were formed. At no time was there a complete linkage nor was there a formation of sharp line corresponding to a unique homogeneous solid solution even with 64 hours of grinding. The broadening of CaCO lines was greater than those of $MnCO_3$. This is in accord with the phase diagram obtained by Goldsmith and Graf (1957) which displays a greater solubility of Mn in $CaCO_3$ than vice-versa. The effect of pressure on this system is unknown, but if it is negligible we see again that the local temperatures can not have exceeded 525° C. and must presumably have been below 475° C. to show the large immiscibility gap illustrated by the patterns.

After 17 hours of grinding, the mixture of synthetic $MgCO_3$ and synthetic $MnCO_3$ gave a diffraction pattern showing uninterrupted heterogeneous, solid solution "bands" between the positions of corresponding lines of $MgCO_2$ and $MnCO_3$. Recent work of Goldsmith and Graf (1960) has shown that solid solubility is complete in this system at 450° C., the lowest temperature at which equilibrium reaction could be carried out.

The $MgCO_3$-$CdCO_3$ grind gave still different behavior in that, not only did the $CdCO_3$ lines broaden in the direction of those of $MgCO_3$ (which remained moderately sharp) but they shifted their peak of maximum intensity also toward $MgCO_3$ indicating a fairly "complete" reaction. No CdO was discerned in the *x*-ray patterns.

C. Decomposition of Carbonates by Grinding

Several experiments on pure carbonates resulted in decomposition to the oxides. It is rather difficult to obtain any quantitative information from these decompositions since neither the CO_2 pressure or O_2 pressure is well defined for a particle during grinding. It is not sufficient to assume that atmospheric partial gas pressures prevail since the actual partial pressures at the stressed surface of a particle are dependent on the ease with which a released gas may escape in the case of CO_2, or the partial pressure of a confined gas, possibly trapped and compressed by surrounding particles in the case of O_2. If the local partial pressure of CO_2 in these experiments were truly atmospheric, all the pure carbonates that were ground would have decomposed, with the possible exception of $BaCO_3$. Actually the decompositions seem to fall into two classes. The first class being reactions of the type

$$MCO_3 \rightarrow MO + CO_2$$

in which the oxygen is supplied by the carbonate itself and hence the reaction is essentially independent of oxygen partial pressures and dependent only on the CO_2 content of the trapped gas. If we assume a nominal partial pressure of .01 atmosphere for CO_2 in the normal atmosphere, and if the reasoning earlier on solids is correct, in compression of any included atmosphere a maximum CO_2 pressure (from atmospheric CO_2) of 200 atmospheres could be reached. The decomposition of smithsonite to ZnO behaved in this fashion. A rough extrapolation of the data of Harker and Hutta (1956) indicate that $ZnCO_3$ is almost unstable under natural conditions at the earth's surface, so with the application of the stresses and temperatures of grinding it is not surprising that $ZnCO_3$ decomposes. In addition, the oxidation relations of ZnO are simple. Apparently the decomposition of $CdCO_3$ falls in this class also.

The second class of decomposition may be exemplified by

$$6MCO_3+O_2\rightarrow 2M_3O_4+6CO_2.$$

Now the oxygen pressure (assuming 20% normal) can be as high as 4000 atmospheres by the above argument, certainly highly oxidizing conditions. Due to the uncertainty of local O_2 and CO_2 pressures as mentioned in the beginning of this section, it would take much more experimental work to actually know what the various physical processes occuring in the case of $FeCO_3$ and $MnCO_3$ are. Kissinger *et al.* (1956) report that $FeCO_3$ decomposes and oxidizes in air to Fe_2O_3, the change being essentially complete at 500° C. This is analogous to our results. Keller (1955) has also reported the oxidation of iron in montmorillonite by grinding. Kissinger *et al.* (1956) report that on heating $MnCO_3$ in air Mn_2O_3 appears at 600° C. while if $MnCO_3$ is heated in CO_2, MnO and Mn_3O_4 appear, the MnO disappearing by the time a temperature of 600° C. was reached. In our grind of a natural sample, the greenish color suggest the formation of MnO, but this was not detected by *x*-ray diffraction. A comparison of the grinding results with those of Kissinger *et al.* (1956) would suggest that our partial pressures of CO_2 were greater than that in normal air. The apparent direct transition of synthetic $MnCO_3$ to Mn_2O_3 indicates the delicate balance of physical parameters involved since the same material when mixed with $MgCO_3$, formed a heterogeneous solid solution which then decomposed, the oxide formed being Mn_3O_4. Again the same material mixed with $CaCO_3$ formed only a heterogeneous solid solution and no decomposition occurred. And again, the addition of $MgCO_3$ to $CdCO_3$ apparently prevented decomposition. These results suggest that the rate of solid solution formation is great enough to at least "armor" the surface, and inhibit oxidation or decomposition for the materials studied.

D. Miscellany

In some grindings, especially after two or more days, mullite lines from the mortar and pestle became obvious in the *x*-ray diffraction patterns. These were readily "discarded" in analyzing the results, but they do point out that prolonged grinding may produce a degree of contamination detrimental to experimental accuracy in various other work; mullite is of course present before it develops in amounts sufficient for *x*-ray detection. The oxidation reactions found, produced apparently by high local O_2 pressures, may very well also occur in the grinding of certain silicates prior to calorimetric studies. In these cases, an uncertainty is

introduced into the experimental data. The same may be said for structural degradation during grinding.

Conclusions

Prolonged grinding does to a partial extent duplicate the results of high pressure experimentation, however its use for this purpose at least with ordinary laboratory equipment is somewhat ambiguous. Heterogeneous solid solutions of various carbonates may be formed by grinding. A systematic study of carbonate decompositions and oxidations could give information on local gas pressures during grinding as the equilibrium diagrams for carbonate systems are becoming known. The grinding of mixtures can be used in a rough way to amplify our knowledge of miscibility in some solid systems in which no experimental work has been performed. Finely ground materials used for solution calorimetry etc., should be carefully examined for phase changes and degradation effects.

References

Acampora, F. M., Tompa, A. S., and Smith, N. O. (1956): Homogenization of Solid Solutions. A Proposed New Technique, *J. Chem. Phys.*, **24,** 1104.

Bowden, F. P. and Tabor, D. (1950): The Friction and Lubrication of Solids, Oxford.

Bowden, F. P. and Thomas, P. H. (1954), The Surface Temperature of Sliding Solids. *Roy. Soc. Lond. Proc. ser. A.* **223,** 29.

Bradley, W. F., Burst, J. E., and Graf, D. L. (1953), Crystal Chemistry and Differential Thermal Effects of Dolomite. *Ill. State Geol. Surv., Rept. of Investigations No.* **167.**

Bridgman, P. W. (1936), Shearing Phenomenon at High Pressure of Possible Importance for Geology. *J. Geol.*, **44,** 653.

——— (1937), Shearing Phenomena at High Pressures, Particularly in Inorganic Compounds. *Proc. Amer. Acad.*, **71,** 387.

Burns, J. H. and Bredig, M. A. (1956), Transformation of Calcite to Aragonite by Grinding. *J. Chem. Phys.*, **25,** 1281.

Clark, S. P. (1957), A Note on calcite-aragonite equilibrium. *Am. Mineral.*, **42,** 564.

Eitel, W. (1954), The Physical Chemistry of Silicates, Univ. of Chicago Press.

Faivre, R. (1946), Etude, par diffraction des rayon X, des carbonates mixtes de calcium et de baryum. *Compt. Rend.*, 222, 227.

Goldsmith, J. R. and Graf, D. L. (1957), The System CaO-MnO-CO_2: Solid Solution and Decomposition Relations. *Geochim. et Cosmochim. Acta* **11,** 310.

——— (1960), Subsolidus relations in the system $CaCO_3$-$MgCO_3$-$MnCO_3$. *Jour. Geol.* (In Press)

Graf, D. L., and Goldsmith, J. R. (1958), The solid solubility of $MgCO_3$ in $CaCO_3$: A revision. *Geochim. et Cosmochim. Acta* **13,** 218.

Harker, R. I. and Hutta, J. J. (1956), The stability of Smithsonite. *Econ. Geol.* **51,** 375.

Jamieson, J. C. (1953), Phase Equilibrium in the System Calcite-Aragonite. *J. Chem. Phys.*, **21,** 1385.

Keller, W. D. (1955), Oxidation of Montmorillonite during laboratory grinding. *Am. Mineral.*, **40,** 348.

King, R. F. and Taber, D. (1954), The Strength Properties and Frictional Behavior of Brittle Solids. *Roy. Soc. Lond. Proc. ser. A*, **223,** 225.

Kissinger, H. E., McMurdie, H. F. and Simpson, B. S. (1956), Thermal Decomposition of Manganous and Ferrous Carbonates, *J. Am. Ceram. Soc.*, **39,** 168.

Lea, R. F. (1893), On Endothermic Decompositions obtained by Pressure. Second Part. Transformations of Energy by Shearing Stress. *Am.J. Sci.*, (*5*), **46,** 413.

MacDonald, G. J. F. (1956), Experimental determination of calcite-aragonite equilibrium relations at elevated temperatures and pressures. *Am. Mineral.*, **41,** 744.

Roy, R. and Osborn, E. F. (1952), Some Simple Aids in the Hydrothermal Investigations of Mineral Systems. *Econ. Geol.*, **47,** 717.

Roy, D. M. and Roy, R. (1955), Synthesis and Stability of Minerals in the Systems MgO-Al_2O_3-SiO_2-H_2O, *Am. Mineral.*, **40,** 147.

Vegard, L. and Hauge, T. (1927), Misch-kristalle und ihre Bildung durch Kontakt fester Phasen und durch Fallung von Lösungen. *Z. Physik*, **42,** 1.

Winchell, A. N. (1951), Elements of Optical Mineralogy, New York.

Manuscript received November 11, 1959.

PARTICLE SIZE AS A FACTOR INFLUENCING EXPANSION OF THE THREE-LAYER CLAY MINERALS

EDWARD C. JONAS, *The University of Texas, Austin, Texas,*
AND HERMAN E. ROBERSON, *Harpur College,*
Endicott, New York.

ABSTRACT

Expansion properties of three-layer clay minerals are the result of an interaction between a binding force, which acts from particle to particle through interlayer cations, and an expansion force created by the adsorption of liquid molecules on interlayer surfaces. The binding force between two particles is a function of the charge density on the interlayer surfaces and the areal extent of the particles. The influence of areal extent of the particles on expansion properties is studied in a comparison between two size fractions of a single sample and between two samples before and after grinding. Fine fractions always contain more expanding layers than coarse fractions. Ground samples always expand more completely than unground samples. It was concluded that mica layers with a high surface charge density can expand provided they have a sufficiently small particle size. There is no simple correlation that can be made between charge density (or silicate composition) and expansion properties.

INTRODUCTION

Expansion is a property of the three-layer clay minerals which may be easily measured with diffraction techniques. Expansion in response to a prescribed treatment has commonly been used to make a distinction between two clay mineral groups, the illites and the montmorillonites. It has been generally accepted that minerals of the montmorillonite group are characterized by lower Al^{+3} for Si^{+4} tetrahedral substitution and/or lower octahedral substitution than are minerals of the illite group. A two-fold classification of these clay minerals has resulted: illites having highly charged silicate layers that do not expand when soaked in ethylene glycol, and montmorillonites having relatively low-charged silicate layers that do expand under this treatment. This classification is thought to be based on compositional variations in the silicate layers.

There is no reason to believe that the degree of isomorphous substitution is not a continuous variable in the clay minerals, ranging from a minimum in the clay equivalent of the talc-pyrophyllite minerals to a maximum in the clay muscovite-biotite minerals. If expansion is truly related to the charge on the silicate layer and the charge is controlled by isomorphism, then expansion properties should be viewed as a continuous variable. With this concept of the three-layer clay minerals in mind, the wisdom of basing a two-fold classification on expansion properties becomes doubtful. It has become apparent (Walker, 1957; Weaver, 1958b) that this two-fold classification *is* artificial and that the three-

layer clay minerals actually do exist as a continuous series of silicate layer charges. Furthermore, Walker (1958) has shown that a single specimen varies markedly in its expansion depending on the manner in which this property is tested. It is therefore important to understand all fundamental attributes of a clay layer which will control its tendency to enter into expansion.

Fundamentals of Clay Expansion

Expansion in three-layer clay minerals is an interaction between two forces. On the one hand, liquid molecules adsorbed onto the oxygen surface of the silicate layer require space between the layers and act through their adsorption forces as a lever to pry the layers apart. Their effectiveness in separating the silicate layers is determined by the strength of this adsorption force. On the other hand, this tendency of the adsorbed liquid molecules to separate the silicate layers is resisted by binding forces exerted through whatever charged interlayer material is present. Expansion occurs when the adsorbed liquid molecules exert a separating force which exceeds the binding force acting through the interlayer material between the silicate layers. The layers remain unexpanded when the binding force exceeds the separating force.

At this point it should be mentioned that the liquids commonly used to expand the clay minerals vary widely in the strength of their adsorption onto the silicate surface. Walker (1958) and Johns and Tettenhorst (1959) have shown that some clay layers that cannot be expanded with glycerol will expand when soaked in ethylene glycol. In the authors' laboratory, diethylene glycol monoethyl ether has been placed in the solvation strength series below ethylene glycol and above water by the observation that clay layers not expanded by water can be expanded by either diethylene glycol monoethyl ether or ethylene glycol, and those not expanding with either ether or water can be expanded by ethylene glycol.

The binding force between silicate layers is a result of a coulombic attraction between the negatively charged silicate layer and the positively charged interlayer ions. The negative charge on the silicate layer originates with isomorphism. Assuming that each negative charge on the silicate layer is neutralized by a singly charged interlayer cation, the binding force should be proportional to the number of interlayer cations per layer. This number of interlayer cations would be, in turn, equal to the product of the charge per unit area of surface (charge density) and the areal extent of each particle. Figure 1 is a graph showing a possible relationship among these three variables. The binding force is an increasing function of charge density. When charge density is low,

the effect of particle size on the binding force is small. For silicate layers that are more highly charged, the particle size exerts a strong control over the binding force acting between two silicate layers.

Assuming that there is a possible continuously varying charge on the silicate layer, hence a continuously varying number of cations between layers of a given size, it seems reasonable to consider that there would be natural clays with all possible interlayer binding strengths. For particles of uniform surface charge density, the binding force would vary directly with surface area of the particle.

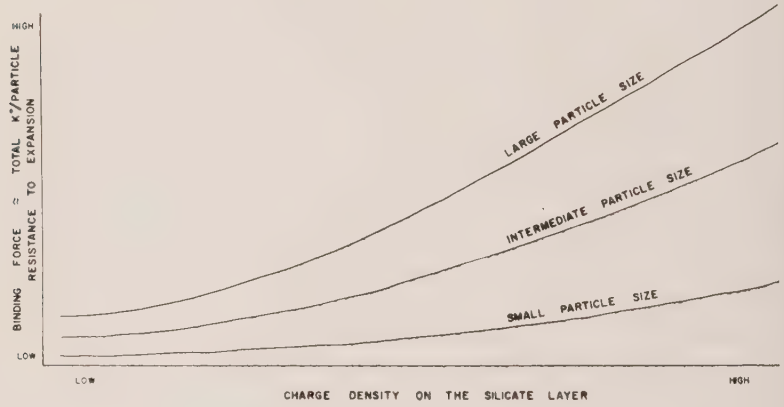

FIG. 1. A proposed relationship between resistance to expansion in three-layer clay minerals and charge density for varying particle size layers.

Besides being dependent on the number of interlayer ions, the binding force also depends on the *character* of the interlayer ions. There are in the literature numerous references to expanding three-layer clay minerals which will exchange potassium, contract to a 10 Å spacing, and resist expansion with water and ethylene glycol (Weaver, 1958a; Walker, 1950). The fact that many micaceous clay minerals will expand with Ca^{+2}, Mg^{+2}, or Na^{+1} as the interlayer ion but become non-expanding when K^{+1} occupies the interlayer position suggests that the binding force through potassium ions is much stronger than that through these other ions. Other clays can be supplied with an excess of K^{+1} to neutralize all of the charge sites and still never gather enough binding strength to develop a force sufficiently strong to prevent expansion with water. For these clays it has been assumed that the particles have a low charge density resulting from a low degree of isomorphous substitution, and therefore the number of potassium ions necessary to neutralize the charge deficiency on the clay particles would be so small as to preclude a

binding force of sufficient strength to render the layers non-expanding. However, it might also be argued that particles with high charge densities having very small areal dimensions would exhibit identical expansion properties after potassium saturation as particles with low charge densities. (See authors' scheme in Fig. 1.)

It may also be proper to assume that in any one natural sample there is a wide distribution of particle sizes. If this be the case, it is expected that particles in spite of having a uniform charge density would exhibit various expansion characteristics.

In dealing experimentally with a system in which there are many variables, the effects of one of the variables can only be viewed under conditions designed to hold the remainder of the variables constant. The variables which determine the expansion of a clay layer are (1) charge density on the silicate, (2) character of the interlayer ion, (3) the adsorbed liquid, and (4) the areal extent of the layer.

Charge density on the silicate layer can be eliminated as a variable if expansion properties are compared only on samples of a single clay mineral that has been variously treated in the laboratory. It must be assumed that the silicate layers are not altered in composition by the mild chemical laboratory treatments and therefore are not changed in charge density. The interlayer ion can be kept from varying by saturating all of the samples with K^{+1} before expansion properties are measured. If expansion properties among the variously treated samples are compared with only one solvating liquid, the effects of non-uniform adsorption forces can be avoided. These were the conditions selected to study the effect of particle size variation on the expansion of three-layer clay minerals, in the belief that they effectively held all the other controlling variables constant.

Procedure

The samples examined in this study were selected because their physical properties and chemical compositions were such that an induced change in particle size would possibly result in strikingly different expansion characteristics. It can be seen from Fig. 1 that only the relatively small particle size material is expanding when the layer charge has a high density; therefore, it would be of little value to grind a coarse-grained, well-crystallized mica or illite in an effort to produce an expanding material. The severe grinding necessary to reduce large particles to particles small enough to expand would have a tendency to damage the structure. Likewise, there would be little value in reducing the particle size of material with a low charge density. The resistance to expansion would already be low and would vary little with particle size. Size reduction would be unlikely to yield observable differences in expansion properties.

The authors have been particularly fortunate in having available for study two samples which are thought to have none of the undesirable properties just described. One sample (0–13) was selected because it was discovered that a great deal of the $<2\mu$ fraction is composed of a three-layer 15 Å clay mineral which will expand to 17 Å after ethylene glycol solvation and will also contract to a non-expanding 10 Å spacing after being treated with a 1 N KCl solution. It was reasoned that this expanding mineral could be characterized by a high charge density and a relatively large particle size. However, it should be pointed out that the expanding material in the 0-13 sample differs from illite (10 Å, non-expanding, K^{+1} irreversibly held in the interlayer position under normal laboratory ion exchange experiments) in that the 0–13 sample probably consists of particles which are smaller and/or possess a somewhat lower charge density. This may be suggested in view of the fact that the 15 Å material in the 0–13 sample, after having been rendered non-expanding by potassium saturation, may be re-converted into the expanding form by exchanging Ca^{+2} for K^{+2} in the interlayer position. This suggests a lower binding force through potassium for the material in the 0–13 sample than for normal illite. Material in the 0–13 sample could be ground while still in the expanded state as highly charged single layers of considerable areal extent. It is thought that size reduction by short-time grinding can be accomplished without severe damage to the silicate layer structure.

The other sample selected for study was an Ordovician metabentonite (8-ONY) of which the $<2\mu$ fraction is composed of approximately 80 to 90 per cent non-expanding layers and 10 to 20 per cent interstratified expanded layers. It was anticipated that short-time grinding of this sample would reduce the size of some of the particles to such an extent that they would no longer remain non-expanding after potassium saturation.

Recognizing that the individual particles of the 0-13 sample must cover a wide range of sizes, they therefore must possess varying total charges and binding forces. It was reasoned that separation of fine particles from relatively coarser ones might enable one to observe differences in expansion qualities. Following Hathaway's (1956) formula for centrifugal size separation, two size fractions ($1–2\mu$ and $<.5\mu$) were obtained. Separation of the natural sample into various size grades appeared to be a direct experimental approach to study the effect of particle size on expansion properties. Three problems detract from the utility of the data gathered from a size fractionation sequence and, in the authors' opinion, make the conclusions drawn from the data only tentative. These three problems are: (1) It is highly probable that all particles of a

specimen are never completely dispersed and that the size fractionation may be only a measure of the aggregate size instead of the size of the individual particle; (2) the composition of the particles may not remain constant through all the size grades, thus introducing a new uncontrolled variable; and (3) the character of the adsorbed ions, which have been shown to vary with the particle size fraction (McAtee, 1955; Roberson, 1959), would undoubtedly influence the expansion characteristics of the particles. With these difficulties in mind, it was decided that careful grinding over a short period of time would introduce fewer complications than size separations and would provide greater confidence in the experimental relationships observed.

Several attempts have been made to determine changes in physical properties which may be brought about by grinding clay minerals. Most of these investigations have been concentrated on measuring changes in the ion exchange capacity of clays after severe grinding. Kelley and Jenny (1936) have shown that the ion exchange capacities of muscovite, biotite, kaolinite, and montmorillonite may be greatly increased by grinding from 48 to 72 hours. Others (Laws and Page, 1946; Perkins, 1948; MacKenzie and Milne, 1953) have shown not only that the ion exchange capacities can be increased by grinding but also that long-time grinding seriously damages the structure of muscovite and kaolinite. The great increase in ion exchange capacity is attributed to the fact that grinding causes a decrease in particle size, an increase in surface area, and an increase in the number of broken bonds at particle edges. There appears to have been little attention directed toward detecting changes in the expansion properties of micaceous clays caused by short-time grinding.

Specimens weighing 0.50 grams were dispersed in a small volume of water and ground in a Bakelite capsule of a Wig-L-Bug. Wet grinding was preferred over day grinding because it was reasoned that particles in a disaggregated state would be thinner and more effectively reduced in size than thick packets of layers in the dry state. It also is possible to maintain a low temperature during wet grinding. The Wig-L-Bug was thought to be the best means of reducing the particle size without damaging the structure because grinding is effected by impact instead of shear, as produced by grinding with a mortar and pestle. The only apparent disadvantage of this grinding technique is the dilution of the clay by the addition of the fine particles of Bakelite from the cylinder.

The potassium treatments were carried out by suspending 0.50-gm. portions of the samples in 50 ml. of a 1 N KCl solution. The samples were allowed to stand overnight, concentrated after decantation, and washed three times with a total of 150 ml. of distilled water.

Ethylene glycol solvation was carried out in vapor at 60° C. overnight.

Heating to remove molecular interlayer water was carried out at 300° C. for one hour in an electric muffle furnace. The samples were then air-quenched and analyzed immediately.

Diffraction tracings show only the 00l peaks because oriented slides were prepared for analysis. Diffraction was registered with a GE XRD-3 with filtered CuKα radiation.

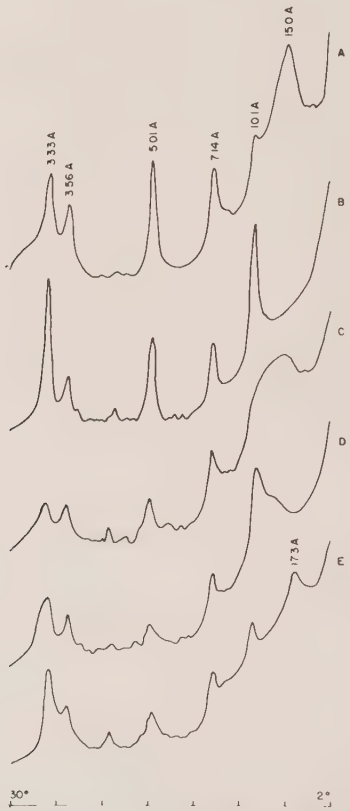

FIG. 2. Diffraction traces showing variable expansion properties for two size fractions of the three-layer clay mica (0–13).

A. 1–2 μ natural sample, hydrated at 50 per cent RH.

B. 1–2 μ potassium treated, expanded with ethylene glycol.

C. 0.1–0.3 μ natural sample, hydrated at 50 per cent RH.

D. 0.1–0.3 μ potassium treated, hydrated at 50 per cent RH.

E. 0.1–0.3 μ potassium treated, expanded with ethylene glycol.

RESULTS

Figure 2 shows clearly that the diffraction characteristics of material in the 1–2μ fraction of the 0–13 sample are quite different from those of

material in the 0.1–0.3μ fraction. The 1–2μ fraction of the sample is mainly composed of particles with a 15 Å spacing which expands to 17 Å after glycolation, non-expanding particles with a 10 Å spacing (illite), and kaolinite particles. The 0.1–0.5μ fraction contains less illite than does the 1–2μ fraction, indicating that many of the illite particles are relatively large. The diffraction tracing of the 0.1–0.3μ fraction also shows that the 15 Å peak is broad and asymmetrical, whereas the diffraction tracing of the 1–2μ fraction exhibits a rather sharp, symmetrical peak. The broadening and the asymmetry of the peak may be caused by an interlayering of Na^{+1} particles with Ca^{+2} particles. It has been shown that particles in the fine fractions of bentonites often carry a higher percentage of sodium ions as the exchange cation (McAtee, 1955; Roberson, 1959).

The most striking difference between coarse and fine fractions is shown after potassium treatment. After the particles in the 1–2μ fraction are treated with potassium their spacing is contracted to 10 Å, and expansion cannot be effected even with ethylene glycol. However, it can be seen that after potassium treatment of the particles in the fine fraction, there is still present some material which will expand with water and ethylene glycol. If it can be assumed that the composition does not change with particle size (*i.e.*, charge density remains constant), then it follows that the difference in expansion properties is directly related to variation in particle size. However, because of the difficulties inherent in size fractionation experiments which have been discussed previously, careful grinding of the 1–2μ fraction was undertaken to determine if size reduction by this means would produce the same results.

The diffraction patterns shown in Fig. 3 illustrate the effect of particle size reduction produced by short-time grinding of the 1–2μ fraction of sample 0–13. By comparing the patterns labeled 3A and 3B with the pattern labeled 2B, it can be readily observed that a considerable proportion of the particles in the 1–2μ fraction, which were initially non-expanding after potassium saturation, cannot be bound together strongly enough by interlayer potassium ions to resist expansion with water or ethylene glycol after being ground for one hour in the Wig-L-Bug. Because of the gentle conditions under which the grinding was performed, it is assumed that little or no composition change was brought about, and therefore the sole factor controlling expansion under these conditions is thought to be the size of the particles.

Figure 4 shows the effect of particle size reduction on the expansion properties of an Ordovician metabentonite (8-ONY). As can be seen from the tracings labeled 4A and 4B, the $<2\mu$ fraction of the natural sample consists of non-expanding layers randomly interstratified with expanding layers. After grinding for $1\frac{1}{2}$ hours, diffraction from two sep-

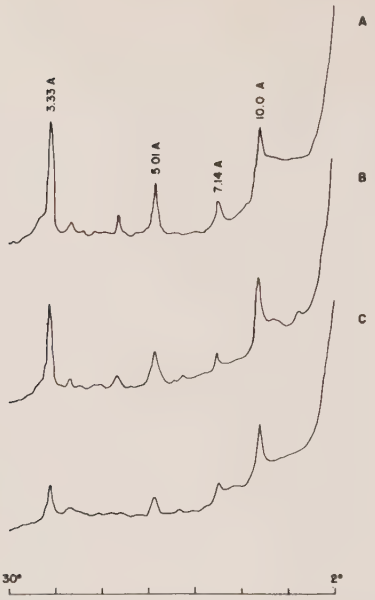

FIG. 3. Diffraction traces showing the expansion properties of the three-layer clay mica (0–13) after grinding 1 hour and potassium treatment.

A. Hydrated at 50 per cent RH.

B. Expanded with ethylene glycol.

C. Heated to 300° C.

arate phases—discrete non-expanding material and material which expands with water—is recorded. The expanding phase cannot be made non-expanding by potassium treatment. The ground material was heated to 300° C. to determine if the expanding material could be contracted to 10 Å. As can be seen from 4D, most of the expanding material collapsed to a 10 Å spacing.

SUMMARY

Jonas and Thomas (1959) have shown that as the effective surface charge density decreases in a series of clay micas of uniform particle size distribution, the interlayer binding force decreases. Those clay micas with effective high surface charge densities resist the expansion forces of even the strongest solvating agents. Clay micas with progressively lower effective surface charge densities yield to the expansion forces of strong solvating agents and continue to resist those of the weaker solvating agents. The clay micas with relatively low effective surface charge densities yield to the expansion forces of even weak solvating agents.

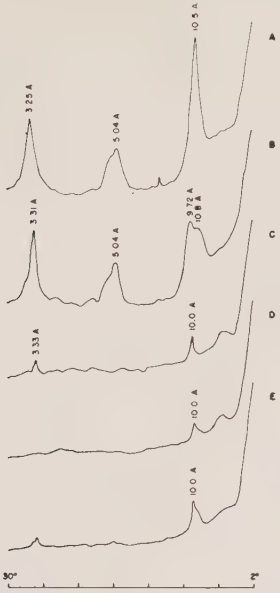

FIG. 4. Diffraction traces showing the effect of grinding on expansion properties of an Ordovician metabentonite (8-ONY).

A. Natural sample, hydrated at 50 per cent RH.
B. Natural sample, expanded with ethylene glycol.
C. 1½ hours grinding, hydrated at 50 per cent RH.
D. 1½ hours grinding, potassium treated, and hydrated at 50 per cent RH.
E. 1½ hours grinding, heated to 300° C.

Expansion properties of micas are also determined by particle size. The actual forces involved in separating the silicate layers during expansion cannot be measured directly. It is therefore not possible to write a specific formula for the relationship between interlayer binding force, surface charge density, and particle area. The relative strengths of the forces are clearly demonstrated by the expansion or lack of expansion. Effects of the two controlling factors are studied here and in the experiment by Jonas and Thomas outlined in the preceding paragraph.

In spite of the qualitative nature of the data, at present it is still possible to state that mica layers with a high surface charge density can expand provided they have a sufficiently small particle size. The belief that expanding clay micas are all of a lower surface charge density than non-expanding micas is, in the light of the foregoing reasoning, not well founded. There are undoubtedly many expanding clay micas whose surface charge density is erroneously judged to be low because of this property. With a fundamental relation between surface charge and isomor-

phism, any assumptions (based on expansion properties) concerning th composition should be only tentative.

Experimental observations of the effect of particle size on expansion properties of other clay mineral groups, such as vermiculite-chlorite montmorillonite-chlorite, and vermiculite-montmorillonite, might b fruitful in light of the data reported herein.

Acknowledgments

The authors wish to express their gratitude to C. E. Weaver for sup plying sample 0–13 and to H. D. Glass for supplying sample 8-ONY. A research grant from the National Science Foundation made the investiga tion possible.

References

Hathaway, J. C. (1956), Procedure for clay mineral analyses used in the sedimenta petrology laboratory of the U. S. Geological Survey: *Clay Minerals Bulletin*, **3,** 8–1

Johns, W. D., and Tettenhorst, R. T. (1959), Differences in the montmorillonite solva ing ability of polar liquids: *Am. Mineral.*, **44,** 894–896.

Jonas, E. C., and Thomas, G. L. (1959), Hydration properties of potassium deficie micas: *Seventh National Conference on Clays and Clay Minerals, Norman, Oklahon* (abstract).

Kelley, W. P., and Jenny, H. (1936), The relation of crystal structure to base-exchang and its bearing on base-exchange in soils: *Soil Sci.*, **41,** 367–382.

Laws, W. C., and Page, J. B. (1946), Changes produced in kaolinite by dry grindin *Soil Sci.*, **62,** 319–336.

MacKenzie, R. C., and Milne, A. A. (1953), The effect of grinding on micas. I. Musco vite: *Mineralogical Mag.*, **30,** 178–185.

McAtee, J. L. (1955), Heterogeneity in montmorillonite: *Proc. of the Fifth National Con ference on Clays and Clay Minerals, National Academy of Science-National Researc Council Pub.* **566,** 277–288.

Perkins, A. T. (1948), Kaolin and treated kaolins and their reactions: *Soil Sci.*, **65,** 185 192.

Roberson, H. E. (1959), Petrology of Tertiary bentonites of Texas: Ph.D. Thesis, Uni versity of Illinois.

Walker, G. F. (1950), Trioctahedral minerals in the soil clays of northeast Scotland *Mineralogical Mag.*, **29,** 72–84.

——— (1957), On the differentiation of vermiculites and smectites in clays: *Clay Mineral Bulletin*, **3,** 154–163.

——— (1958), Reactions of expanding lattice clay minerals with glycerol and ethylen glycol: *Clay Minerals Bulletin*, **3,** 302–313.

Weaver, C. E. (1958a), The effects and geologic significance of potassium "fixation" by expandable clay minerals derived from muscovite, biotite, chlorite, and volcani material: *Am. Mineral.*, **43,** 839–861.

——— (1958b), A discussion on the origin of clay minerals in sedimentary rocks: *Proc. o the Fifth National Conference on Clays and Clay Minerals, National Academy of Science National Research Council Pub.* **566,** 159–173.

Manuscript received October 11, 1959.

IRON-RICH MUSCOVITIC MICA FROM THE GRANDFATHER MOUNTAIN AREA, NORTH CAROLINA*

MARGARET D. FOSTER, BRUCE BRYANT, AND JOHN HATHAWAY,
U. S. Geological Survey, Washington 25, D. C.

ABSTRACT

The metamorphic arkoses and arkosic quartzites in the Grandfather Mountain area, North Carolina, contain green micas that have high indices of refraction with the β index ranging from 1.603 to 1.619. Detailed study of mica having the highest indices of refraction showed that it is dioctahedral in character, falling between muscovite and phengite in the trisilicic-tetrasilicic dioctahedral potassium mica series, with considerable proxying of Fe^{+3} for octahedral Al. The green color and high indices of refraction are attributed to the high iron content and to the presence of both Fe^{+3} and Fe^{+2} (8.11 per cent Fe_2O_3 and 2.55 per cent FeO).

INTRODUCTION AND REGIONAL GEOLOGY

In the course of geologic mapping in the Grandfather Mountain area, North Carolina, (one of us (B. B.)) observed rocks containing a fine-grained green mica. The green aspect of the rocks strongly suggests the presence of chlorite in addition to mica. However, thin section study showed that no chlorite is present; the green color of the rocks is due entirely to the mica. Preliminary optical study showed that the mica is muscovitic in type but has much higher indices of refraction than usual in such micas. The high indices of refraction, and the color, incited our interest in making a more detailed study of this mica.

The Grandfather Mountain area is on the eastern edge of the Blue Ridge province 56 miles northeast of Asheville, N. C. The area is underlain by early Precambrian basement rocks and late Precambrian and early Cambrian sedimentary and igneous rocks. These rocks are surrounded by early Precambrian schists, amphibolites, gneisses, and granitic rocks. Keith (1903) interpreted the structure of this area as a complex synclinal downfold bordered by opposing thrusts. A. I. Jonas and G. W. Stose (Geologic map of the U. S., 1932) first recognized this structure as a window, and the present workers agree with that interpretation. For a summary of the regional geology see King (1955).

Retrogressive metamorphism of the basement rocks has produced a cataclastic foliation and recrystallization with development of new biotite and albite in rocks of appropriate composition both within the window and in the upper plate adjacent to the window. Progressive metamorphism in the late Precambrian and early Cambrian rocks was of the same grade.

In the window two sequences of sedimentary rocks are recognized:

* Publication authorized by the Director, U. S. Geological Survey.

an autochthonous sequence unconformably overlying the basement rocks and an allochthonous sequence in thrust contact with members of the allochthonous sequence and the basement rocks (Reed and Bryant, 1958). The upper sequence consists of arkosic quartzite, phyllite, and quartzite underlying dolomite, which appears to be equivalent to the Shady dolomite of the Valley and Ridge province. The lower sequence consists of an interbedded and interlensing sequence of meta-arkose, calcareous biotite phyllite, phyllite, metasiltstone, metagraywacke, and greenschist.

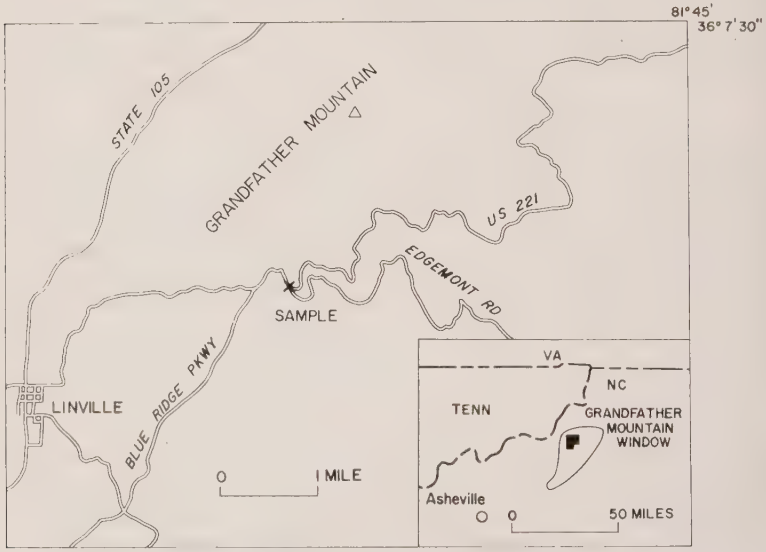

Fig. 1. Location of sample.

The Green Mica

Most of the metamorphosed arkoses and arkosic quartzites in both sequences contain green muscovitic mica; the rocks range from light greenish-gray to green. The β index of the mica from some of the greener rocks ranges from 1.603 in some specimens to 1.619 in others. A sample containing mica of the highest index of refraction found was chosen for further study.

The sample selected was collected from a roadcut on U. S. Highway 221 about 1,000 feet southeast of the junction with the Edgemont road on the southeast side of Grandfather Mountain one-half mile east of the crest of the Blue Ridge (Fig. 1). This specimen is a green micaceous arkosic quartzite from the lowest member of the autochthonous sequence.

The rock displays cleavage cutting bedding at an angle of 15°. Green mica is concentrated along the cleavage planes, which are as much as 2 mm. apart in the coarser beds. Quartz and microcline clasts up to 2 mm. and plagioclase clasts up to 0.7 mm. in diameter occur in a matrix of recrystallized quartz which has an average grain size of 0.1 mm. Feldspar at least as small as 0.1 mm. retains its clastic outline, whereas quartz as large as 0.3 mm. is recrystallized and participates in mosaic texture. The mica is well aligned parallel to the cleavage and from 0.02 to 0.5 mm. long. It includes aggregates of sphene and leucoxene.

Mode of sample

quartz	45.8
potassium feldspar	14.5
plagioclase	8.1
green mica	29.2
sphene and leucoxene	1.7
epidote	.3
apatite	.3
zircon	tr.

Optical properties

The green mica has the following optical properties:

$\alpha = 1.580 \pm 0.001$ (colorless)	$\gamma - \alpha = .043 \pm .01$
$\beta = 1.6195 \pm .0005$ (light green)	optic sign = negative
$\gamma = 1.6230 \pm .0005$ (light green)	$2V = 35° \pm 3°$

The indices were determined with Na light in oils graduated in two thousandths. The α index was determined on the spindle stage (Wilcox, 1959) and the optic axial angle by Mallard's method.

Separatory Procedure

The sample was crushed and divided into two fractions: 100–200 mesh and 200–400 mesh. The mica was separated by a process of repeated treatment in a Bendix ultrasonic transducer and separation in a Frantz isodynamic separator. Each fraction was treated for two 20-minute intervals in the ultrasonic transducer and run through the isodynamic separator with 25° forward tilt and 15° side tilt at 1.0 amperes. The magnetic fraction from this run was treated again in the transducer and run through the separator at 0.9 amperes. This process was repeated, at each run decreasing the amperage by about 0.1 ampere. The treatment in the ultrasonic transducer shredded the mica flakes and freed minute inclusions of sphene, quartz, and feldspar which went into suspension and were decanted.

An amperage of 0.55 separated the green mica from the less magnetic

constituents. This fraction was run again at 0.45 amperes to remove magnetite, yielding a concentrate of about 99% mica in the 200–400 mesh fraction, and about 98% in the 100–200 mesh fraction. The impurities were very fine grained, but were probably chiefly sphene and leucoxene.

X-RAY ANALYSIS

Both *x*-ray powder photographs and diffractometer patterns were used in the examination of the green mica. Two different diffractometers were used, operated at the following settings:

Radiation: Cu/Ni
KVP—40; MA—20
Scanning speed $\frac{1}{8}$° per minute
Low 2θ cutoff
Divergence slit 1°
Receiving slit 0.003 inch
Scatter slit 1°

Scale factor 4
Multiplier 1
Time constant 4
Sample length 20 mm.

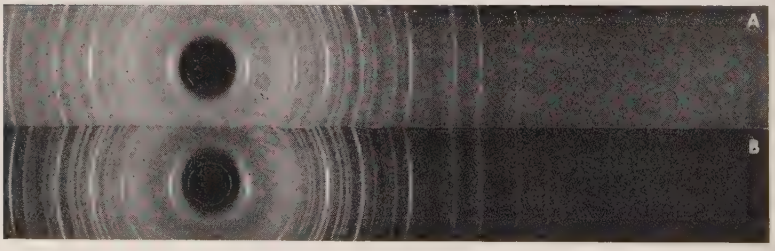

FIG. 2. *X*-ray powder photographs of: (A) Green mica from the Grandfather Mountain area, N. C., and (B) 2M Muscovite, Ontario 114.59 mm camera, CuKα, Ni filtered radiation.

The powder photographs were made of both relatively coarse and of finely ground material, with 114.59 mm. diameter cameras using exposures of about 12 hours.

The similarity between the green mica and 2M muscovite is shown in Fig. 2. Some slight differences may be noticed between the patterns, in particular the spacing of the 060 reflection. Other differences became apparent when an attempt was made to index the pattern by comparison with the muscovities listed in the ASTM *x*-ray diffraction data card file (1958). It was found necessary to calculate provisional unit-cell parameters using assumed indices. This unit cell is confirmed by the good agreement of the observed and calculated spacings shown in Table 1.

The a_0 and b_0 dimensions are larger than normal for muscovite, whereas the c_0 dimension is slightly smaller:

TABLE 1. *X*-RAY DATA FOR GREEN MICA FROM GRANDFATHER MOUNTAIN AREA, NORTH CAROLINA

a_0 5.249Å b_0 9.064Å c_0 19.991Å $\beta = 95°45'$

hkl	*d* (calc.)	*d* (obs.)	I/I_1	*hkl*	*d* (calc.)	*d* (obs.)	I/I_1
002	9.945	9.958	100[1]	$12\cdot\bar{1}\bar{1}$	1.6440	1.6442	5
004	4.972	4.972	19[1]	$31\bar{5}$	1.6298	1.6276	8
110	4.525	4.525	50	228	1.6054	1.6047	14
$11\bar{1}$	4.497	4.498	73	049	1.5822	1.5818	5
021	4.419	4.421	18	155	1.5546	1.5608	13
111	4.331	4.326	20	$13\cdot10$	1.5462	1.5456	5
022	4.124	4.130	15	$13\cdot\bar{1}\bar{1}$	1.5235	1.5239	20
112	3.990	3.992	10	060	1.5108	1.5107	36
$11\bar{3}$	3.898	3.897	51	$24\bar{7}$	1.5105		
023	3.742	3.748	46	331	1.4952	1.4939	2
113	3.595	3.590	8	061	1.4937		
$11\bar{4}$	3.501	3.501	75	335	1.4527	1.4515	15
024	3.350	3.349	85	$15\bar{8}$	1.4326	1.4316	8
006	3.315	3.316	100[1]	$00\cdot14$	1.4206	1.4198	12[1]
114	3.211	3.208	94	$33\bar{6}$	1.4201		
115	3.126	3.120	14	$11\cdot13$	1.4126	1.4112	10
025	2.990	2.993	100	065	1.4123		
115	2.867	2.864	79	158	1.3892	1.3882	5
$11\bar{6}$	2.793	2.792	64	066	1.3747	1.3757	8
200	2.611	2.612	29	$13\cdot\bar{1}\bar{3}$	1.3504	1.3506	44
$13\bar{1}$	2.610			$04\cdot12$	1.3378	1.3376	31
131	2.576	2.579	90	$11\cdot14$	1.3230	1.3223	15
$11\bar{7}$	2.506	2.504	20	$22\cdot13$	1.3217		
132	2.499			400	1.3055	1.3042	21
008	2.486	2.486	12[1]	$20\cdot14$	1.3040		
204	2.413	2.409	32	$13\cdot13$	1.2926	1.2931	7
027	2.407			$04\cdot13$	1.2680	1.2689	8
133	2.392	2.394	36	170	1.2569	1.2568	9
134	2.268	2.266	12	$35\bar{2}$	1.2571		
040	2.266			351	1.2475	1.2485	5
135	2.237	2.242	9	$00\cdot16$	1.2431	1.2431	9[1]
204	2.222	2.217	7	173	1.2295	1.2289	4
$20\bar{6}$	2.159	2.158	18	353	1.2177	1.2174	10
135	2.137	2.139	36	$35\bar{7}$	1.1804	1.1807	3
223	2.087	2.081	4	$22\cdot14$	1.1587	1.1580	8
044	2.062	2.060	3	$11\cdot\bar{1}\bar{7}$	1.1573		
$22\bar{5}$	2.044	2.043	5	$24\cdot\bar{1}\bar{4}$	1.1302	1.1294	8
$24\bar{3}$	1.9897	1.9897[2]	80[1]	357	1.1190	1.1194	5
$00\cdot10$	1.9889			$31\cdot12$	1.1189		
$13\bar{7}$	1.9742	1.9741	55	083	1.1169	1.1175	4
$22\bar{6}$	1.9491	1.9517	21	$22\cdot17$	1.0781	1.0776	3
$11\cdot\bar{1}0$	1.8819	1.8830	8	$35\cdot\bar{1}\bar{1}$	1.0681	1.0677	2
$13\bar{8}$	1.8488	1.8471	3	$20\cdot\bar{1}\bar{8}$	1.0563	1.0566	4
$02\cdot10$	1.8213	1.8195	5	$13\cdot17$	1.0485	1.0483	14
$22\bar{8}$	1.7506	1.7480	10	429			
$11\cdot\bar{1}\bar{1}$	1.7316	1.7314	13	$33\cdot\bar{1}5$	1.0417	1.0416	3
$13\bar{9}$	1.7313			$51\bar{1}$	1.0416		
$31\bar{2}$	1.7131	1.7134	13	282	1.0296	1.0296	5
150	1.7127			$37\bar{4}$	1.0294		
227	1.6995	1.6998	8	373	1.0172	1.0173	2
$20\cdot10$	1.6646	1.6631	30	$33\cdot\bar{1}6$	1.0029	1.0028	2
312	1.6577	1.6578	10[1]	$11\cdot\bar{2}0$	.98944	.98961	10
$00\cdot12$	1.6574			Plus at least 22 additional weak lines.			
139	1.6477	1.6485	64				

[1] The strongest 00*l* and *hkl* lines were each assigned an intensity of 100 because preferred orientation could not be eliminated in the specimens used and the true intensity relationships between 00*l* and *hkl* reflections could not be determined. The intensities of all of the 00*l* reflections are relative to the 002.

[2] $\lambda = 1.54050$Å for this and all smaller spacings. For large spacings $\lambda = 1.5418$Å.

	a_0	b_0	c_0	β
Green mica	5.249 Å	9.064 Å	19.991 Å	95°45′
Muscovite[1]	5.19 Å	9.03 Å	20.05 Å	95°46′
Synthetic 2M muscovite[2]	5.189 Å	8.995 Å	20.097 Å	95°11′

The b_0 dimension calculated from the structural formula of the green mica by the method described by Brown (1951, p. 160, 161) is in good agreement with the observed b_0.

Calculated: $b_0 = 9.066$Å
Observed: $b_0 = 9.064$Å

A further difference between the green mica and normal muscovite lies in the relative intensities of the 00*l* reflections:

		I/I_1	
	002	*004*	*006*
Green mica (oriented aggregate)	100	19	100
Muscovite[1]	95	31	100
Synthetic 2M muscovite[2]	>100	55	>100

The intensities I/I_0 for a mica having the composition of the green mica calculated by the method of Brown (1955) for an oriented aggregate in which 8 per cent of the particles behave as a randomly oriented powder (amount necessary to produce equal 002 and 006 intensities) are as follows:

3 Al:1 Fe in octahedral coordination: *002*(100); *004*(23); *006*(100).

As more iron would tend to depress the intensity of the 004 reflection and the green mica studied has slightly more total iron than the 3:1 ratio used in the calculation, the observed intensity of 19 (for 004) is in good agreement with that calculated.

The *x*-ray data for the green mica reveal a larger a_0 and b_0 but slightly smaller c_0 than for the usual muscovite. The b_0 dimension and the relative intensities of the 00*l* reflections are in close agreement with those calculated for a material of the composition of the green mica.

Chemical Composition

The chemical analysis of the green mica was carried out by standard methods by one of us (MDF) except for determination of Na and K, which were made by means of the flame photometer by Ivan Barlow U. S. Geological Survey. The analysis, which is given in the first column of Table 2, shows the presence of a small amount of TiO_2 and CaO. As the sample contains a small amount of impurities, which are probably

[1] Gillery, 1956.
[2] Yoder and Eugster, 1955, p. 246.

Table 2. Analysis of Green Mica

	As determined	Constituents in mica	Adjusted to 100 per cent
SiO_2	47.28	47.08	47.62
TiO_2	.30	—	—
Al_2O_3	24.46	24.46	24.74
Fe_2O_3	8.02	8.02	8.11
FeO	2.52	2.52	2.55
MgO	1.86	1.86	1.88
MnO	.08	.08	.08
CaO	.14	—	—
Na_2O	.11	.11	.11
K_2O	10.6	10.6	10.72
H_2O	4.00	4.00	4.05
F	.14	.14	.14
Total	99.51	98.87	100.00
$-O=F$	.06		
	99.45		

Specific gravity 2.879.

chiefly sphene and leucoxene, the TiO_2 and CaO reported in the analysis are attributed to these impurities. Sphene and leucoxene also contain SiO_2, consequently 0.20 per cent SiO_2 was deducted from the SiO_2 reported as attributable to these impurities. The adjusted analysis, calculated to 100 per cent, given in Table 2 column 3, yields the following calculated formula for the green mica,

$$[\underbrace{(Al_{1.27}Fe^{+3}_{.42}Fe^{+2}_{.15}Mg_{.19})}_{2.03}(Si_{3.27}Al_{.73})O_{10}(OH)_2]^{-.98}(K_{.94},Na_{.02})^{+.96}_{.96}$$

The points of particular interest in this formula, as compared to that of muscovite,

$$[Al_{2.00}(Si_{3.00}Al_{1.00})O_{10}(OH)_2]^{-1.00}K^{+1.00}_{1.00},$$

are, (1) the octahedral-tetrahedral charge relation, (2) the higher Si and lower tetrahedral Al, (3) the number of octahedral sites occupied by bivalent cations, and (4) the relatively high Fe^{+3} content.

The composition of some of the high silica sericites and their relation to muscovite was explained by Schaller (1950, p. 407–415) as due to their being members of a trisilicic-tetrasilicic series. Foster (1956, p. 67–77) showed that this series, of which muscovite is the trisilicic end member,

is characterized by a gradual shift in the seat of the inherent unit charge from the tetrahedral layers to the octahedral layer. This shift is brought about by the replacement of octahedral aluminum by bivalent cations, usually Fe^{+2} and Mg. As this replacement is ion for ion, and the total number of octahedral cations remains the same, there is a deficiency in positive octahedral charges necessary to neutralize the anions associated with this layer, and it develops a negative charge, this charge being the greater the greater the replacement of trivalent cations by bivalent cations. Coincident with this replacement and the development of a negative charge on the octahedral layer, there is an equivalent decrease in the negative tetrahedral charge, due to increase in Si and decrease in tetrahedral Al. Replacement of half the octahedral trivalent cations by bivalent cations produces the tetrasilicic end member, in which all the inherent unit-layer charge is on the octahedral layer, and the tetrahedral layers, completely filled by Si, are neutral, as illustrated below:

$$\overset{.00}{[Al_{2.00}}(\overset{-1.00}{Si_{3.00}Al_{1.00}})O_{10}(OH)_2]^{-1.00}K^{+1.00}_{1.00}, \text{ (muscovite);}$$

$$\text{(phengite), } [\underbrace{(R^{+3}_{1.50}R^{+2}_{.50})}_{2.00}(\overset{-.50}{Si_{3.50}Al_{.50}})O_{10}(OH)_2]^{-1.00}K^{+1.00}_{1.00};$$

$$\text{(celadonite), } [\underbrace{(R^{+3}_{1.00}R^{+2}_{1.00})}_{2.00}\overset{.00}{Si_{4.00}}O_{10}(OH)_2]^{-1.00}K^{+1.00}_{1.00}.$$

In the formula for the green mica from the Grandfather Mountain area, North Carolina, about one-fourth of the negative inherent unit-layer charge of 0.98 is on the octahedral layer—three-fourths on the tetrahedral layers. Thus this mica falls about halfway between muscovite and phengite in its octahedral-tetrahedral charge relationship. The R^{+2} ions responsible for the octahedral charge are made up almost equally of Mg and Fe^{+2}.

Trivalent iron and total iron are much higher than is usually found in micas in the muscovite-phengite part of the series. As Foster has pointed out, this end of the series is characterized by aluminum; it is the tetrasilicic end of the series that is characterized by iron both ferric and ferrous. No analysis of a muscovitic mica was found in the literature that contained as much Fe_2O_3, or as much total iron as Fe (7.57 per cent) as was found in this specimen. The highest Fe_2O_3 recorded is in an analysis reported by Clarke (1908, p. 286), which reports 6.10 per cent Fe_2O_3. However, as no FeO is reported, this figure probably represents total iron as Fe_2O_3 and not necessarily that present as Fe_2O_3. Total iron as Fe in this analysis is 4.27 per cent, an amount lower than that

found in an analysis reported by Ginzburg (1920, p. 9), which contains 5.64 per cent Fe_2O_3, and 1.27 per cent FeO. Total iron as Fe in this analysis is 4.94. A third analysis (Tolman and Goldich, 1935, p. 236) has a higher total iron as Fe content, 5.54 per cent, but is lower in Fe_2O_3, 3.94. Thus the mica herein studied is unique, for its position in the series, in its content of Fe_2O_3 and of total Fe.

Relation between Indices of Refraction and Iron Content

Winchell (1951, p. 368) concluded that the mean index (that is, the intermediate principal index, β) of muscovitic micas increases rapidly with increase in ferric iron content. Volk (1939, p. 263) agreed with Winchell's conclusion. Both Winchell and Volk used a three component diagram for plotting end member compositions of which the micas studied were presumed to be composed, Winchell using the end members muscovite, $KAl_2(Si_3Al)O_{10}(OH)_2$, ferrimuscovite, $K(AlFe^{+3})(Si_3Al)O_{10}(OH)_2$, and picrophengite, $K(Al_{1.5}Mg_{0.5})(Si_3Al)O_{10}(OH)_2$, and Volk using the end members muscovite, ferrimuscovite, and phengite $K[Al(Fe^{+2}Mg)](Si_3Al)O_9(OH)_3$. Of these end members only muscovite occurs in nature; the others, ferrimuscovite, picrophengite, and phengite are hypothetical and were postulated for the purpose of interpreting the composition of dioctahedral micas in terms of end members. However, neither Winchell's nor Volk's diagram showed a close relationship between ferric iron content and mean index; both showed considerable scatter of points. None of their micas had as high an index nor as high a content of ferric iron as the green mica herein studied. The relation between the β index and Fe_2O_3, in terms of molecular equivalents and between the β index and (Fe_2O_3+Fe), in terms of molecular equivalents in a number of muscovitic micas is shown in Fig. 3. The unnumbered points in this diagram represent micas used by Volk that contained both Fe_2O_3 and FeO; the numbered points represent some muscovitic micas reported in the literature for which both analyses and indices of refraction are given. The numbers refer to analyses given in Table 3. Although a very general trend toward increase in β index with increase in Fe_2O_3 and with increase in (Fe_2O_3+FeO) content is suggested, the relationship is not close and it would not be feasible to try to predict even the approximate iron content from the β index or vice versa for muscovitic micas. However, the points representing the much higher β index and iron content of the North Carolina mica are in line with the general upward trend of the points representing these properties in other micas.

Cause of Color

A semiquantitative spectrographic analysis by John C. Hamilton of the U. S. Geological Survey, shows that the green mica from North

Carolina contains between 0.002 and 0.005 per cent V, between 0.001 and 0.002 per cent Ni, between 0.0005 and 0.001 per cent Cr, and between 0.0002 and 0.0005 per cent Cu. The amounts of these elements present seem too low to account for the color, and Fe remains the most probable cause of the green color in this mica.

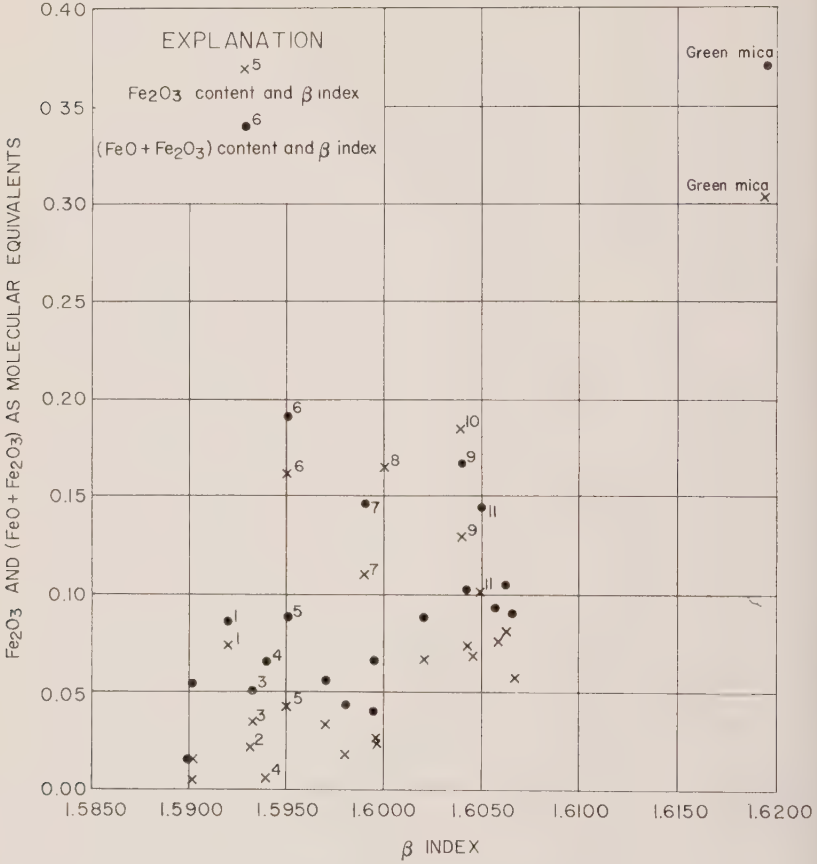

FIG. 3. Relation between Fe_2O_3 and $(FeO+Fe_2O_3)$ content and β index in muscovite micas.

Fersman (1937, p. 201-204) showed that the color of many minerals depends on the relative proportions of different valences of the same atom. Thus, he states that Fe^{+2} alone is characterized by yellow-green, and Fe^{+3} alone by reddish brown, but that both ions in the same mineral depresses the color to a deep blue or black. Grigoriev and Kotulsky (1941) also found that the presence of Fe^{+2} and Fe^{+3} together produces a

TABLE 3.—ANALYSES OF MUSCOVITIC MICAS, OTHER THAN VOLAS, USED IN PREPARING FIG. 2
ARRANGED IN ORDER OF INCREASING β INDEX

	Per cent										
	1	2	3	4	5	6	7	8	9	10	11
SiO_2	45.56	44.87	45.12	44.77	45.50	45.84	50.79	43.67	44.73	46.10	45.66
TiO_2	0.47	0.02	0.51	0.00	0.20	—	1.10	0.72	0.34	2.04	0.31
Al_2O_3	35.78	37.72	34.19	35.36	33.20	31.11	26.53	29.76	30.67	30.54	31.80
Fe_2O_3	1.92	.54	.85	.28	1.03	4.31	2.94	4.36	3.42	3.43	2.69
FeO	.51	none	.64	2.13	1.41	1.06	1.34	none	1.42	1.96	1.53
MnO	.11	trace	.02	.15	.04	.04	.05	.59	.02	.00	—
MgO	.94	.32	.92	.87	.96	1.10	2.80	1.19	1.56	1.71	.92
CaO	—	.36	.25	.00	trace	trace	—	.06	none	.07	.09
Na_2O	1.07	1.04	.71	.95	.52	2.27	1.01	.54	.53	3.82	.60
K_2O	10.03	9.83	10.33	10.81	10.49	9.66	9.71	10.00	10.18	6.54	10.34
H_2O^-	3.72	.38	1.57	4.54	1.10	4.49	3.90	2.24	1.43	3.83	.36
H_2O^+		4.72	5.05		5.37			6.28	5.17		5.32
F	—	n.d.	.05	.15	.18	.15	—	.95	.02	.05	.37
Total	100.11	100.24[1]	100.32[2]	100.01	100.12[3]	100.03	100.17	100.41[4]	100.23[5]	100.09	99.99
β index	1.592	1.5930	1.5932	1.5938	1.595	1.595	1.599	1.595–1.607	1.604	1.604	1.605–1.606

[1] Includes 0.27 per cent Cr_2O_3, 0.09 per cent V_2O_3, 0.08 per cent P_2O_5, and trace of Li_2O.
[2] Includes 0.01 per cent V_2O_3 and 0.10 per cent P_2O_5.
[3] Includes 0.04 per cent BaO, 0.05 per cent P_2O_5, and 0.03 per cent S.
[4] Includes 0.05 per cent BaO.
[5] Includes 0.66 per cent BaO, 0.02 per cent V_2O_3, 0.03 per cent P_2O_5, and 0.03 per cent S.

1. Claro, Tessin, Jakob, 1925, p. 445, no. 11.
2. Whitcombe Valley, Mikonui, New Zealand, Hutton, 1940, p. 330B.
3. Duffer Creek, Westland, New Zealand, Hutton, 1940, p. 330B.
4. Finnbo, Dalecarlia, Sweden, Eckermann, 1927, p. 231.
5. Mariner's Peak, South Westland, New Zealand, Hutton and Seelye, 1945, p. 161.
6. Mansjö Mountain, Sweden, Eckermann, 1927, p. 231.
7. Rossa, Val Calanca, Tessin, Jakob, 1925, p. 445, no. 18.
8. Ultevis district, Jokkmokk, Sweden, Ödman, 1950, p. 18.
9. Henry Pass, George Sound, New Zealand, Hutton and Seelye, 1945, p. 161.
10. Wissahickon Valley, Philadelphia, Pa., Postel and Adelhelm, 1944, p. 285.
11. Mattawan Township, Nipissing District, Ontario, Ferguson, 1943, p. 40.

darker color than either alone. Depth of color produced by Fe^{+2} and Fe^{+3} together, or by either alone, also depends on the amounts present. Another factor affecting the color produced by coloring ions in minerals is crystal structure (Grum-Grzhimailo, 1945, p. 933–46). Iron is responsible for green colors in biotites (Hall, 1941, p. 29–33) and for the green color in glauconite. In both of these minerals Fe is usually present both as Fe^{+2} and Fe^{+3}. Wyoming bentonite, which consists almost entirely of montmorillonite, is olive-green when Fe^{+3} predominates over Fe^{+2}, but is blue-gray when Fe^{+2} predominates over Fe^{+3} (Foster, 1956, 1003). In glauconite also, Fe^{+3} is ordinarily in excess of Fe^{+2}. As these minerals have the same crystal structure as the mica from North Carolina, it is concluded that its green color is due to the presence of both Fe^{+3} and Fe^{+2}, with Fe^{+3} predominant over Fe^{+2}.

Summary

A detailed study of a green mica associated with metamorphosed arkoses and arkosic quartzites in the Grandfather Mountain area, North Carolina, showed it to be a dioctahedral potassium mica about midway between muscovite and phengite in its layer charge relationship. For its place in the trisilicic-tetrasilicic dioctahedral mica series, this mica is unusually high in content of ferric iron and of total iron. Its high indices of refraction are attributed to this high iron content, and its color is attributed to the presence of both Fe^{+3} and Fe^{+2} in the structure, with Fe^{+3} predominant over Fe^{+2}.

Acknowledgments

Our appreciation is expressed to John C. Reed, Jr., coworker on the Grandfather Mountain project, and to Leonard B. Riley, both of the U. S. Geological Survey, for their encouragement and interest.

References

Brown, G. (1951), The mica clay minerals, Part II Nomenclature of mica clay minerals: *in* G. W. Brindley, ed., X-ray identification and crystal structures of clay minerals: London, The Mineralogical Society, 155–172.

——— (1955), The effect of isomorphous substitutions on the intensities of (00*l*) reflections of mica- and chlorite-type structures: *Mineralog. Mag.* **30,** 657–665.

Clarke, F. W. (1910), Analyses of rocks and minerals from the laboratory of the United States Geological Survey, 1880–1908: *U. S. Geol. Survey Bull.* **419,** p. 286.

Eckermann, Harry von (1927), The optical and physical properties of two Swedish muscovites: *Geolog. Fören. Stockholm Förh.* **49,** 229–234.

Ferguson, R. B. (1943), Muscovite from Mattawan Township, Nipissing District, Ontario: *Univ. Toronto Studies, Geol. ser. no.* **48,** 31–41.

Fersman, A. E. (1937), The color of minerals: *Acad. sci. U.S.S.R. Comptes rendus,* **17,** 201–204.

Foster, M. D. (1956), Correlation of dioctahedral potassium micas on the basis of their charge relations: *U. S. Geol. Survey Bull.* **1036-D,** 67–77.

Gillery, F. H. (1956), Muscovite: X-ray powder data file Am. Soc. for Testing Materials, Philadelphia, cards 6-0263, 6-0264; *X-ray powder data file* **1958,** *Am. Soc. for Testing Materials, Philadelphia.*

Ginzburg, I. I. (1920), Mica, its properties, application, and distribution in Russia, Materials to the knowledge of the natural productive forces of Russia: *Petrograd, no.* **34,** 128 p., 40 figs.

Grigoriev, D. P., and Kotulsky, A. V. (1941), Diagram showing dependence of coloration of magnesian-ferriferous micas on the content of iron oxides: *Akad. Nauk. S.S.S.R. Doklady* **31,** 691–693.

Grum-Grzhimailo, S. (1945), The effect of the structure of crystals on the color produced by chromium, manganese, iron, nickel, cobalt, and copper: *Acta Physicochim. U.R.S.S.,* **20,** 933–946.

Hall, A. J. (1941), The relation between colour and chemical composition in the biotites: *Am. Mineral.* **26,** 29–33.

Hutton, C. O. (1940), Optical properties and chemical composition of two micas from Westland, South Island, New Zealand: *New Zealand Jour. Sci. and Technology, no. 6B,* **21,** 330B–331B.

Hutton, C. O., and Seelye, F. T. (1945), Contributions to the mineralogy of New Zealand, Part 1: *Roy. Soc. New Zealand Trans.* **75,** 160–168.

Jakob, Johann (1925), Beiträge zur chemischen Konstitution der Glimmer. II. Mitt.- Die Muskovite der Pegmatite, I. *Zeits. Kriste.* **62,** 443–453.

Keith, A. (1903), Description of the Cranberry quadrangle (N. C.-Tenn.): *U. S. Geol. Survey Geol. Atlas, Folio* **90.**

King, P. B. (1955), A geologic section across the southern Appalachians -an outline of the geology in the segment in Tennessee, North Carolina, and South Carolina, *in* Russell, R. J., ed., Guides to southeastern geology, p. 332–37, geol. map.

Ödman, O. H. (1950), Manganese mineralization in the Ultevis district, Jokkmokk, north Sweden. Part 2: Mineralogical notes: *Sveriges Geolog. Undersökning Årsbok,* **44,** 28 p.

Postel, A. W., and Adelhelm, William (1944), White mica in the Wissahickon complex: *Am. Mineral.* **29,** 279–290.

Reed, J. C., Jr., and Bryant, Bruce (1958), Stratigraphy of the western part of the Grandfather Mountain window, North Carolina (abs.): *Geol. Soc. Amer. Bull.* **69,** 1633.

Schaller, W. T. (1950), An interpretation of the composition of high-silica sericites: *Mineralog. Mag.* **29,** 406–415.

Tolman, C., and Goldich, S. S. (1935), The granite, pegmatite, and replacement veins in the Sheahan quarry, Graniteville, Missouri: *Am. Mineral.* **20,** 236.

Volk, G. W. (1939), Optical and chemical studies of muscovite: *Am. Mineral.* **24,** 255–266.

Wilcox, R. E. (1959), Use of the spindle stage for determination of the principal indices of refraction of crystal fragments: *Am. Mineral.* **44,** 1272–1293.

Winchell, A. N., and Winchell, H. (1951), Elements of optical mineralogy, Part II, 4th end.: John Wiley and Sons, Inc., New York, 368.

Yoder, H. S., and Eugster, H. P. (1955), Synthetic and natural muscovites: *Geochim. et Cosmochim. Acta,* **8,** 225–280.

Manuscript received September 1, 1959.

MULTIPLE GROWTH TWINNING IN $BaTiO_3$ SINGLE CRYSTALS

R. C. De Vries, *General Electric Research Laboratory, Schenectady, New York*

Abstract

A novel form of multiple growth twinning in $BaTiO_3$ single crystals is described. The crystal contains three (111) primary twin planes and one (115) secondary twin interface. The twinned crystal appears to have grown from a nucleus which contained all the twin elements and not by successive twinning separated by intervals of growth. From a hard sphere model of the various forms of growth twinning in $BaTiO_3$, it is suggested that TiO_6 octahedra can share up to two faces.

Introduction

The purpose of this paper is to describe a novel form of multiple (111) growth twinning (spinel type) in $BaTiO_3$; to propose some ideas relative to its origin; and to call attention to the type of packing of TiO_6 octahedra necessary for multiple twinning in this compound as deduced from a hard sphere model.

Description of the Twin Crystal

A twin crystal which is occasionally found in the crystal assemblage grown from a supersaturated KF-$BaTiO_3$ solution (the Remieka (1954) technique) is illustrated in plan and perspective views, and photographs of the crystals are shown in Fig. 1.

The crystal can be considered as consisting of a twinned spine from which have grown flat plates bounded by {100} faces.* The (111) plane is both the twin plane and composition plane just as has been described for the more common "butterfly" twin. Curien and LeCorre (1955) and White (1955). The plates are identical to the wings of the usual butterfly twin crystals; contrary to the latter, the wings are not paired but alternate right and left along the axis. When viewed down the axis of the spine a V-shaped cross section is seen if the wing growth is approximately equal on both sides (upper plan view, Fig. 1*a* and Fig. 1*b*). In many crystals however, the wing has grown essentially on only one side (lower plan view, Fig. 1*a* and Fig. 1*c*); *i.e.*, in the plan view the wings on one side are very poorly developed. The terminal end of the spine is a (110) plane common to all members of the twinned crystal. In Fig. 2 are shown {110} sections taken along the length of the spine and transverse to the spine axis of a typical multiple twin. The sections were etched and polished simultaneously using a technique described by Kontoleon and

* $BaTiO_3$ is tetragonal at room temperature, but the crystals are grown in the stability region of the cubic phase and all discussion is in terms of the cubic system.

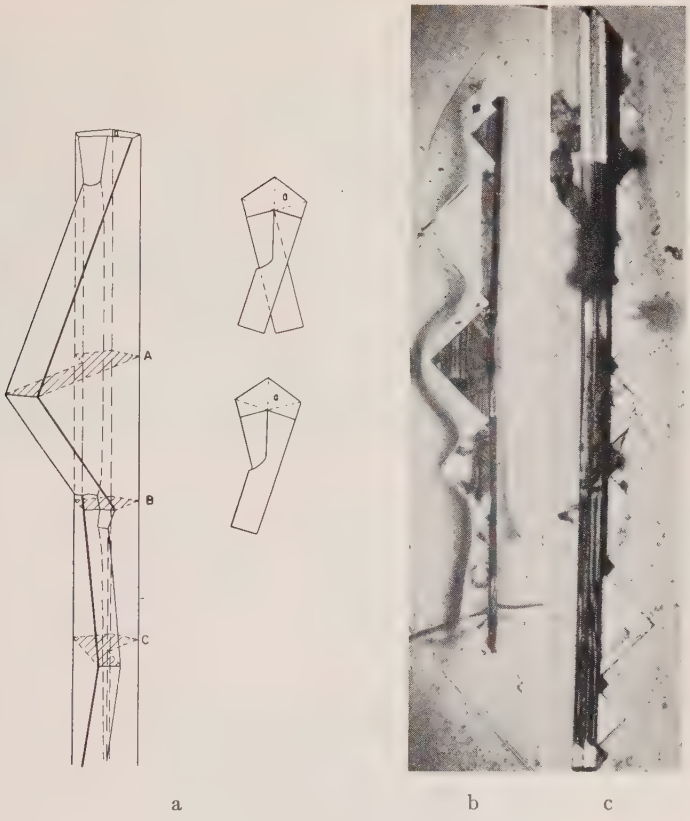

FIG. 1(a). Plan and perspective views of a multiple twin of $BaTiO_3$. The position of the (111) twin planes are shown as light dashed lines in the plan view only. A, B, and C are the approximate locations of the sections in Fig. 2. With the exception of the face "*a*" which is a (110) plane, all planes are {100}.

(b and c).—Side views of actual twinned crystals. (b) Wing development approximately equal. The small triangular wing at the top points into the plane of the paper; the wing below is tilted slightly up from this plane and so on down the length of the crystal. ×33. (c) Wing development very unequal. The large plates point slightly into the plane of the paper; these alternate with the small wings which are tilted upward. ×140.

Hurd (1956). The sections illustrate the change in crystal shape from one wing to the next where the wing development is approximately equal; Fig. 2b is essentially a section of the spine alone. Three {111} twin plane traces (made visible by etching) divide the crystal into four parts and the relationship to the usual butterfly twin (two twin plane traces) is made clear by comparison with Fig. 3, which is a similar polished section of a typical butterfly twin.

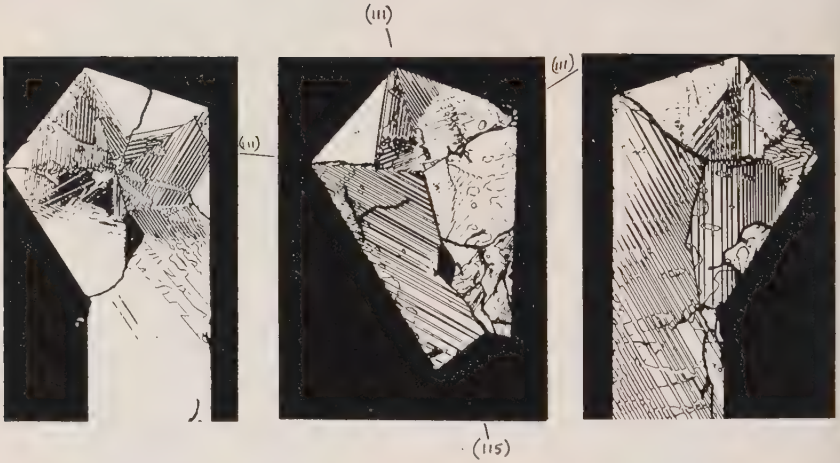

FIG. 2. Polished and etched sections of a multiple twin. Approximate positions of the sections relative to the crystal are given in Fig. 1. The main features of interest to the discussion are indicated. The fine twin structures which show discontinuities at the (111) and (115) traces are (101) tetragonal twins. ×210.

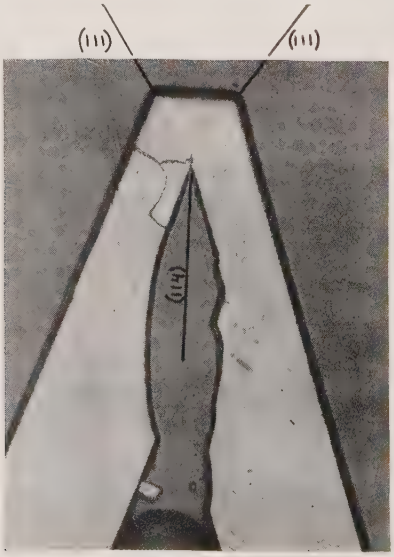

FIG. 3. Cross-section of a typical "butterfly" twin crystal with two (111) twin planes. The "wings" do not converge to form an interface as in the twin with three twin planes. ×50.

In contrast to the usual butterfly twin in which an interface between the wings does *not* develop DeVries (1959) (the most simple interface would be (114)), in the multiple twin under consideration, rapid growth in a [110] direction of the outer wings causes them to converge and a crystallographic interface (115) is formed. As a result, the two outer members of the multiple twin are related as if they were twinned across this plane. As would be expected this interface etches much more easily than the lower energy (111) twin interface. The length of the (115) trace as seen on {110} sections (Fig. 2) varies from a maximum near the region between alternate wings to a minimum near the center of a

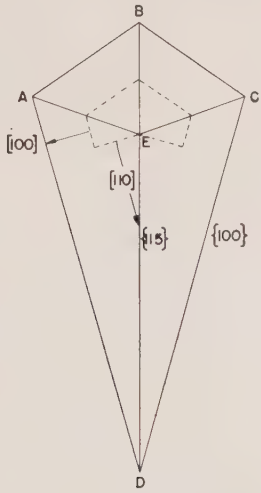

FIG. 4. Ideal cross-section of the multiple twin. AE, BE and CE are traces of (111) twin planes; DE is the trace of a (115) plane. The form described by dashed lines is considered in the text. All external faces are {100}.

wing; in contrast to this variation the length of the {111} traces is essentially constant throughout the length of the crystal. A cavity is often found at the end of the (115) trace (but none has ever been found at the intersection of the twin traces), and the remainder of the grain boundary between the outer members of the twinned crystal is usually noncrystallographic, although occasionally the interface is more regular as seen in Fig. 2a.

As a result of the geometry of the spinel type twinning in the multiple twin of $BaTiO_3$, the (115) interface is coincident with the central (111) twin plane. The traces of these planes are conveniently shown on a (110) section because all the planes involved are perpendicular to this section, and Fig. 4 is used to prove the coincidence of the (115) and (111) traces.

Thus, given the angle $\{111\} \wedge \{100\}$ equals 54°44′ (*e.g.*, angles EBC, ECB, ECD) it can easily be shown that the angle EDC of Fig. 4 as computed by difference from 180° in the triangle BCD (formed by the extension of BE) is identical to the calculated interfacial angle between $\{115\}$ and $\{100\}$; *i.e.*, 15°48′.

Growth of the Twinned Crystal

It has been established that some of the multiple twins are formed late in the crystallization process; for example, they are found in random orientation on top of the large butterfly twins. However, some have probably grown at the same time as the usual butterfly twins. The microstructural features suggest that the crystal grows from a nucleus which contains all the twinning elements rather than by repeated twinning separated by periods of growth.* If the latter were true, it would be difficult to explain the equal length of the $\{111\}$ traces, the overall symmetry of the cross sections about the (115) trace, and the consistent absence of voids at the center. It seems more reasonable to describe the end result in terms of growth outward from a twinned nucleus.

If it be assumed that in the early stages the crystal has a $\{100\}$ habit with $\{111\}$ twin planes, the outline as seen on a (110) section would be represented by the dashed line of Fig. 4. The potential "wing" portions of this crystal are free to grow rapidly outward along [110] directions (as is characteristic of $BaTiO_3$ grown from a KF flux) while the $\{100\}$ faces grow more slowly. Since the (115) interface does form, there also exists the possibility of the re-entrant angle at E (Fig. 5) serving as a deposition site. As a result the growth rate along the (115) plane would be increased, and at some stage in the growth process the symmetrical form illustrated by the solid lines of Fig. 4 would be reached provided there is no marked anisotropy in growth rates of the potential wings in the [110] direction shown in the figure. Since the alternating wing habit does form, an undefined singularity in growth conditions is assumed. For example, this singularity might be an external condition such as a concentration gradient or a poisoning effect; or it might be an internal singularity such as a dislocation. Whatever the condition which causes one wing to grow more rapidly than the other, the more rapidly growing side serves as a barrier to further growth of the other side, and a noncoherent boundary is formed. The more rapidly growing wing reaches a maximum size which is a resultant of growth both along and away from the spine, and the com-

* This is in contrast to the previously reported Kontoleon and Tomlinson (1956) sequence of events in doubly twinned [211] dendrites and in some butterfly twins in which twin planes are definitely separated as would occur during a period of growth of individual members of the twinned crystal.

pletion of the growth of one wing removes the restriction to growth of its opposite as the spine advances. Equal development of alternating wings suggests that neither one has either an internal or external singularity in growth conditions and therefore no marked difference in growth rates. However, many crystals show very unequal wing growth (i.e., one side developed almost exclusively, Fig. 1*c* and lower plan view Fig. 1*a*) and barring anisotropic conditions related to position in the solution, *e.g.*, near sides of the crucible, it is suggested that these crystals most likely have a dominant internal singularity.

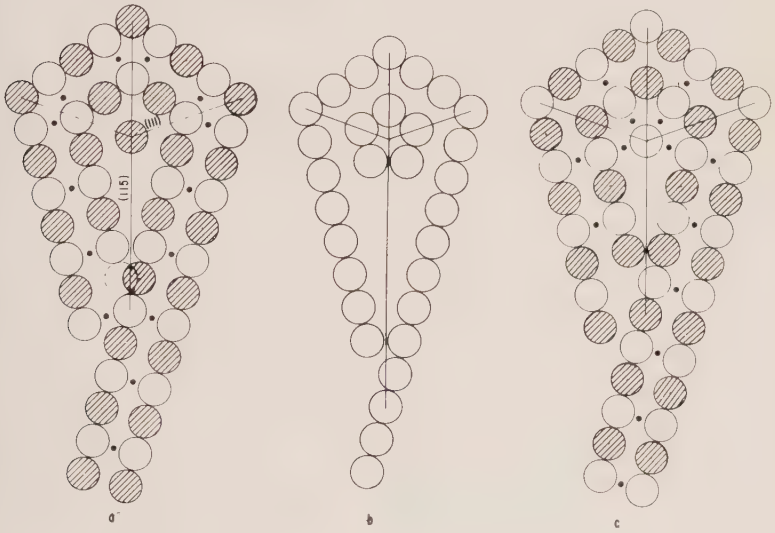

FIG. 5. Arrangement of atoms on {110} sections of a multiple twin of $BaTiO_3$. The significance of the traces is as previously described. Open circles = oxygen; shaded circles = barium; solid dots = titanium. Repeated stacking of these layers in the sequence *a*, *b*, *c* develops the multiple twin structure. The central Ba^{2+} and O^{2-} ions of *a* and *c*, respectively, form a Ba-O-Ba-O chain common to all parts of the twin and the coordination around the Ba^{2+} ion is shown in Fig. 6.

DEDUCTIONS FROM THE HARD SPHERE MODEL

Oxygen coordination around Ba^{2+}

{110} sections showing the atomic arrangement in a hard sphere model of the twinned crystal are shown in Fig. 5. Repetitive stacking of these layers in the sequence shown results in a central Ba-O-Ba-O chain common to all members of the twin. Furthermore, in contrast to the normal 12-fold cubo-octahedral (f.c.c.) and 12-fold twinned cubo-octahedral (h.c.p.) packing of oxygen ions around a Ba^{2+} ion in untwinned

and singly-twinned crystals, respectively, the 12-fold coordination around a Ba^{2+} ion in the common chain is in the form of a pseudo-pentagonal prism with pyramidal ends (Fig. 6).

Face-sharing arrangements in TiO_6 octahedra

The close approach of Ti^{4+} ions at the twin planes in comparison to the normal Ti-Ti distance is also shown in the {110} sections. In terms of Ti-O groups, the basic unit at the twin plane is the Ti_2O_9 group formed by face-sharing of two TiO_6 octahedra; such a coordination is also found for 2/3's of the octahedra in the hexagonal modification of $BaTiO_3$. Burbank and Evans (1948). The variations in multiple (111) twinning in

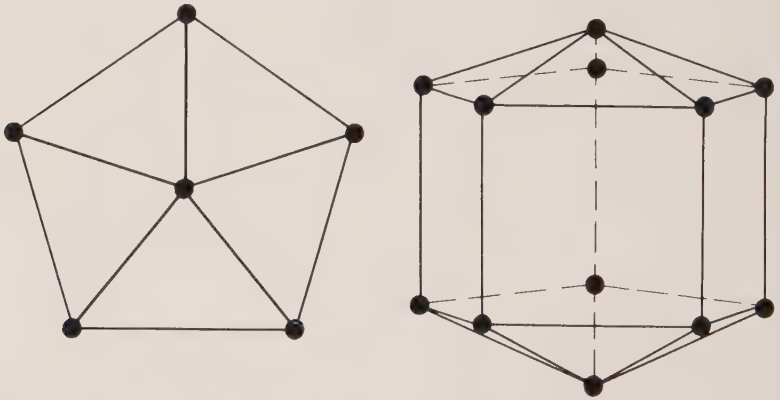

FIG. 6. Plan (left) and perspective view (right) of the type of arrangement of oxygen ions (solid dots) around a barium ion (not shown) common to all parts of the twinned crystal. The packing is in the form of a pseudo-pentagonal prism with pyramidal ends.

$BaTiO_3$ can be described by other still more complex arrangements of TiO_6 octahedra. Thus, a Ti_3O_{12} (three face-shared TiO_6 groups) unit would be a descriptive nucleus of the ordinary butterfly twin (two twin planes); a Ti_4O_{15} group, the nucleus of the multiple twin described here; and the last possibility of this type, a Ti_5O_{18} group as a nucleus of a pseudo-pentagonal shaped crystal ($5 \times 70° \ 32' = 352° \ 40'$) with four {111} twin planes. Schematic illustrations of these arrangements are shown in Fig. 7.

If one considers the ways of stacking octahedra, it will be clear that there are several possible ways of putting together face-shared TiO_6 groups. From the previously reported structures and from the present description of the twinned crystals, the arrangements actually found are (1) face-sharing of two octahedra to form Ti_2O_9 groups as in hexagonal

$BaTiO_3$ and in simple (111) twins; (2) collinear groups of three face-sharing octahedra as found in some impure hexagonal barium titanate forms Burbank and Evans (1948) and (3) cyclic, coplanar groups in which an octahedron can share *two* faces as in the multiple twin described here and in "butterfly" twins (Fig. 7). No morphological evidence has been found which could be interpreted on the basis of the possible forms resulting from a complex group involving face-sharing on more than two faces. This probably represents a limit for this type of coordination for TiO_6 units.

From the external morphology of the twinned crystals it is possible to conclude which of the octahedral faces are more likely to be shared.

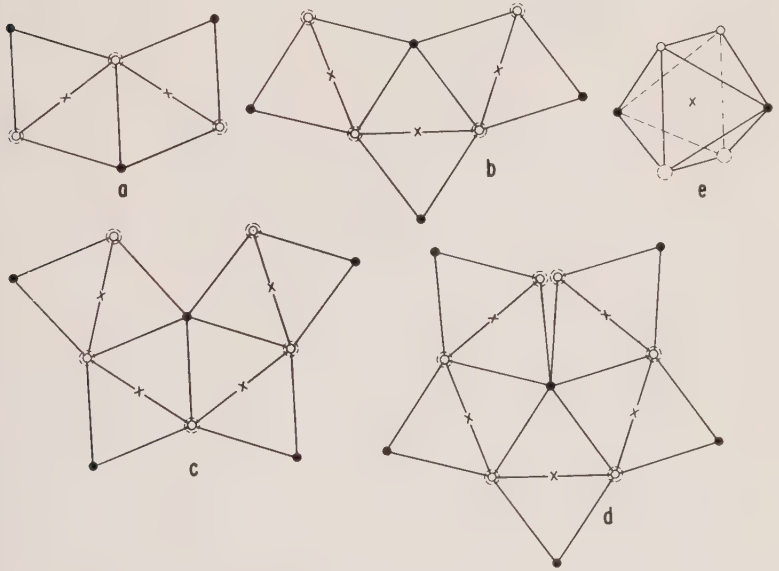

FIG. 7. Schematic representation of the different types of arrangements of TiO_6 octahedra from which the multiple twin structures can be developed. The arrangement of oxygen ions in the projections *a*, *b*, *c*, and *d* is shown in an octahedron in *e*. X = titanium. *a*, Ti_2O_9; *b*, Ti_3O_{12}; *c*, Ti_4O_{15}; *d*, Ti_5O_{18}. Sharing of more than one face of an octahedron is shown in *b*, *c* and *d*.

Given a Ti_2O_9 group formed from two octahedra in twinned relationship as shown in Fig. 8, one can conclude from the multiple twin structures that the faces of the type illustrated by BEC are face-sharing positions. However, there are no crystal forms which can be ascribed to face-sharing of faces of the type ABE or BCF which are sides of re-entrant angles resulting from twinning the octahedral habit. On these planes the orienta-

tion of new material is probably determined by nucleation at the re-entrant angle growth site and a new twinned relationship would not be energetically feasible until the crystal had grown somewhat larger. The evidence for addition of material on the end face of the Ti_2O_9 group such as CDE is derived not from morphological considerations but from crystal structure work on impure forms of $BaTiO_3$ in which collinear groups of three face-sharing octahedra have been reported Blattner *et al.* (1948).

Experimentally it has been qualitatively established, again using the

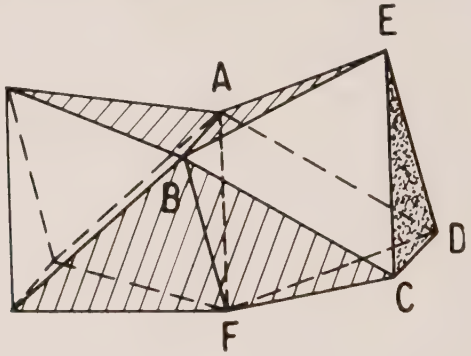

FIG. 8. Perspective view of two octahedra in twinned arrangement as in a Ti_2O_9 group.

external morphology criteria, that the rate of cooling influences which type of face-sharing will take place in the $BaTiO_3$ structure. Thus under rapid cooling conditions it is concluded that the single twin (one shared face) form is the more stable on the basis of profuse amount of singly-twinned dendrites and the metastable quenching of the hexagonal form of $BaTiO_3$. Also with rapid cooling there occurs in some dendrites a type of overgrowth which is related to face-sharing on end faces of the type CDE (Fig. 8). With slow cooling the multiple twins (two and three twin planes) predominate; *i.e.*, given sufficient time, the more stable sites for further twinning are the faces of the type BEC. Why only the unique cyclic pattern of twinning develops when other equivalent sites are available is yet another interesting, unanswered question.

SUMMARY

A multiple spinel twin of $BaTiO_3$ with four (111) twin planes grows from KF-$BaTiO_3$ solutions in the form of flat {100} plates alternating right and left along an elongated common spine. From an interpretation of the morphological features of the twinned crystals, it has been suggested that this crystal grows from a nucleus containing all the twinning

elements. With a hard sphere model of this twin and the other variations of (111) twinning in $BaTiO_3$, complex fundamental groups resulting from face-sharing of TiO_6 octahedra can be described. It is suggested from these units and the types of crystals seen, that there is a maximum of two shared faces per octahedron and that certain faces of two octahedra in twinned relationship are more likely than others to participate in face-shared groups.

Acknowledgment

Mary Houle's skillful preparation of the polished sections and photographs of the delicate twinned crystals is gratefully acknowledged.

The author is grateful for helpful and encouraging discussions with G. W. Sears, J. E. Burke and M. L. Kronberg. Both M. L. Kronberg and J. H. Westbrook critically reviewed the manuscript.

References

Blattner, H., Granicher, H., Kanzig, W., and Merz, W. (1948), Die Kristallstruktur des hexagonalon und rhombischen Barium-Platinat-Titanats; *Helv. Phys. Acta* **21,** (5), 341.

Burbank, R. D., and Evans, H. T., Jr. (1948), The Crystal Structure of Hexagonal Barium Titanate; *Acta Cryst.* **1,** 330.

Curien, H., and LeCorre, Y. (1955), Butterfly-type Twins in Barium Titanate; *Bull. Soc. Franc. Mineral. Crist.*, **78,** 604–607.

DeVries, R. C. (1959), Observations on the Growth of $BaTiO_3$ Crystals from KF Solutions; *J. Am. Cer. Soc.*, **42,** (11), 547–558; also *G.E. Research Lab. RL*-2188.

Kontoleon, D., and Tomlinson, J. (1956), Micro-examination of Barium Titanate; *Metal Progr.* **69** (No. 5) 98.

Remeika, J. P. (1954), A Method of Growing Barium Titanate Single Crystals; *J. Am. Chem. Soc.*, **76,** 940–941.

White, E. A. D. (1955), Twinning in Barium Titanate Crystals; *Acta Cryst.*, **8,** 845.

Manuscript received October 8, 1959.

THE MICROSCOPIC DETERMINATION OF THE THICKNESS AND PLANENESS OF PLATELETS IN FINE MATERIALS

CHARLES B. SCLAR AND LEE DILLINGER, *Battelle Memorial Institute, Columbus, Ohio.*

ABSTRACT

A procedure has been developed for the direct microscopic determination of the thickness and planeness of both opaque and nonopaque platelets which constitute fine powders ranging from a limiting size of 100 mesh to a nominal size of 5 microns. The procedure consists of (1) orienting the platelets by dusting the sample over the meniscus of an epoxy resin, (2) sectioning the resultant catalyzed resin mount normal to the meniscus and, correspondingly, the broad faces of the platelets, (3) remounting the sectioned block in additional resin to protect the thin layer of oriented platelets, and (4) polishing the sectioned face for microscopic examination in incident light.

The thickness of the platelets exposed on the polished surface of the mount may be measured with a micrometer ocular. The error in the measured or apparent thickness due to deviation of the platelets from the preferred orientation should typically be less than 15 per cent of the true thickness. The planeness or unevenness of the broad faces of the platelets may be assessed by visual inspection of their outlines on the polished mount. These outlines are the profiles of the platelets observed in a direction parallel to their principal plane.

The possibility of extending this method to include the direct measurement of the thickness of platy clay-mineral particles by means of the electron microscope and replication methods is under study.

INTRODUCTION

Many properties of finely divided materials are dependent on the shape, dimensions, and surficial roughness of the constituent particles. Accordingly, the industrial mineralogist is frequently requested to evaluate these characteristics. If the particles are roughly equidimensional, their diameters may be measured and the shape and roughness of the grains ascertained with either the light or the electron microscope. When the particles are either platy or lath-shaped, however, the problem of measuring their short dimension and of assessing the roughness or relief of their broad faces becomes formidable.

This paper is a description of a procedure by means of which the short dimension and the planeness of both opaque and nonopaque platelets may be directly measured and assessed with the light microscope.

CLASSICAL MICROSCOPIC METHODS FOR MEASUREMENT OF PLATELET THICKNESS AND ASSESSMENT OF PLATELET PLANENESS

General Discussion

In order to measure the short dimension of platy particles the platelets must be oriented so that their short dimension lies in the plane of the stage of the microscope. This type of preferred orientation is virtually

impossible to obtain by conventional techniques for petrographic examination and the usual procedure by which opaque particles are mounted in Lucite, Bakelite, or other suitable media so that they may be polished for microscopic examination in incident light.

A high degree of orientation is obtained with standard immersion methods, but the platelets are then oriented with their short dimension parallel to the optical axis of the microscope. A discussion of the applicability of classical methods for determining the thickness and planeness of nonopaque anisotropic platelets in this orientation follows.

Chaulnes Method

In the Chaulnes method (Winchell, 1937, pp. 75–76, 84–85) the true thickness of the platelet is the product of the apparent thickness, as measured on the micrometer screw of the microscope, multiplied by the index of refraction of the platelet. The platy particles of most micaceous minerals oriented with their short dimension parallel to the optical axis of the microscope have a birefringence of section which is less than 0.01 (Taylor, 1948). As a result, the intermediate index of refraction (β) may be used in the Chaulnes formula without significantly affecting the calculated thickness. It appears, therefore, as though the Chaulnes method should be suitable for the determination of platelet thickness. In practice, however, the usefulness of the method is limited because the surfaces of the platelets in sized fractions obtained by wet elutriation methods are essentially free from microscopically visible surface dust, and it is almost mandatory that subsieve powders (those passing a 325-mesh Tyler screen which has an aperture of 44 microns) be closely sized if reliable quantitative data are to be obtained. The absence of fixed reference points (dust particles) on which to focus leads to confusion in regard to the critical selection of the upper and lower surfaces of the platelets. Furthermore, the diameter-to-thickness ratio of minus 325-mesh platelets is almost invariably greater than 3 to 1 so that the true thickness of subsieve platelets is characteristically less than 15 microns. Inasmuch as one interval on the micrometer screw of most polarizing microscopes is 1 micron or greater, the error in the measurement of platelet thickness by the Chaulnes method could be excessive.

Multiple thickness determinations are required to detect thickness variations in a platelet by the Chaulnes method. Such a procedure, however, yields inadequate results even if dust particles for critical focusing occur on both the upper and lower surfaces of the platelet.

Differential Retardation

Variations in the interference color from point to point on the broad face of a single-crystal platelet between crossed nicols represent variations

in thickness. Most micaceous minerals, however, have a very low birefringence of section in this orientation, and the combination of a low birefringence with a very thin platelet (<15 microns) results in interference colors that are, at most, shades of first-order gray. Insertion of the gypsum plate or the quartz wedge will enhance small differences in retardation from point to point within a low-retardation platelet and, when the stage of the microscope is rotated, the platelets with a variable thickness have a variegated appearance. A qualitative impression of the degree of roughness of the broad surface of a low-retardation platelet can thereby be obtained, but this is hardly adequate for critical comparative studies of the surfaces of platelets in different powders.

*Berek Compensator**

The thickness of an anisotropic platelet is the quotient of its retardation, as measured with the Berek Compensator, divided by its birefringence of section. Platelets mounted on a slide in an immersion liquid will orient themselves with their broad faces parallel to the stage of the microscope. Consequently, the birefringence of section of the platelets of the any micaceous substance so mounted will be a constant, which for a known substance can be obtained directly from handbooks and for an unknown substance can be determined by measuring its refractive indices in this orientation. In theory, therefore, the Berek Compensator should provide a means of determining the thickness of thin anisotropic platelets, but in actual practice its applicability is limited. This is due to the combined effect of (1) the thinness of the platelets, which are typically less than 15 microns thick in powders finer than 325 mesh, and (2) the characteristically low effective birefringence (<0.006) of micaceous minerals oriented with their broad faces normal to the optical axis of the microscope (Taylor, 1948). The net result is a low retardation manifested by either quasi-extinction or grays of the first order which cannot be measured accurately with the Berek Compensator. Furthermore, the calculated thickness of the platelets is subject to serious error when the birefringence of section is less than 0.006 because such values approach the usual limits of accuracy for refractive index measurements. For example, if the birefringence of section is 0.004, deviations of ± 0.002 change the calculated thickness by -33 per cent and $+100$ per cent of the true thickness, respectively.

Method Proposed in This Paper

The method is a procedure whereby the platelets are oriented in a resin matrix, sectioned normal to the broad faces of the platelets, and

* Descriptions of this instrument are given by Winchell (1937, pp. 132–135), and Rogers and Kerr (1942, pp. 19, 75–78).

polished for microscopic examination in incident light. The method has been successfully employed on a variety of opaque and nonopaque minerals, which, when finely ground, tend to have platy and lath-shaped particles. These include molybdenite, graphite, energite, muscovite, talc, pyrophyllite, and brucite.

Procedural Details

Mounting the Sample

An aluminum foil mold in the form of a rectangular parallelepiped is filled with Epon No. 828,* a cold-setting epoxy resin that is liquid at room temperature. A liquid catalyst, triethylene tetramine,† is added to the resin in the ratio of 10 parts resin to 1 part catalyst to make the resin consolidate at room temperature in about 1 hour. The curing time for the catalyzed resin can be shortened markedly by heating it in a laboratory oven at 275° F. for about 15 minutes and then quenching it in tap water.

The powder to be mounted is dusted over the surface of the catalyzed liquid resin in the mold until the meniscus is thinly coated with the powder. The minute platelets in the powder orient themselves with their broad faces parallel to the meniscus of the resin and slowly settle downward. Particles of the minerals listed above (specific gravity 2.3 to 4.7) that are finer than 150 mesh settle between 0.15 mm. and 0.70 mm. in the 45 to 60 minutes required for the catalyzed epoxy resin block to solidify at room temperature.

The sample to be mounted should preferably be closely sized for the purposes of quantitative microscopic analysis, and in order to obtain (1) good dispersion of the platelets in the mount and (2) platelets with surfaces free of fine particles which would otherwise obscure their surficial relief. Suitable size fractions may be obtained from material coarser than 325 mesh by wet screening on standard testing sieves. Equally acceptable size fractions may be obtained from material finer than 325 mesh by either wet elutriation, through the use of standard sedimentation methods or laboratory mechanical classifying devices, or dry elutriation by means of the Haultain Infrasizer. Mounts with a satisfactory dispersion and with dust-free platelets have been prepared from minus 200-mesh talc and muscovite which were deslimed at nominal limiting sizes of between 5 and 15 microns. For less rigorous quantitative studies, therefore, desliming of a minus 200-mesh sample by sedimentation prior to mounting is probably adequate preparation in order to insure a satisfactory finished mount.

Sectioning the Mounted Sample and Remounting the Sectioned Block

The aluminum foil is removed by hand from the resin block that contains the sample, and the mount is sectioned normal to the original upper liquid surface (meniscus) of the resin with a Carborundum cut-off wheel. The sectioned face is then placed face down in another rectangular mold of aluminum foil whose dimensions are about twice those of the original mold. The mold is then filled with additional catalyzed Epon No. 828 epoxy resin. The sectioned surface of the original cast resin block which contains the sample is now exposed on the lower face of the newly cast resin block (see Fig. 1). The exposed cross section of the sample is surrounded by resin and is now sufficiently protected so that it can withstand the stresses of grinding and polishing.

* Manufactured by the Shell Chemical Corporation, Union Commerce Building, Cleveland 14, Ohio.

† Obtained from the Carbide and Carbon Chemicals Company, 30 East 42nd Street, New York 17, New York.

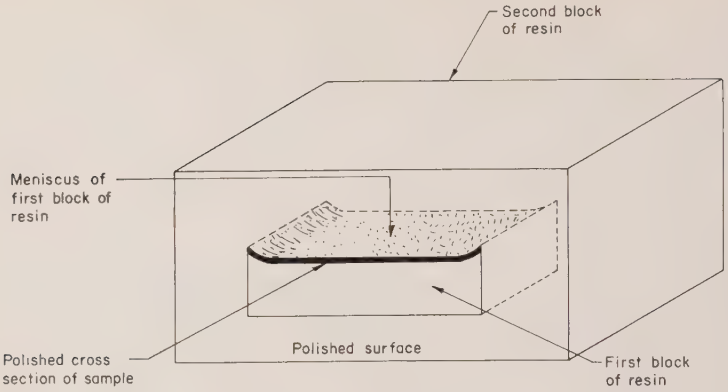

FIG. 1. Diagram of a finished mount.

Grinding and Polishing

The choice of a grinding and polishing procedure will depend principally on the nature of the mounted material. The method described here is a simple and rapid procedure which has given consistently satisfactory results for a number of materials with diverse physical properties.

The face of the mount on which the sectioned sample is exposed is ground on a 600-grit silicon carbide paper backed disk which is mounted on a wheel rotating at 1250 rpm. The disk is lubricated with Johnson's Stik Wax.* The ground surface is then polished with rouge on a water-lubricated wheel covered with Buehler Miracloth† which rotates at 250 rpm. The mount is now ready for microscopic examination in incident light.

The maximum elapsed time for the preparation of a finished mount by the method described above is about 2 hours and 20 minutes. Two hours represent the curing time at room temperature of the two successive blocks of resin required for each mount; this interval can be shortened by the application of heat. Grinding and polishing takes less than 5 minutes.

The Finished Mount

The sectioned sample on the polished surface of the finished mount is confined to a zone less than 1 mm. in thickness (Fig. 1). At magnifications greater than 250 diameters, the sectioned platelets are readily discernible and appear as long thin rods on the polished surface (Fig. 2). Many platelets of nonopaque micaceous minerals show the traces of their cleavage planes oriented parallel to the long axes of the rods. Although the reflectivity of many nonopaque micaceous minerals in polished section is close to that of the resin matrix, the platelet boundaries are still easily recognized. Their distinctiveness is enhanced by the positive relief of even the softest platelets, such as those of talc, on the polished surface when the mount is first prepared. If the mount is repolished by the same procedure after 3 or 4 weeks, however, the differential relief between the particles and the matrix changes. Talc particles, for example, no longer stand up in positive relief but are essentially

* Manufactured by S. C. Johnson and Son, Inc., Racine, Wisconsin.

† Obtained from Buehler Limited, 2120 Greenwood Street, Evanston, Illinois. Miracloth is a blend of 85 per cent cashmere and 15 per cent silk; it has a medium nap.

flush with the polished surface of the resin. This change in the relative polishing hardness of the resin and the platelet cross sections is probably due to post-solidification curing of the resin which increases its intrinsic polishing hardness.

Measurement of Thickness

If, as the platelets settled in the resin, they increasingly deviated from the preferred orientation, a systematic trend of increasing apparent thickness from the original meniscus to successively lower levels of the

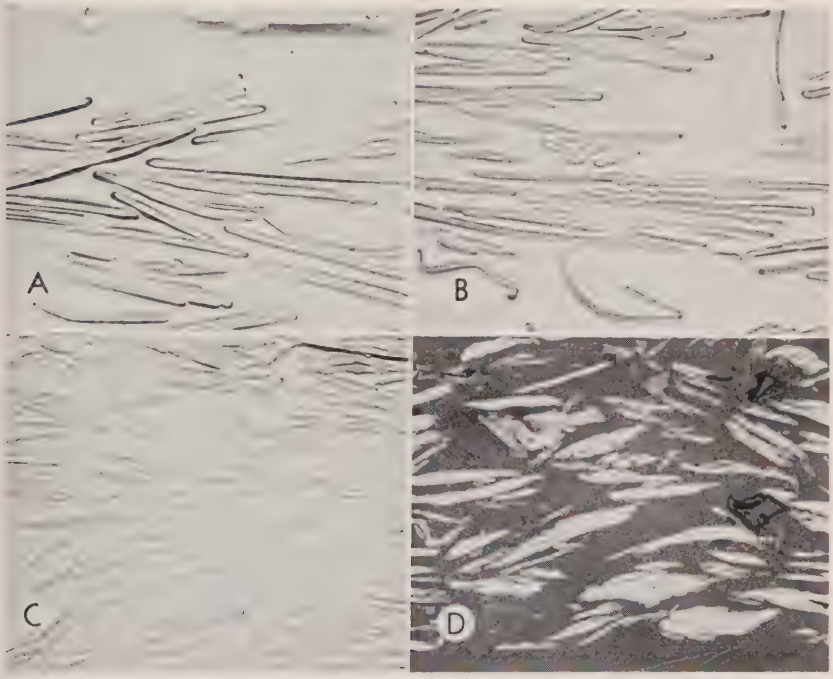

FIG. 2. Photomicrographs of ultrasonically disintegrated muscovite and of commercial flake graphite mounted in accord with methods described in this paper. Incident light. ×220.

A. Muscovite: −150 +325-mesh fraction. Note trace of meniscus at top.

B. Muscovite: −150 +325-mesh fraction. Note deformed particles (center and lower left) and "peeled back" cleavage flake (center).

C. Muscovite: −325-mesh fraction (unsized).

D. Graphite: −270-mesh (unsized).

mount should be evident, inasmuch as the true thickness of a platelet is its minimum thickness. The absence of such a trend in mounts of closely sized samples suggests that deviations from the preferred orientation are probably of little importance with respect to the average or median

thickness which is calculated from the measured thicknesses of a statistically representative number of platelets.

The relationship of the true thickness of a platelet to its apparent thickness as measured on the polished surface of a mount prepared by the method described in this paper is

$$\text{Apparent Thickness} = \frac{\text{True Thickness}}{\text{Cosine } (90 - \alpha)}$$

where α is the angle between the normal to the polished surface of the mount and the pole of the platelet. The ratio of the interplatelet distance to the diameter of the platelets is typically less than 0.5 in mounts prepared by this method. This means that, for any platelet, the maximum deviation of α from 90° will be 30° because of the physical resistance offered by adjoining platelets. Although the magnitude of the error introduced into the apparent thickness by the deviation of α from 90° increases exponentially as the deviation of α increases linearly, a limiting deviation of 30° corresponds to a maximum error in the apparent thickness of only 15 per cent of the true thickness. The permissible error will, of course, be greater if (1) the platelets in adjoining levels are arranged in echelon so that there is little or no opposition to the deviation of an intervening platelet from the preferred orientation by those in adjoining levels, (2) two or more platelets rotate in unison which would result in an increase in the effective interplatelet distance and a corresponding increase in the permissible deviation of α, and (3) the ratio of interplatelet distance to diameter of the particles in a particular mount is greater than 0.5. With respect to the first two circumstances, however, a statistically significant number of thickness measurements should suppress any exceptionally large individual errors in apparent thickness due to exceptionally large deviations of α.

Assessment of Platelet Planeness

The outlines of the platelets in the polished mounts represent the profiles of the platelets as viewed in a direction parallel to the principal plane (principal cleavage) of the flakes (Fig. 2). Significantly, the profiles reflect the degree of irregularity or unevenness of the broad surfaces of the platelets. The cross sections of the platelets may be classified into three overlapping but distinctive categories as follows:

(1) *Platelets with plane parallel sides*

In cross section these particles appear as long rod-shaped forms with rectilinear boundaries. Cleavage traces parallel to the length of the rods may be visible, particularly in nonopaque minerals.

(2) *Platelets with rough or uneven surfaces*

In cross section these particles appear as elongate forms with irregular boundaries. These irregularities reflect either convexities and concavities in the broad surfaces of the platelets or structurally controlled "treads and risers" wherein the "tread" represents the broad surface of a cleavage flake which was peeled off the platelet, and the "riser" represents the fracture along which the cleavage flake was torn off the platelet. The cleavage traces of the platelets run approximately parallel to the elongation of the irregular cross sections, but do not conform to the irregularities in their outlines.

(3) *Deformed platelets*

Platelets which have been warped, bent, crumpled, and otherwise deformed appear as elongate forms which have been bowed, singly or multiply folded, crimped on one or both ends, deformed into S-shapes, etc. The traces of the cleavage planes run parallel to the outlines of the deformed platelets. This is a useful criterion for differentiating deformed platelets from platelets with uneven surfaces.

By classifying a statistically significant number of platelets on this basis or some modification of it that is of greater significance for the particular material under study, it is possible to assess quantitatively the comparative planeness of the platelets in various samples which constitute a suite.

Within the confines of the two-dimensional polished surface of the resin mount, it is possible for a rough particle to appear as a plane particle if the irregularities on the broad surfaces of the platelet are nonuniformly distributed. The recorded percentage of plane particles in a sample will, as a result, be greater than the true value. On the other hand, this error should not seriously affect the usefulness of the acquired statistical data on planeness for comparative purposes.

Possible Extension of the Proposed Method to Platy Clay Minerals

The dimensions of clay particles are of considerable technological importance because in large part they control the colloidal properties of clay suspensions. The diameters of platy clay particles may be determined directly with the electron microscope, although some uncertainty as to the exact equivalence of their diameters as measured on the electron micrograph and that of the particle in suspension is introduced because the sample must be dried in order to prepare it for electron-optical study. Electron microscopy is evidently the ideal method for the determination of particle thickness, but the thickness of platy clay particles cannot be determined readily from ordinary electron micrographs in which the broad faces of the platelets lie in the plane of the micrograph. Shadowing techniques may be employed, but they yield results that are usually

difficult to evaluate quantitatively. Kahn (1959) has recently attempted to determine the thickness of platy clay particles by combining electro-optical birefringence data with ultracentrifuge data and viscosity data. The two sets of derived thicknesses show a fair correlation with respect to trends in their relative magnitude, but the absolute thicknesses obtained by these methods are widely divergent.

Studies are now in progress to extend the method described in this paper to the determination of the thickness of platelets within the particle-size range of clays. When techniques for obtaining a preferred orientation of clay platelets in a resin mount have been developed, it should be possible to replicate the polished surface for direct measurement of the thickness of the clay platelets with the electron microscope.

Acknowledgments

The authors are indebted to R. D. Buchheit of the Battelle staff, who provided helpful suggestions during the development of the method described in this paper and subsequently reviewed the manuscript. Raymond Flauhaus and John Foley drafted Fig. 1.

References

Kahn, A. (1959), Studies on the Size and Shape of Clay Particles in Aqueous Suspension, Proc. Sixth Nat. Conf. on Clays and Clay Minerals, Berkeley, Calif., 1957, Pergamon Press, New York and London, pp. 220–236.

Rogers, A. F. and Kerr, P. F. (1942), Optical Mineralogy, Second Edition, McGraw-Hill, New York.

Winchell, A. N. (1937), Elements of Optical Mineralogy, Part I. Principles and Methods, Fifth Edition, John Wiley and Sons, New York.

Taylor, E. D. (1948), Optical Properties in Cleavage Flakes of Rock-Forming Minerals, Laval Univ., Geol. and Mineral. Contrib. No. 78.

Manuscript received September 15, 1959.

Note Added in Press

A recent paper by Sahama (*Am. Mineral.*, **44**, 1959, 1303–1305) directed our attention to the applicability of the rotating elliptical mica compensator (the Sénarmont 1/4 λ plate and the Brace 1/10 to 1/30 λ plate) in determining the thickness and planeness of fine platelets. These compensators can be used to measure accurately small retardations in the 1 to 50 $m\mu$ range which is the approximate retardation range of fine platelets oriented parallel to the microscope slide in the particle-size range considered in this paper. Errors in the calculated thickness may be large, however, because it is difficult to determine the birefringence of section with a precision greater than ± 0.001. For example, if the birefringence of section is 0.004, deviations as small as ± 0.001 will change the calculated thickness by -20 per cent and $+33$ per cent of the true thickness, respectively. The elliptical compensators could be quite useful for differentiating platelets with plane-parallel sides from rough-sided platelets of variable thickness, but the profile method proposed in this paper should be superior for differentiating crumpled and deformed platelets from undeformed rough-sided platelets of variable thickness.

NOTES AND NEWS

NEW DATA ON BIRNESSITE AND HOLLANDITE*

C. Frondel, U. B. Marvin and J. Ito, *Harvard University, Cambridge, Massachusetts.*

Birnessite

Natural delta-MnO_2 or "manganous manganite" was first described under the name birnessite from a manganese-rich hardpan in fluvioglacial gravel at Birness, Scotland, by Jones and Milne (1956), who summarize the work on synthetic manganese manganites identical with or related to δ-MnO_2. An occurrence of the same mineral in Canada had been reported earlier by McMurdie and Golovrato (1948). We have identified birnessite by x-ray study in specimens collected at Cummington, Massachusetts, and Sterling Hill, New Jersey.

At Cummington, small discontinuous lenses or beds containing rhodonite, rhodochrosite, tephroite, spessartite, alleghanyite, cummingtonite and a manganoan and ferroan variety of dolomite occur conformably in metamorphosed sedimentary rocks, chiefly mica schist (Mosier and Thomas, 1949). The ore oxidizes very readily and the outcrop is overlain and penetrated along cracks by hard to friable crusts of black manganese oxide. Blocks of pink primary ore thrown on the waste heap of the mine quickly weather black. Although the black oxidation product appears to the eye to be homogeneous, it is usually found on x-ray and optical examination to consist of granular rhodonite, rhodochrosite, garnet or quartz with the secondary manganese oxide present in very minor amount, often as little more than a stain along grain boundaries. When separated, the manganese oxide generally does not give a distinct x-ray pattern, although we have identified cryptomelane in some samples. On a few specimens small patches were found of a soft, fine-grained black mineral which gave a relatively sharp x-ray pattern of δ-MnO_2 (Table 1). The four lines recorded in the pattern probably are orders of $(00l)$, from a layer-structure. This mineral is opaque under the microscope. Other samples of soft black material proved to be mixtures of birnessite and γ type MnO_2. The patches rich in birnessite appear to have been produced by the oxidation of a particular mineral in the primary ore which we have not been able to identify. The earlier work on the x-ray powder pattern of δ-MnO_2 is summarized by Jones and Milne (1956).

A chemical analysis of a bulk sample purified as far as possible by heavy liquid and sedimentation techniques, but which still contained about 10 per cent of impurities, is cited in Table 2. The x-ray pattern of

* Contribution from the Department of Mineralogy, Harvard University, No. 397.

TABLE 1. *X*-RAY DATA FOR BIRNESSITE AND HOLLANDITE

Fe radiation, Mn filter, in Angstroms

Patterns taken on film in 114 mm. diameter cameras

Birnessite Cummington, Mass.		Birnessite Sterling Hill, N. J.		Hollandite Langenberg, Saxony	
I	*d*	I	*d*	I	*d*
10	7.31	10	7.36	5	6.98
5	3.60	9	3.67	3	4.93
7	2.44	8	2.46	8	3.47
8	1.418			10	3.13
				1	2.68
				9	2.40
				½	2.24
				8	2.15
				½	1.98
				6	1.83
				¼	1.74
				2	1.65
				7	1.55
				2	1.43
				2	1.363

this sample showed some faint extra lines corresponding to the darkest lines in the patterns of quartz, spessartite, rhodochrosite, and γ-MnO_2. The chemical analysis is hardly more satisfactory than that of Jones and Milne (1956) for the purpose of deriving a formula. If the MnO_2 and MnO determinations are taken at face value the atomic ratio of total Mn:O is 1.78, with $Mn^4:Mn^2 = 3.38:1$. The material of Jones and Milne is near $Mn:O = 1:1.91$ with $Mn^4:Mn^2 = 9.51:1$. Both values fall into the range of composition of synthetic manganous manganite, with Mn:O between about 1.74 and 1.96. The role of the Ca, Mg, alkalies, and H_2O in our material is speculative, if indeed these cations are essential constituents. Possibly the Ca, Mg and alkalies occupy vacant lattice sites, analogous to the relation of the hollandite group of minerals to α-MnO_2, and the general formula can then be written $(Ca, Mg, Na_2, K_2)_x(Mn^4, Mn^2)(O, OH)_2$, where x may be compensated by variation in the $Mn^4:Mn^2$ or O:OH ratios.

Birnessite also was identified by its *x*-ray pattern (Table 1) as a secondary mineral associated with chalcophanite as a weathering product of franklinite—willemite ore from the old surface workings of the Noble

TABLE 2. CHEMICAL ANALYSES OF BIRNESSITE AND HOLLANDITE

	1. Birnessite Cummington	2. Hollandite Langenberg
MnO_2	66.66	70.38
MnO	16.07	8.98
MgO	0.23	0.20
CaO	1.05	0.05
BaO	—	13.32
K_2O	0.09	0.98
Na_2O	0.16	0.03
Fe_2O_3	0.86	0.11
Al_2O_3	0.83	0.39
SiO_2	2.62	0.40
H_2O	10.83	4.76
Rem.	1.47	0.74
Total	100.87	100.34

1. Birnessite. Rem. is SrO∼0.01, Li_2O∼0.005, NiO 0.01, CuO 0.005, SO_3 0.14, MoO_3 ∼0.005, Sc_2O_3 tr., (Zr, Nb, Ti) oxides 1.29. Al_2O_3 contains some (Y, Yb). Analyst: J. Ito.
2. Hollandite. Rem. is SrO∼0.01, Li_2O∼0.005, CoO∼0.05, NiO∼0.05, CuO 0.14, PbO 0.001, ZnO 0.01, SO_3 0.17, P_2O_5 0.28, V_2O_5∼0.01, ZrO_2 0.01, TiO_2∼0.001. Analyst: J. Ito.

pit at the south end of the ore-body at Sterling Hill, New Jersey. It occurs very sparingly as black crusts varying from hard and dense to earthy in consistency. The earthy material appears under the microscope as minute laths and needles that barely transmit light; the extinction is parallel, but the indices of refraction could not be measured.

HOLLANDITE

A specimen labelled "wad" from Langenberg, Saxony, collected prior to 1865 and acquired by the Harvard Museum from the J. B. Pearse collection, consists of a botryoidal crust with a radial-fibrous to fern-like internal structure (Fig. 1). The mineral is dark brownish-black in color; the powder is dark brown, and tends to smear out in the mortar to a glistening film. It has the general appearance of todorokite, but it contains barium and on *x*-ray study and chemical analysis was identified as hollandite. The spacings are given in Table 1. The specific gravity and hardness could not be measured accurately because of the fibrous habit. The earthy manganese and iron oxide deposits at Langenberg (Beck, 1902, 1909) are secondary concentrations derived by the weathering

and erosion of veins and stockworks containing fine grained varieties of silica with barite, calcite, manganite, braunite, pyrolusite, hausmannite, hematite. Hollandite occurs as a product of metamorphism of sedimentary manganese deposits, as in India and Sweden, and is found in other types of hypogene environments, but at Langenberg it is a supergene mineral. Numerous other supergene occurrences of hollandite are mentioned by Hewett and Fleischer (1960).

FIG. 1. Hollandite from Langenberg, Saxony. About ½ natural size.

Chemical Composition

The members of the hollandite group can be considered as derivatives of the α-MnO_2 structure, for which the idealized unit cell contents can be written $V_2Mn_8O_{16}$ (where V denotes vacant structural sites), as shown by A. and A. M. Byström (1950, 1951). Infilling of the vacancies by divalent or monovalent cations, which in the members of the hollandite group are large 8-coordinated cations Ba, Pb or K, is, in natural material, compensated electrostatically by a valence shift in the manganese ions as indicated in the formula $(V_{2-x}A_x)_x(Mn^4{}_{8-x}Mn^2{}_x)_8O_{16}$ where A is Ba, Pb, K, and possibly also NH_4 (Butler and Thirsk, 1952) or H_2O. Vacancies also can occur to a small extent in the 6-coordinated (Mn^4, Mn^2) positions, and OH can substitute for O. The analysis of the Langenberg mineral, cited in Table 1, indicates that A is chiefly Ba with minor K and that x is approximately 1. The approximate formula also can be

written (Ba, K_2, Mg, Ca, Na_2, Co, Ni)$Mn^2Mn^4{}_7O_{16}\cdot nH_2O$, with Ba:K ~8:1. The amount of essential water, if any, is uncertain; the analysis is close to $2H_2O$.

References

Byström, A. and A. M. (1950), The crystal structure of hollandite, the related manganese oxide minerals, and α-MnO_2: *Acta Cryst.* **3**, 146–154.

Byström A. and A. M. (1951), The positions of the barium ions in hollandite: *Acta Cryst.* **4**, 469.

Butler, G. and Thirsk, H. R. (1952), Electron diffraction evidence for . . . a cryptomelane modification of manganese dioxide prepared in absence of potassium: *Acta Cryst.* **5**, 288–289.

R. Beck (1909), Lehre von den Erzlagerstätten. Berlin, vol. 1, 268.

R. Beck (1902), Über die Erzlager der Umgebung von Schwarzenberg im Erzgebirge: *Freiberger Jb. Berg. und Hütt.*, **1902**, 64.

Jones, L. H. P. and Milne, A. A. (1956), Birnessite, a new manganese oxide mineral from Aberdeenshire; *Scotland: Min. Mag.* **31**, 283–288.

Hewett, D. F. and Fleischer, M. (1960), Deposits of the manganese oxides: *Econ. Geol.* **55**, 1–55.

McMurdie, H. F. and Golovrato, E. (1948), Study of the modifications of manganese dioxide: *J. Res. Nat. Bur. Stand.* **41**, 589.

Mosier, M. and Thomas, M. L. (1949), Investigation of Anson Betts Manganese Mine, Hampshire County, Mass.: *U. S. Bureau of Mines, Rept. Investig.* **4443**, 8 pages.

THE AMERICAN MINERALOGIST, VOL. 45, JULY–AUGUST, 1960

CHEVKINITE IN VOLCANIC ASH*

E. J. Young and H. A. Powers, *U. S. Geological Survey, Denver, Colorado.*

Chevkinite, a titano-silicate of the cerium earths, first found as large crystals presumably from a nepheline syenite pegmatite (Rose, 1839), has been found in samples of volcanic ash of rhyolitic composition. Noteworthy are its apparent paragenesis, its trifling abundance and its wide distribution. It occurs as separate phenocrysts embedded in volcanic glass in all the samples, and as inclusions within phenocrysts of fayalite, ferroaugite, and sanidine in several samples. Its abundance is on the order of a thousandth of a per cent; only a few crystals can be concentrated from ten grams of sample. It has been separated from a tuffaceous sand in the Dubose member of the Whitsett formation of Eocene age from Texas, an early Pleistocene ash from Idaho, and from the so-called

* Publication authorized by the Director, U. S. Geological Survey.

Pearlette ash beds of middle Pleistocene age from Texas, Kansas, Colorado, Nebraska, Wyoming, Utah, and Nevada.[1] The widespread so-called Pearlette ash deposits are thought to represent not more than four separate volcanic eruptions (Powers, *et al.*, 1958).

Physical and Optical Properties

The prismatic chevkinite crystals are approximately 0.03 by 0.17 mm. They vary from slender elongated forms to short stubby ones, and break conchoidally, showing no cleavage. In reflected oblique light they appear

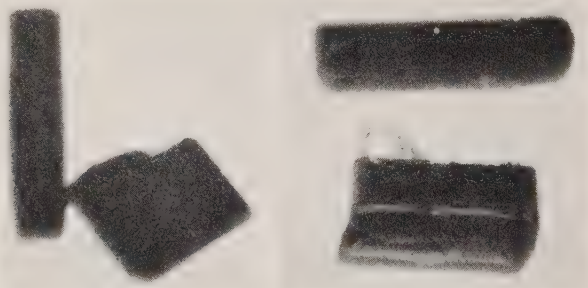

Fig. 1. Photomicrograph of four chevkinite grains from near Mercury, Nevada, taken in plane polarized transmitted light. The short stubby grain with volcanic glass adhering to it is not entirely opaque to transmitted light, showing the property of lesser absorption for α. $\times 130$.

black and have a bright splendent luster. In transmitted light (Fig. 1) their most striking diagnostic feature is virtually complete absorption of polarized light for β and γ so that even the smallest fragments appear opaque in at least one position; α shows least absorption, and is yellow to brown in color.

$\alpha \perp$ elongation, 1.97 to 2.01, moderate absorption (yellow to brown)
$\beta \perp$ elongation, >2.00, virtually complete absorption
$\gamma \parallel$ elongation, >2.00, virtually complete absorption
Birefringence -0.020 to 0.030.

Attempts to obtain the optic sign and 2V with the universal stage failed due to the intense absorption.

Some portions of crushed chevkinite crystals showing refractive indices less than α values suggest alteration or metamictization even in this Pleistocene chevkinite.

The x-ray patterns of chevkinite from 3 samples of volcanic ash match

[1] Robert L. Smith of the United States Geological Survey reports (written communication, July 6, 1959) chevkinite from the Bandelier tuff in New Mexico.

the pattern of monoclinic chevkinite from New Hampshire and Arizona (Jaffe *et al.*, 1956). The monoclinic symmetry cannot be confirmed by optical methods because the prismatic crystals are elongated parallel to *b*.

Chemical

Hydrochloric and nitric acids do not affect chevkinite but hot hydrofluoric acid attacks most of the chevkinite strongly, leaving behind a whitish soft isotropic skeleton which has a refractive index of 1.556 ±0.002. Some of the chevkinite grains appear fresh and unchanged after the treatment, and many grains were only partially altered and still possessed cores of presumably fresh chevkinite.

Radioactivity of a group of several chevkinite grains was measured on a micro-alpha-counter as approximately 7 per cent equivalent Th, which

Table 1. Semiquantitative Spectrographic Analysis of a Chevkinite Concentrate from Pleistocene Volcanic Ash from the La Sal Mountains, Utah

Analyst: John C. Hamilton, U. S. Geological Survey

	Element	Per cent		Element	Per cent
	Si	M		Mg	0.7
	K	M		Y	0.7
Major	Ti	M		Nb	0.7
	Ce	M		Mn	0.3
	La	M		Dy	0.3
				Er	0.3
	Fe	7		Gd	0.3
	Ca	7	Trace	Sc	0.07
	Nd	7		Yb	0.07
Minor	Al	3		Ba	0.03
	Pr	3		Cu	0.015
	Th	3		Mo	0.015
	Sm	1.5		Cr	0.007
	Zr	1.5		Sr	0.003

Notes: The chevkinite concentrate consists of the following minerals:

chevkinite	50%
fayalite	10%
ilmenite	2–5%

The remainder is tourmaline, hornblende, ferroaugite, plagioclase.

Figures are reported to the nearest number in the series 7, 3, 1.5, 0.7, 0.3, 0.15, etc. in per cent.

Sixty per cent of the reported results may be expected to agree with the results of quantitative methods.

M = Major constituent—greater than 10 per cent.

agrees with a semiquantitative spectrographic analysis of a 50 per cent chevkinite concentrate shown in Table 1.

The spectrographic analysis was made on only 8 mg. of sample; this was all that was available in one of the samples richest in chevkinite. Major amounts of Ti, Ce, and La and relatively large amounts of several other rare earths confirm the identification of chevkinite. The high content of K may be due to volcanic glass coatings surrounding many of the grains.

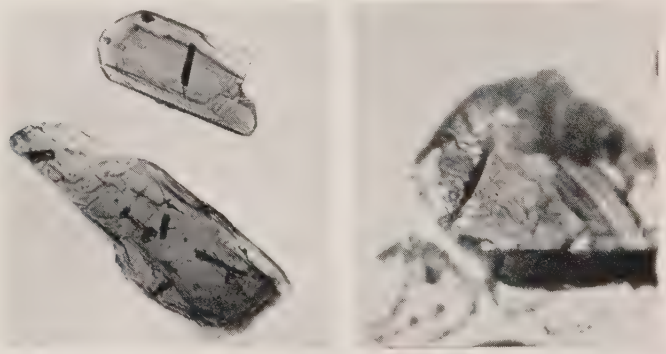

FIG. 2. Photomicrographs of ferroaugite and fayalite with chevkinite inclusions from near Mercury, Nevada, taken in plane polarized transmitted light. (a) the larger ferroaugite grain contains four chevkinite inclusions. The two small nonopaque inclusions in the center of the grain are not chevkinite, and are unidentified. Note that the two chevkinite inclusions in approximately horizontal position show lesser absorption due to α of the chevkinite being transmitted. $\times 100$. (b) The relatively large inclusion of chevkinite in the fayalite is also in position for α to be transmitted and is consequently nonopaque. $\times 330$.

CHARACTERISTICS OF HOST MATERIALS

In large pumice fragments in a tuff in Forty Mile Canyon near Mercury, Nevada, chevkinite crystals are embedded within phenocrysts of fayalite and ferroaugite (Fig. 2). The inclusions were removed from the host grains and identified by immersion methods.

The fayalite grains are rounded (resorbed) and generally clear yellow in color. Others contain a thin reddish skin presumed to be hematite. Optical data for the fayalite are:

$\alpha = 1.810 \pm 0.01$, $\beta = 1.850 \pm 0.01$, $\gamma = 1.860 \pm 0.01$
Pleochroism is $\alpha = \beta$ pale yellow, γ = almost colorless
Absorption formula is $\alpha = \beta > \gamma$, $2V(-) = 48° \pm 2°$ (universal stage).

According to the data of Winchell (1951) the measured 2V would place the mineral almost at the fayalite end of the forsterite-fayalite series. The β refractive index would indicate a composition of $Fo_{5\text{-}11}$ $Fa_{95\text{-}89}$. Using an x-ray method of Yoder and Sahama (1957) accurate

measurement of the (130) spacing, which was 2.825 Å, indicates a composition of $Fo_{11}Fa_{89}$. Optical data for the ferroaugite are:

$\alpha=1.729$, $\beta=1.735$, $\gamma=1.762$ (± 0.005)
$Z\wedge c=49°$, average (variation from 48°–52°)
$2V(+)=56°$, average (variation from 54°–67°)
Extinction angles and 2V determined on the universal stage.
Pleochroism is faint with $\alpha=\beta$ green, $\gamma=$ yellowish green.
Using the determinative chart by Hess (1949) the green pyroxene fits in the ferroaugite field and has the following cation ratio: Fe: Ca: Mg=58:34:8.

The pumice has the following chemical composition (in weight per cent), with and without phenocrysts.

	Pumice	*Pumice (phenocrysts extracted)*
	D-1756[1]	D-1757[1]
SiO_2	69.44	70.98
Al_2O_3	12.56	12.28
Fe_2O_3	1.60	1.46
FeO	.54	.53
MgO	.63	.34
CaO	1.12	.78
Na_2O	3.41	3.48
K_2O	5.24	5.35
H_2O^-	1.16	.72
H_2O^+	3.01	3.04
TiO_2	.13	.13
CO_2	.52	.27
P_2O_5	.01	.01
F	.14	.12
MnO	.08	.07
	99.59	99.56
Less 0	.06	.05
	99.53	99.51

[1] Analysis number—U. S. Geological Survey, Denver rock analysis laboratory. Analyst, Dorothy F. Powers.

Comparative Data on the Occurrences

In this study chevkinite has been identified from 60 samples of silicic volcanic ash from 20 different localities; it is believed, however, that these samples are from the products of not more than six different volcanic eruptions at centers whose location is not yet known. One tuffaceous sand that contains chevkinite is of Eocene age in the Dubose member of the Whitsett formation of Texas; one ash bed from Hagerman, Idaho, is of Early Pleistocene age; the other beds are believed all to be

parts of the so-called Pearlette ash (four separate closely-spaced eruptions) of middle Pleistocene age (Powers *et al.*, 1958). No chevkinite was found in samples of about sixty other ash beds of late Cenozoic age; hence, about 50 per cent of the volcanic ashes examined contained chevkinite. Perhaps chevkinite has been a rare species because its presence has been overlooked, and future mineralogic studies of heavy mineral concentrates may find it to be an expectable accessory constituent of some varieties of igneous rocks. Chevkinite is an early-formed mineral in a magma as shown by its common appearance as inclusions in early-formed ferroaugite and fayalite.

A comparison of several features of some of the chevkinite-bearing ashes is given in Table 2.

Table 2. Comparative Data on Some Chevkinite-Bearing Volcanic Ashes

	1	2	3	4	5	6	7
Chevkinite, α refractive index	1.99	1.99[1]	1.99[1]	1.99	1.98	1.98	1.97
Associated phenocryst heavy minerals[2]							
Fayalite		x		x			
Augite, β1.695±	x						
Ferroaugite, β1.736		x	x	x	x		
Hornblende, red-brown			x	x	x	x	x
Hornblende, olive-brown	x				x	x	x
Hornblende, blue-green					x	x	x
Zircon, colorless	x	x	x	x	x	x	x
Zircon, pink		x	x	x	x	x	x
Partial chemical composition of volcanic glass (phenocrysts extracted)							
SiO_2, water free	74.3	74.1	75.5	76.5	76.5	76.3	77.1
TiO_2, water free	0.13	0.14	0.13	0.13	0.13	0.12	0.11
Na_2O+K_2O, water free	9.6	9.2	8.8	8.9	8.8	8.9	9.2

1. Ash, Hagerman, Idaho.
2. Pumice blocks from tuff, Forty Mile Canyon, Mercury, Nevada.
3. Ash, Pine Valley, Nevada.
4. Ash, La Sal Mountains, Onion Creek, Utah.
5. Ash, Meade County, Kansas.
6. Ash, Pine Valley, Nevada (probably different from 3).
7. Ash, Valley County, Nebraska.

[1] Identity of chevkinite verified by x-ray diffraction.

[2] All samples contain ilmenite and magnetite.

REFERENCES

Hess, H. H. (1949), Chemical composition and optical properties of common clinopyroxenes, Part I: *Am. Mineral.*, **34,** 621–666.

Jaffe, H. W., Evans, H. T., Jr., and Chapman, R. W. (1956), Occurrence and age of chevkinite from the Devil's slide fayalite-quartz syenite near Stark, New Hampshire: *Am. Mineral.*, **41,** 474–487.

Powers, H. A., Young, E. J., and Barnett, P. R. (1958), Possible extension into Idaho, Nevada, and Utah of the Pearlette ash of Meade County, Kansas (Abs.): *Bull. Geol. Soc. Amer.*, **69,** 1631.

Rose, G. (1839), Beschreibung einiger neuen Mineralien des Urals: *Annalen der Chemie und Physik*, **48,** 551–554.

Winchell, A. N. (1951), Elements of Optical Mineralogy, Part II: Descriptions of Minerals, Fourth Edition, John Wiley and Sons, New York, 551 p.

Yoder, H. S., Jr., and Sahama, Th. G. (1957), Olivine *x*-ray determinative curve: *Am. Mineral.*, **42,** 475–491.

THE AMERICAN MINERALOGIST, VOL. 45, JULY–AUGUST, 1960

AN IMPROVED THERMAL HEAD FOR D.T.A. OF CORROSIVE MATERIALS

James A. Dunne and Paul F. Kerr, *Columbia University, New York, N.Y.*

Differential thermal analysis of sulfides and other minerals that corrode metal containers when heated in air was made practical through the development of specially designed receptacles described by Kopp and Kerr (1957). Research on the differential thermal analysis of sulfides supported by the National Science Foundation has recently resulted in the development of apparatus which is a further refinement of this equipment.

The thermal head, shown in Fig. 1, is machined out of 18-8, Cr-Ni stainless steel round stock. Specimen well holes are designed to contain nests of alundum insulator tubing which are supported in the head by a thin transite disc. The nests can be prepared in advance from commercially available stock and are quickly interchanged when thermocouples require replacement. Head temperature is measured by the reference thermocouple using an ordinary triple lead arrangement as described by Mackenzie (1957, p. 36, Fig. II, 4). The writers are indebted to Mr. E. M. Bollin of the mineralogy group at Columbia University for calling this procedure to their attention.

The simplification of the head design permits rapid and inexpensive machining, and facilitates the removal of used specimen wells and cement. The specimen well assemblies are constructed with the aid of brass gauges which have been made in order to insure constant well

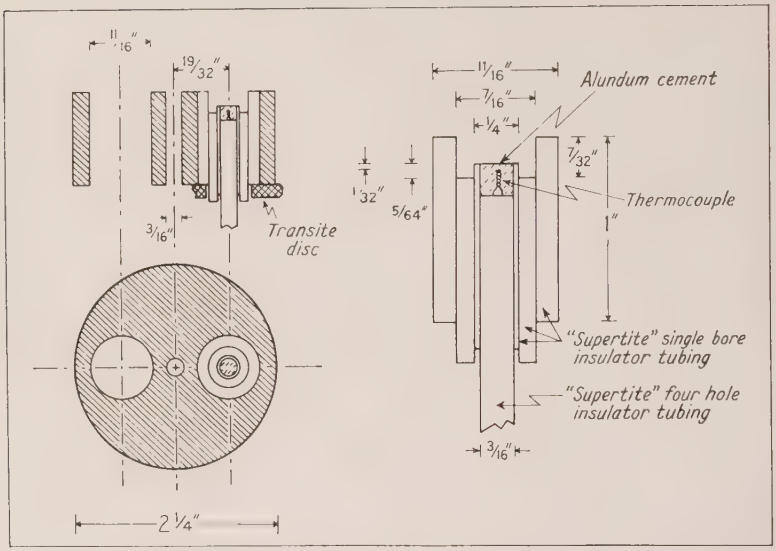

FIG. 1. A sectional view of the thermal apparatus. The metal head is shown on the left and the well nest assembly of ceramic insulator tubing on the right.

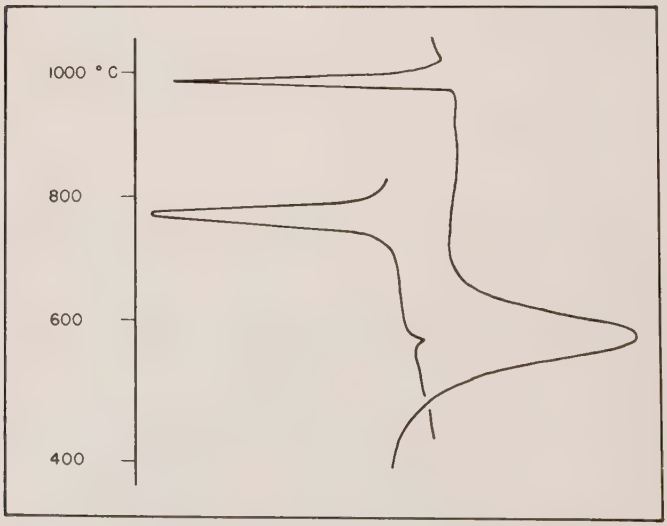

FIG. 2. D.T.A. curves of galena, Wood River, Idaho (left) and kaolinite (API No. 17; right). The latter shows the sensitivity of the apparatus for familiar materials.

dimensions and sample-to-thermocouple distances, as indicated in Fig. 1. This feature furnishes head-to-head reproducibility. Experimental data collected using the modified apparatus show reproducibility to be essentially a function of chart reading error. The 6″ chart of the Leeds and Northrup Speedomax H single point continuous recorder which is used for the majority of sulfide analyses can be read to an accuracy of $\pm 5°$ C.

The positive nature of the alundum shielding protects the thermocouples to such an extent that curves for 25 to 30 sulfide samples may be obtained without replacement. The sensitivity of the apparatus compares favorably with that of equipment normally used for clays, carbonates and other thermally active materials. The D.T.A. curve of a reference sample of kaolinite (No. 17, Am. Pet. Inst. Research Project No. 49) obtained from the modified apparatus is given in Fig. 2. The amplitude of the exothermic peak indicative of recrystallization of the sample to mullite represents a thermocouple emf of approximately 0.47 millivolts. A curve for galena from the Mayflower Mine, Wood River, Idaho is displayed to the left of the kaolinite curve in Figure 2. The exothermic peak at 790° C. represents sample oxidation. The well defined nature of the oxidation peak has been found to be characteristic of galena.

The apparatus described herein has been applied to the study of the PbS-PbSe system (Dunne and Kerr, 1960), in combination with recently developed equipment which allows D.T.A. in vacuo and furnishes differential thermal records of the reactions involved in mineral pyrosynthesis (Bollin, Dunne and Kerr, 1960).

References

Bollin, E. M., Dunne, J. A. and Kerr, P. F. (1960), Differential Thermal Pyrosynthesis: *Science* **131,** No. 3401, p. 661–662.

Dunne, J. A. and Kerr, P. F. (1960), Differential Thermal Analysis of Galena and Clausthalite: *Am. Mineral.* (in press).

Kerr, P. F., *et al.*, (1951), Reference Clay Minerals: American Petroleum Institute Research Project 49.

Kopp, O. C. and Kerr, P. F. (1957), Differential Thermal Analysis of Sulfides and Arsenides, *Am. Mineral.* **42,** 445.

Mackenzie, R. C. (1957), The Differential Thermal Investigation of Clays, Mineral. Soc. London, 456 pp.

THE AMERICAN MINERALOGIST, VOL. 45, JULY–AUGUST, 1960

OCCURRENCE OF MULTI-FORM FLUORITE FROM MEXICO*

PAUL E. DESAUTELS, *United States National Museum, Washington, D.C.*

The mineral collection of the United States National Museum contains many fine specimens from Las Chispas Mine, near Arizpé, Sonora, Mexico. Among them is a specimen of polybasite (U.S.N.M. R7867) weighing 82 pounds. Such a mass of polybasite is unique in its own right. However, disseminated throughout the mass are myriads of small fluorite crystals of such unusual habit as to invite description.

The mine which produced this specimen took its name from the fine "chispas" or crystals of silver minerals occurring there. Activity at Las Chispas Mine began in the 1880's. Because of poor mine management and extensive ore stealing, profitable operation did not begin until 1907. At that time the properties were incorporated as the Pedrazzini Gold and Silver Mining Company. (Russell, 1908). Extensive mine workings were eventually developed and fine specimens obtained for a number of years.

Dufourq (1910) describes the country rock as rhyolite which has been brecciated and re-cemented by secondary silica. Two rhyolite beds, varying in thickness from 300 to 400 feet, are separated by an altered volcanic tuff. The Chispas vein, filled mainly with quartz containing rhyolite fragments, lies along a small vertical fault. The ore body, apparently formed by secondary enrichment, continued downward to 900 feet below the outcrop. Below the 200-foot level mineralization consists of pyrite, polybasite, stephanite, argentite and small amounts of chalcopyrite. One stope described by Dufourq, after rising fifty feet and producing ore not assaying over eleven ounces of silver per ton, came suddenly into five feet of ore averaging two thousand ounces per ton across the entire face. This occurrence of bonanza ore zones was one of the unique features of the Chispas vein. A seven-foot thick vein mentioned by Dufourq contained a center band of pyrargyrite eight inches thick. On each side was a rib of quartz outside of which were two to three-inch bands of argentite mixed with quartz.

Because of the exceptional size and quality of the crystallized silver minerals, specimens from Las Chispas Mine are found in all the great mineral collections. Ford (1908) and Ungemach (1910) described the unusually fine stephanite and polybasite crystals from this vein. The 82-

* Published by permission of the Secretary, Smithsonian Institution, Washington, 25, D.C.

pound mass of polybasite in the United States National Museum probably represents the largest preserved as a single piece. It was assayed by the United States Mint at 16,868 ounces of silver per ton. The surface of the specimen has been dulled by oxidation but internally it is an open network of splendent polybasite crystals. Throughout the mass, crystal surfaces are partially covered with druses of well formed pyrite, chalcopyrite, quartz and fluorite.

The fluorite occurs in two generations, the first in spherical sub-parallel crystal aggregates and the last as limpid, highly modified individuals ranging in diameter from one-half to one millimeter. Under 30× magnification their beauty is most striking. The crystals show little or no malformation but their unusual clarity and high complexity makes vis-

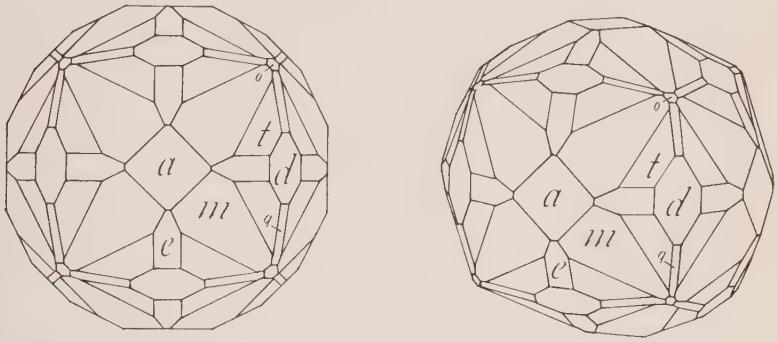

Fig. 1. Orthographic and clinographic projections of fluorite from Mexico.

ual identification of the faces difficult. A unique feature of most of the fluorite crystals is the occurrence, on a single crystal, of one each of all seven type forms of the hexoctahedral class.

Highly modified fluorite crystals are relatively common. Goldschmidt (1918) shows highly complex fluorites with a greater total number of forms but lacking at least one of the basic seven. In Shepard (1857) is a drawing of a Rossie, New York crystal having all seven forms but indices are not given. The forms appear to be different from those reported here and the crystal of a more usual habit with the octahedron dominant.

The appearance of a typical Las Chispas crystal, with practically no idealization, is shown in Fig. 1. Forms present are the cube (*a*), octahedron (*o*), dodecahedron (*d*), tetrahexahedron (*e*) {012}, trapezohedron (*m*) {113}, trisoctahedron (*q*) {133}, and hexoctahedron (*t*) {124}. The faces of {012} and {111} are always etched. The cube, dodecahedron and trapezohedron are about equally dominant with the other forms of lesser importance. The relative size of the hexoctahedron varies consid-

erably. Similar crystals observed on other Las Chispas specimens had fewer forms. In every case, however, at least {100}, {110}, {113}, and {012} are present. Despite this variation the great majority of these transparent crystals show all of the holohedral isometric forms.

References

Dufourq, E. L. (1910), Minas Pedrazzini Operations near Arizpé, Sonora: *Engineering and Mining Journal*, **90,** 1105–1106.

Ford, W. E. (1908), Stephanite Crystals from Arizpé, Sonora, Mexico: *American Journal of Science and Arts*. **25,** 244–248.

Goldschmidt, V. (1918), Atlas der Krystallformen. Band IV, Tafel 2–13.

Russell, B. E. (1908), Las Chispas Mines, Sonora, Mexico: *Engineering and Mining Journal*. **86,** 1006–1007.

Shepard, C. U. (1857), Treatise on Mineralogy. Third Edition. Volume 2, p. 95, figure 211.

Ungemach, M. H. (1910), Contribution à la Minéralogie du Mexique: *Bulletin Société Francaise de Minéralogie*. **33,** 394–395.

THE AMERICAN MINERALOGIST, VOL. 45, JULY-AUGUST, 1960

AN INTERLAYER MIXTURE OF THREE CLAY MINERAL TYPES FROM HECTOR, CALIFORNIA

Meredith E. Ostrom,* *Illinois State Geological Survey, Urbana, Illinois.*

The occurrence of mixed-layer clays in relatively pure clay deposits has been reported by various authors. Randomly interstratified mixed-layer silicates are found commonly as intermediate stages in the alteration of micas and other silicates to clay minerals. Random mixed-layer clays are minerals in which the layers occur in random intergrowth. A sample of clay from Hector, California, exhibits peculiarities inconsistent with existing data for the clay mineral hectorite. The clay is trioctahedral with an expanding lattice and has a pH of 9.8. In addition, the sample contains a small amount of calcite.

Because the description of the occurrence of such a material might cast some light on the genesis of the Hector deposits, and because of the possibility that the peculiarities attributed to hectorite might be the consequence of a polymineralic character in certain instances, the author believes the data presented herein are significant.

X-ray Analysis

X-ray diffraction curves of the basal 00*l* reflections are incompatible with a normal hectorite structure. By use of Ni-filtered Cu-radiation

* Present address, Wisconsin Geological and Natural History Survey, Madison, Wisconsin.

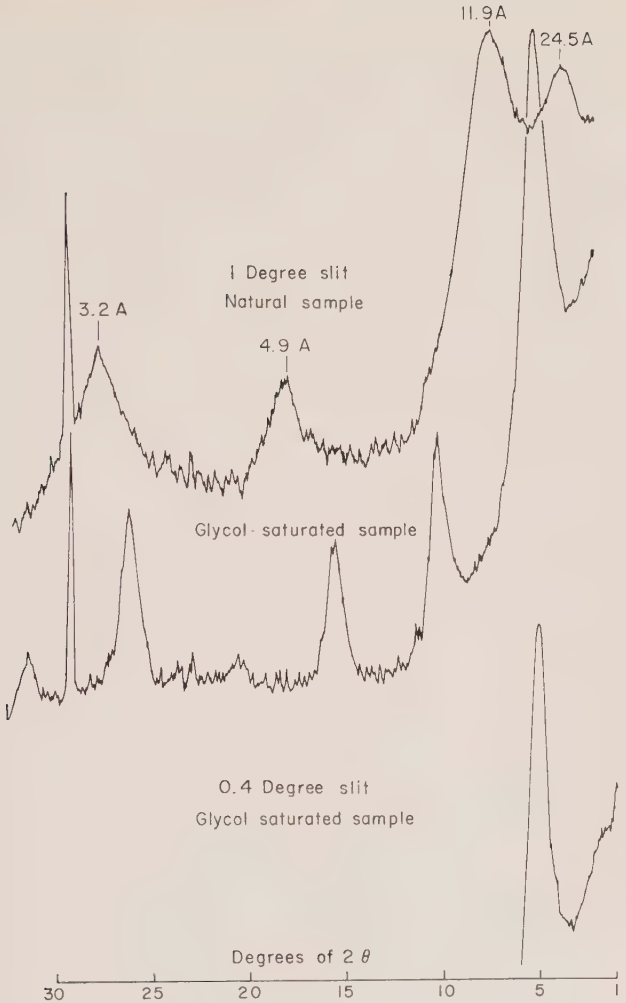

FIG. 1. *X*-ray diffraction curves of natural sample before and after glycol saturation using 1.0 and 0.4 degree slits with Ni-filtered Cu-radiation.

and a 1 degree slit, the *x*-ray diffraction curve for the natural material shows prominent reflections at 24.5 Å, 11.9 Å, 4.9 Å, and 3.2 Å (Fig. 1). Because the 00*l* series is not an integral sequence it is suggested that this clay is polymineralic and that it is composed of several different types of layers that form a random mixed-layer clay.

The identity of the various components was determined by the method described by Weaver (1956). It is assumed that the separate re-

flections represent average values resulting from simultaneous scattering from the different types of layers.

Evidence for the presence of expansible montmorillonite-like layers was obtained by saturating the clay with ethylene glycol. A prominent nearly integral submultiple sequence of reflections appeared at 17.3 Å, 8.7 Å, 5.7 Å, 4.3 Å and 3.4 Å, confirming the abundant presence of montmorillonite in this mixed system. A less intense period of about 55 Å was detected by using a 0.4 degree slit.

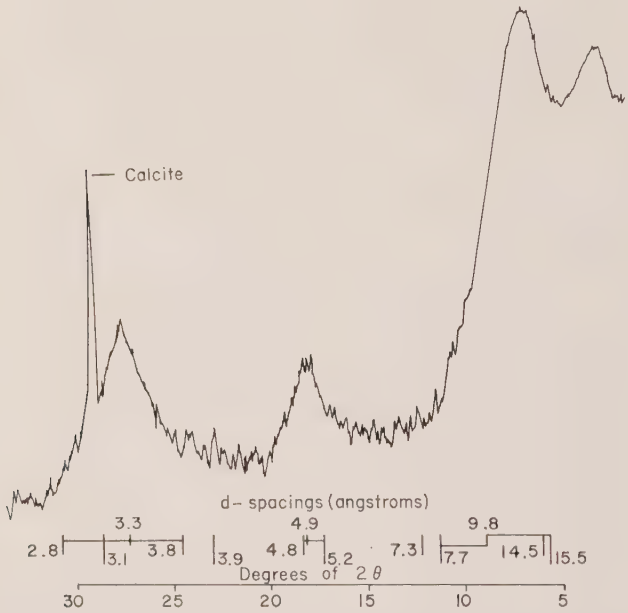

FIG. 2. Relation between observed reflections (*X*-ray diffraction curve), and positions of reflections of the three proposed randomly interstratified clay mineral types (vertical lines).

The vertical lines below the *x*-ray diffraction curve illustrated in Fig. 2 indicate the position of the 00*l* reflections for the three types of layers. The short lines show the position of the 9.8 Å 00*l* series (9.8, 4.9, 3.3), the medium lines the 00*l* reflections of the 14.5 Å layers (14.5, 7.3, 4.8, 3.8, 2.8), and the long lines the 00*l* reflections of the 15.5 Å layers (15.5, 7.7, 5.2, 3.9, 3.1). Horizontal lines connecting adjacent vertical lines show which reflections contribute to the observed reflections.

The close agreement between the positions of the observed reflections and those of the proposed mixed-layer components (Fig. 2) is undeniable. The broad reflection at about 3.3 Å is the sum of contributions

from each component spread over a broad range. That at about 5.0 Å is sharper and is the result of close grouping. A weak but distinct reflection occurs at about 8.5 Å, the sum of contributions from the 9.8 Å and 7.7 Å components, and a very prominent reflection occurs at about 12 Å which is the average of the first order reflections of all three components. The shapes and positions of the maxima suggest that all three types of layers are moderately abundant.

After glycolation the swollen layers strongly predominate indicating that at least two of the three components are expansible. The long period suggests that one species, with an abundance near one-third, differs somewhat from the other two.

Significance

It is suggested that the sample of clay represents an intermediate stage between phlogopite and hectorite. The fact that the 9.8 Å 00*l* series approaches those of the micas permits a certain amount of speculation regarding the material found at Hector. It is suggested that the expansible clay mineral hectorite is the product of the action of hot springs on a nonexpanding trioctahedral magnesium silicate mineral such as phlogopite, with loss of interlayer potassium and an apparent gain of some sodium.

Ames *et al.* (1958) consider hectorite to be the result of the alteration of dacitic tuff through an intermediate zeolite (clinoptilolite) by acid solutions during hot spring activity in a restricted lake environment. Randomly interstratified mixed-layer clays, similar to that described in this paper, are commonly considered to be intermediate stages in the alteration of micas and other silicates to clay minerals, yet such a material has not previously been described from the Hector deposits. It is suggested here that hectorite is derived from the alteration of phlogopite, and that the random mixed-layer material described herein is an intermediate stage between phlogopite and hectorite.

Acknowledgments

The author wishes to express his thanks to Dr. W. A. White who provided the original sample and to Dr. W. F. Bradley who aided in the development of this paper and critically read the manuscript.

References

Ames, L. L., Jr., Sand, L. B., and Goldich, S. S., 1958, A contribution on the Hector, California, bentonite deposit: *Econ. Geol.*, **53,** no. 1, pp. 22–37.

Weaver, C. E., 1956, The distribution and identification of mixed-layer clays in sedimentary rocks: *Am. Mineral.* **41,** 202–221.

THE AMERICAN MINERALOGIST, VOL. 45, JULY-AUGUST, 1960

A DEVICE FOR VIEWING *X*-RAY PRECESSION PHOTOGRAPHS IN THREE DIMENSIONS*

E. C. T. Chao, *U. S. Geological Survey, Washington 25, D. C.*

The understanding of the reciprocal lattice in *x*-ray crystallography is fundamental to the interpretation of the precession photographs taken with a Buerger precession camera. The undistorted *x*-ray diffraction photograph obtained with such a camera from an appropriately oriented single crystal shows the reciprocal lattice in two dimensions. A device is described here to show the photographed reciprocal lattice of the crystal in three dimensions.

In crystal systems with orthogonal axes, the reciprocal axes are also perpendicular to each other and coincide in direction with the direct axes. A precession photograph taken of such a crystal shows a square or rectangular net of reflections. Since the direct axis [*hkl*] is parallel to the reciprocal axis [*hkl*]*, the reciprocal nets of each level will superimpose exactly. In such cases, visualization of the orthogonal reciprocal cell is simple. If the crystal has an oblique cell, the direct axes and the reciprocal axes are not parallel. The reciprocal net of each level will then be displaced along a reciprocal axis by an amount related to the obliquity of the cell. If the displacement is considerable, visualization of the reciprocal cell is not easy.

A device which provides an excellent three-dimensional view of the photographed reciprocal cell can easily be built. It consists of a box made of $\frac{1}{4}$-inch clear plastic material such as Lucite. The side plates are "dadoed" or slotted and held together by screws to a top and a bottom plate. The precession films are inserted along the slots and are held in place one on top of the other. The slots are spaced 1 mm. apart to allow the films to be placed at the approximately correct heights according to the scale. Fig. 1 shows the transparent box with precession films in place. The dimensions of the box are as follows:

Width of cut of slots	$\frac{1}{64}$ inch or 0.4 mm.
Depth of slots	$\frac{1}{16}$ inch or 1.6 mm.
Spacing of slots	$\frac{1}{25}$ inch or 1 mm.
Width between side plates	$5\frac{7}{8}$ inches 12.4 cm.
Overall outside dimension	5 by $6\frac{3}{8}$ by $1\frac{1}{2}$ inches.

A stereoscopic pair of photographs (Fig. 2), is taken of superimposed films in this device and, when viewed with a pocket stereoscope, illustrates the clarity with which the oblique reciprocal cell can be visualized.

* Publication authorized by the Director, U. S. Geological Survey.

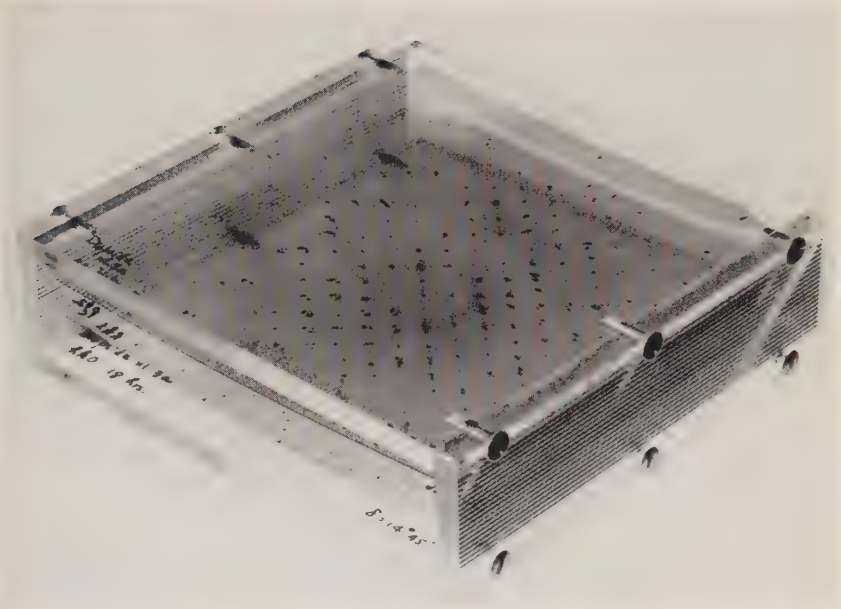

FIG. 1. An oblique view of the box showing the grooved side plates and the precession films in place.

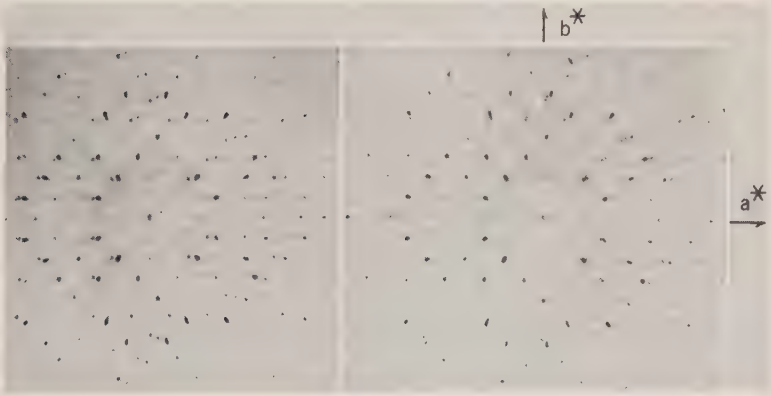

FIG. 2. Stereoscopic pair showing the reciprocal lattice of diopside with precession films of $hk0$, $hk1$ and $hk2$ in place in the device. $+b^*$ is towards the top of the paper, $+a^*$ is to the right and $+c^*$ is about 74° from a^* (c-axis is at the center, normal to the paper towards the viewer).

The crystal chosen for illustration is diopside, (monoclinic: $a=9.74_7$, $b=8.91_8$, $c=5.25_8$ Å, $\beta=105°\ 55'$; space group $C2/c$). The photographs were taken with the x-ray beam parallel to the c axis. The zero level is placed at the bottom, the first level is about 8 mm. above the zero level and the second level (which may not be needed) is placed 8 mm. above the first level. Both upper level nets are displaced towards the viewer's right, along the c^* axis. The reciprocal unit cell chosen is outlined by the reflections. With the three dimensional view of the reciprocal lattice in front of one, the indexing of the reflections is simplified and systematic extinctions of reflections readily observed. If more than one crystal of the substance is used, the device also helps in maintaining a uniform setting or orientation of the reciprocal cell chosen. The device should therefore be useful to experienced crystallographers as well as to students.

I wish to thank my colleague, Joseph F. Abell, who supervised the construction of the box, and to Joan R. Clark and D. E. Appleman for their helpful criticism.

THE AMERICAN MINERALOGIST, VOL. 45, JULY–AUGUST, 1960

ORIGIN OF EMBAYED QUARTZ CRYSTALS IN ACIDIC VOLCANIC ROCKS

ROBERT J. FOSTER, *Department of Earth Sciences, Montana State College, Bozeman, Montana.*

Embayed or rounded quartz crystals are ubiquitous features of acidic volcanic rocks. Most petrology textbooks offer no explanation of why the quartz crystals of these rocks, that contain abundant normative quartz, are not in equilibrium with the groundmass. Almost all authors who have described these features have noted that the embayed quartz crystals are dipyramidal and so have the form of β or high temperature quartz (Cf., Williams, Turner & Gilbert 1954, p. 123 & 126). β quartz inverts to α or low temperature quartz on cooling past its inversion point.

In a recent textbook Moorhouse (1959), in describing rhyolites and quartz latites, notes (p. 207–208),

"Quartz phenocrysts often exhibit "corrosion" effects. . . . In the past these textures have been attributed to corrosion of the phenocrysts by the matrix. The suggestion has also been made that "corroded" quartzes are due to irregular amoeboid growth rather than corrosion. In corroded feldspars, such as those in Fig. 113A (quartz latite, San Juan Mts., Colorado), there can be little doubt that they have been attacked and invaded by the matrix. Surely these are xenocrysts foreign to the magma enclosing them. The same impression is given by the textures of Figs. 15A, B, C (quartz latites, San Juan Mts., Colorado). In these, angular, sometimes corroded chips and fragments of quartz, feldspar and ferromagnesians occur in a glassy or microcrystalline matrix of acid composition. It is

as if the lava of the matrix had picked up innumerable fragments of wall rock and incorporated them with very little effect on itself."

Some embayed quartz crystals probably originated in this fashion, but it appears unlikely that such an accidental origin can account for a ubiquitous feature in common rocks. The shattered quartz crystals can perhaps be explained as due to volume changes in the inversion from high to low quartz and Wright and Larsen (1909) note that such shattering is characteristic of inverted crystals; however, the fact that the dipyramidal form is recognizable in many rocks suggests that well-formed but embayed quartz crystals are common.

Thus it appears that many acidic volcanic rocks contain crystals that are not in equilibrium with the groundmass. Because of the widespread occurrence of this phenomenon, most petrologists interpret it to mean that the crystals formed early, perhaps under different conditions, and are now not in chemical equilibrium with the groundmass (Turner and Verhoogen 1959, p. 63). Reaction rims of pyroxene around quartz crystals such as those described by Moorhouse (1956, p. 191) indicate that the quartz formed at high temperatures. Resorption of early formed feldspar crystals is well explained by Tuttle and Bowen (1958, p. 130–137) in light of their experimental work. Perhaps a similar explanation of embayed quartz crystals in volcanic rocks is possible.

The data presently available offer several possible explanations of embayed quartz crystals. As noted by Moorhouse they may be due to amoeboid growth in a very viscous melt, and rhyolitic magma, especially near the liquidus, is very viscous (Tuttle and Bowen 1958, p. 76–77). The fact that most of the quartz crystals in question have recognizable dipyramidal form argues against this hypothesis.

Perhaps a more likely explanation is that these embayed quartz crystals record the arrested beginning of the recrystallization that Bowen and Tuttle's experimental work indicates occurs in many granites. Tuttle (1952, p. 108–110) summarized the differences between plutonic and volcanic quartz, noting differences in inclusions, form, orientation and extinction. Tuttle and Bowen (1958, p. 137–142) proposed that the textural differences between rhyolites and granites are due to recrystallization during the slow cooling of the latter. In experimental melts (Tuttle and Bowen 1958, p. 28 & 59 61) and in volcanic rocks, quartz forms early euhedral crystals. In plutonic rocks quartz is commonly anhedral and apparently forms late, although as pointed out by Tuttle (1952, p. 120), determining order of crystallization in a plutonic rock, "is a risky undertaking at best."

A major problem in explaining embayed quartz crystals as resolution

as the first step in recrystallization is the lack of a driving force for such a reaction. Tuttle and Bowen (1958, p. 138) have shown why recrystallization of feldspars takes place, but no one has shown why quartz recrystallizes; although Turner (1948, p. 192–211) and Tuttle (1952) have shown that the quartz of many plutonic rocks is recrystallized.

In the light of Tuttle and Bowen's work, the reactions between crystals and groundmass in a volcanic rock probably take place after the rock has solidified but is still hot. Such reactions could be due to a late liquid phase (Tuttle and Bowen, 1958, p. 102–103). They could also be due to a reaction between the hot glassy or cryptocrystalline groundmass and the quartz crystals, perhaps through the medium of an intergranular film.

References

Moorhouse, W. W. (1959), The study of rocks in thin section: Harper and Bros., New York, 514 p.

Turner, F. J. (1948) Evolution of the metamorphic rocks: *Geol. Soc. America Mem.* **30,** 342 p.

——— and Verhoogen, John (1960), Igneous and metamorphic petrology: McGraw-Hill, New York, 694 p. (Second edition).

Tuttle, O. F. (1952), Origin of the contrasting mineralogy of extrusive and plutonic rocks: *Jour. Geol.*, **60,** 107–124.

——— and Bowen, N. L. (1958), Origin of granite in the light of experimental studies in the system $NaAlSi_3O_8$-$KAlSi_3O_8$-SiO_2-H_2O: *Geol. Soc. America Mem.* **74,** 153 p.

Williams, Howel, Turner, F. J. and Gilbert, C. M. (1954), Petrography: W. H. Freeman, San Francisco, 406 p.

Wright, F. E. and Larsen, E. S. (1909), Quartz as a geologic thermometer: *Am. Jour. Sci.*, **27,** 422–447.

THE AMERICAN MINERALOGIST, VOL. 45, JULY–AUGUST, 1960

"HYDROMUSCOVITE WITH THE $2M_2$ STRUCTURE—A CRITICISM"

E. W. Radoslovich, *Division of Soils, Commonwealth Scientific and Industrial Research Organization, Adelaide, Australia.*

A recent paper by Threadgold (1959) has reported chemical, differential thermal and *x*-ray diffraction data on a hydromuscovite from Mt. Lyell in Tasmania. Threadgold gives data which are claimed to show that this hydromuscovite has the $2M_2$ structure, a mica polymorph previously only found amongst the lepidolites (Levinson, 1953). Radoslovich (1959) has recently suggested, however, that the theoretical polymorphs 20, $2M_2$ and 6H, which are based on 60° rotations between layers (Smith

and Yoder, 1956) may be expected to be rare or non-existent among the muscovites, because of the markedly ditrigonal symmetry of the oxygen network (Radoslovich, 1960, in press).

Since this specimen is the first reported $2M_2$ mica other than lepidolite it was decided to re-examine it. A careful survey did not reveal any material sufficiently coarse-grained for single crystal methods, so that powder diffraction techniques must be used. For this purpose a 19 cm. diameter evacuated powder camera was used to record consecutively (under the same conditions) the diffraction patterns of various polymorphs and mixtures of polymorphs. The camera is equipped with knife-edges, and has been carefully calibrated using a quartz standard. A Hilger film-measuring rule was used for obtaining θ values, and the corresponding d spacings were determined by extrapolation from the table published by Rose (1957).

The following mica specimens were photographed under standard conditions.

(a) Hydromuscovite from Lyell Comstock Mine, Mt. Lyell, Tasmania; kindly supplied by I. Threadgold, C.S.I.R.O., Melbourne.
(b) 1M muscovite from Iron Monarch quarries, Sth. Australia; kindly supplied by E. R. Segnit, University of Adelaide.
(c) $2M_1$ muscovite from Spotted Tiger Mine, Central Australia as studied by Radoslovich (in press, 1960).
(d) A 2:1 mixture of (b) and (c).
(e) $2M_2$ lepidolite from the Brown Derby pegmatite, Gunnison County, Colorado, described as #505 by Levinson (1953); kindly supplied by Prof. E. Wm. Heinrich, Univ. of Michigan.

The d spacings for each of these micas are given in Table 1, with the visually estimated intensities.[1] By direct comparison of the photographs—which show high resolution—it is clear that the Mt. Lyell hydromuscovite is not identical with the $2M_2$ lepidolite specimen, but in fact shows considerably better agreement with the 2:1 mixture of 1M and $2M_1$ polymorphs. These are, of course, subtle variations in relative line intensities, but these are not unexpected in layer-silicates, both because of orientation effects and because the hydromuscovite differs a little chemically from the 1M and $2M_1$ specimens. A print of the photographs of specimens (*a*), (*d*) and (*e*) is given in Fig. 1; the detail does not reproduce well.

In view of the slight intensity discrepancies between the Mt. Lyell hydromuscovite and the authentic muscovite polymorphs examined it cannot be claimed categorically that this hydromuscovite is a mixture

[1] Victor (1957) has also given data for a mixture of 70% 2M, and 30% 1M muscovite.

TABLE 1. *X*-RAY POWDER PHOTOGRAPH DATA FOR FIVE MICAS

(*d* values in Å)

a		*b*		*c*		*d*		*e*	
9.96	s	10.07	s	10.02	s	9.97	s	9.93	m
4.97	m	5.00	w-m	4.99	m-s	4.98	m	4.97	m
4.448	vs	4.487	s	4.453	vs	4.460	vs	4.465	s
4.342	w	4.342	w-m			4.343	w	4.327	w
4.258	w			4.278	w	4.268	w		
4.093	vw (br.)	4.093	w-m	4.089	w	4.087	w-m		
				3.951	vw			3.969	w
3.868	m			3.868	m	3.866	w-m	3.855	m
3.780	vw								
3.713	vw			3.721	m	3.718	w-m	3.710	vw
3.647	m-s	3.647	s			3.640	m-s	3.611	m-s
				3.575	vvw				
3.478	m-s	3.482	vvw	3.480	s (br.)	3.478	m	3.473	m-s
3.316	vs	3.337	s	3.326	vs	3.327	vs	3.314	m-s
		3.208	vvw	3.250	vw	3.245	vvw		
3.1820	m			3.190	m-s	3.1836	w	3.195	m-s
3.1180	vw			3.0830	vw			3.0710	m
3.0382	m	3.0593	s	3.0480	vw	3.0570	m		
2.9675	w-m			2.9798	m-s	2.9728	w-m	2.9714	vw
2.9145	w-m	2.9211	w			2.9142	w		
								2.8860	m
2.8454	m			2.8542	m-s	2.8475	w-m	2.8490	m
2.7818	m			2.7818	m	2.7769	w	2.7700	w-m
2.6986	vw	2.6772	w-m			2.6736	w		
2.5745	vs	2.5875	w-m	2.5820	m	2.5783	m	2.5686	vs
2.5495	(br.)	2.5585	v.s. (br.)	2.5530	vs	2.5528	vs		
2.4800	vw	2.4773	vvw	2.4922	vw (br.)	2.4986	vvw	2.4780	vw
				2.4540	w	2.4530	vw		
2.4336	w (br.)	2.4327	w	2.4313	w	2.4319	w		
2.4083	w			2.4075	vvw			2.4148	m (br.)
2.3834	w (br.)	2.3918	w	2.3887	vw	2.3890	w		
				2.3720	m	2.3708	w	2.3744	vw
2.3249	vvw	2.3509	w			2.3525	vw		
2.2934	vvw							2.3006	vw (br.)
2.2666	vvw	2.2440	w						
2.2381	w-m			2.2401	w-m (br.)	2.2384	w	2.2438	m
2.1999	w	2.2096	vw	2.1982	w-m			2.2156	vw
		2.1901	vvw					2.2027	vw
2.1730	w			2.1752	w			2.1733	w
2.1372	w			2.1429	w-m				
2.1180	w	2.1020	vw	2.1224	m-s	2.1236	w-m	2.1230	vw
2.0727	w-m (br.)	2.0766	w-m	2.0590	vw	2.0766	w	2.0902	vw
2.0402	w			2.0475	w			2.0551	w
2.0314	w							2.0266	
2.0144	w								
1.9912	w-m	2.0022	w-m (br.)	1.9944	m (br.)	1.9945	m (v. br.)	1.9824	m-s
1.9628	vvw			1.9658	w-m	1.9637	w		
1.9390	vvw	1.9454	v.w. (br.)	1.9440	w	1.9436	w		
1.9102	vvw								
				1.8881	vw				
				1.8161	vw				
				1.7420	vvw				
				1.7269	w	1.7274	vvw		
1.7079	vw			1.7084	vw	1.7081	vw		
1.6942	vw			1.6947	vw				
1.6821	vw	1.6856	vvw	1.6862	vw	1.6871	vvw	1.6884	m
				1.6723	vvw			1.6731	w-m
1.6581	w (br.)	1.6662	w-m	1.6627	w	1.6629	w (br.)		
1.6407	vw			1.6439	m	1.6423	vw		
1.6302	w-m	1.6307	m (v.br.)			1.6307	w		
				1.6237	w			1.6296	w
				1.6104	w				
1.6011	w			1.5980	w-m	1.5919	vw (br.)	1.6041	w
1.5783	w	1.5717	w			1.5681	vw	1.5856	w
								1.5707	

a Hydromuscovite, Mt. Lyell, Tasmania
b 1M muscovite
c $2M_1$ muscovite
d 2:1 mixture of (b) and (c)
e $2M_2$ lepidolite

vs very strong
s strong
m-s medium to strong
m medium
w-m weak to medium

w weak
vw very weak
vvw just discernible
br broad
bracket = band

TABLE 1 (*continued*)

a		*b*		*c*		*d*		*e*	
1.5594	w			1.5531	w-m	1.5491	vvw		
				1.5406					
								1.5377	vw (br.)
				1.5228	w-m	1.5225	vw		
				1.5065	vw				
1.4947	s	1.4978	vs (br.)	1.4959	vs	1.4955	s	1.4985	s
		1.4791	w	1.4804	vvw	1.4794	w		
				1.4678	vvw				
1.4465	vvw			1.4521	w				
1.4220	w (v.br.)	1.4299	vw	1.4289	vw				
		1.4234	vw	1.3938	vvw				
		1.3746	w (br.)	1.3712	vvw	1.3722	w. band		
1.3483	w	1.3405	w (br.)	1.3516	m				
1.3346	vw			1.3374	w-m	1.3377	w (br.)		
1.3220	vw	1.3293	vvw	1.3206	vw band			1.3123	w (v.br.)
1.2949	w	1.2972	w	1.2923	m band	1.2947	w	1.2957	m-s
1.2904		1.2880				1.2868			
1.2745	vw band			1.2760	w				
				1.2707	w				
1.2463	w-m	1.2484	vw	1.2459	w-m	1.2436	w band		
1.2426		1.2414		1.2369	w-m				
				1.2181	w (br.)	1.2173	w band		
		1.1878	vw						
		1.1624							
1.1694	w-m								
1.1173									
		1.1118	vvw	1.1118	w (br.)				
		1.1015	vw	1.1017	w (br.)				
1.0930	w	1.0923	w (v.br.)						
1.0870									
1.0124	v.w.	1.0136	v.w.						
1.0085		1.0087							

of 1M and $2M_1$ polymorphs, though the diffraction data are in better agreement with this mixture than with $2M_2$ lepidolite. It should be further remarked that the pattern of a $2M_2$ muscovite (when found) will not necessarily be identical with the observed pattern of $2M_2$ lepidolite. This re-examination therefore clearly shows that the Mt. Lyell hydromuscovite has not been proved to be a $2M_2$ polymorph. Indeed it will be very difficult to demonstrate conclusively that the $2M_2$ polymorph of muscovites exists at all, by powder methods. For this reason it will, in the writer's opinion, first be necessary to find a $2M_2$ muscovite (if such exists) by single crystal methods, in order to provide standard $2M_2$ muscovite powder data, against which unknown polymorphs can be compared with certainty.

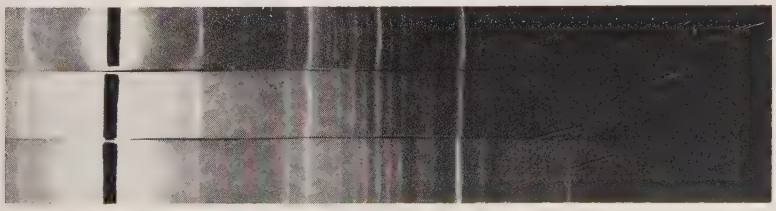

FIG. 1. *X*-ray powder photographs. (Above) 2:1 mixture of 1M muscovite and $2M_1$ muscovite, (*d*). (Middle) Hydromuscovite from Mt. Lyell, Tasmania, (*a*). $2M_2$ lepidolite (*e*).

References

Levinson, A. A. (1953), Studies in the mica group: *Am. Mineral.*, **38,** 88–107.
Radoslovich, E. W. (1959), Structural control of polymorphism in micas: *Nature,* **183,** 253.
Radoslovich, E. W. (1960), The structure of muscovite: *Acta Cryst.* In press.
Rose, A. J. (1957), Tables permettant le dépouillement des diagrammes de rayons X, C.N.R.S. Paris.
Smith, J. V. and Yoder, H. S. (1956), Studies of the mica polymorphs: *Min. Mag.*, **31,** 209.
Threadgold, I., (1959), Hydromuscovite with the $2M_2$ structure; *Am. Mineral.*, **44,** 488.
Victor, Iris. (1957), Burnt Hill Wolframite Deposit, Canada. *Econ. Geol.*, **52,** 149.

THE AMERICAN MINERALOGIST, VOL. 45, JULY–AUGUST, 1960

INTERFERENCE FIGURES OF LARGE CRYSTALS IMMERSED IN A SPHERE OF LIQUID

Louis Navias, *General Electric Research Laboratory, Schenectady, N.Y.*

It is frequently necessary to determine rapidly and non-destructively the approximate orientation of a non-cubic single crystal which either due to its mode of preparation or subsequent treatment is lacking in regular external crystallographic form. A typical example is a corundum boule. Although the orientation can be determined roughly by simply rotating the crystal in air between two crossed polarizers, the conditions for observation can be considerably optimized by immersion of the crystal in a refractive index oil and making the determination under a microscope. If one can then rotate the crystal in a simple way, it is possible to find the orientation by obtaining a centered interference figure. It has been found that with a small spherical flask, all of these conditions can be easily met. The simplicity and usefulness of the technique suggests it may be of interest to others.

The glass spheres should be perfect in shape and free of mold marks, striae and bubbles. The most perfect bulbs experimented with were blown by hand, by Wilmad Glass Co., Buena, N.J., and made of borosilicate glass. Fig. 1A shows a sphere of 40 ml. capacity, 4.5 cm. diameter. Sometimes a chemist's boiling flask is found in stock, which is good enough for the purpose. Fig. 1B shows such a sphere of 33 ml. capacity, 4.0 cm. diameter. To determine the effect of mold marks, we have used two different sizes of machine-made bulbs of a soda-lime-silica glass blown in a two-piece mold. These are General Electric Company bulbs, designation G12-1, 3.9 cm. diameter, 26 ml. capacity, Fig. 1C; and designation G9A2, 3.0 cm. diameter, 11 ml. capacity, Fig. 1D. These bulbs

can be used for many purposes despite distortion in certain directions.

The problem of filling the sphere completely with liquid is solved by using a capillary in the stopper as in the ordinary pycnometer. In the combination 1B the stopper is made of teflon, which is not affected by the immersion liquids, and it contains two holes, one for the brass holder

FIG. 1. Various types of glass spheres and stoppers.

rod, and the other a capillary of 1 mm. bore. The stopper is machined to fit the neck of the flask, of volume 33 ml. In the combination 1A, the ground glass stopper with capillary of 1 mm. bore fits into a ground glass neck. The ground joint is 14 mm. in diameter at the mouth and 12 mm. long, and is attached to a section of clear tubing of about the same length, which was blown with the sphere. The volume of the sphere is about 40 ml. and the wall thickness roughly 1 mm.

The glass stopper is made in two distinct steps. First a length of capillary tubing is sealed centrally in the stopper by means of two ring seals.

Then an extra section of capillary is attached to the lower ring seal, blowing a small bubble in the capillary at the junction. This procedure prevents excess cracking of the stopper during the sealing operation.

The metal specimen-holder is made to fit snugly over the fire-polished capillary as shown in 1A, C and D. In 1A the holder is made of brass, split in four segments to give spring contact around the capillary tube and it has one movable jaw actuated by a screw. In 1C, the movable jaw has been replaced by a bronze spring clamp. In 1D the holder is made entirely of a stiff spring of wire, about 1 mm. in diameter. In 1B the holder is made of a brass rod to which is attached a flat brass plate with a bronze flat spring.

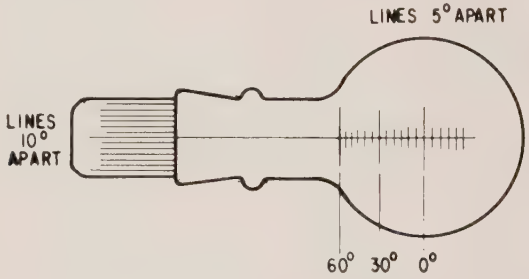

FIG. 2. Sphere and stopper with reference marks.

For the permanent location of the center of the interference figure relative to the geometry of the specimen, it is necessary to have a system of reference marks. By means of a small indexing fixture, scribe marks were made on the surface of the sphere and the stopper as shown in Fig. 2. The sphere is marked with short lines, 5° apart, which are actually parts of great circles, with a common center located at the center of the sphere. The longer line at the center of the drawing is situated at 0° when the device is in the horizontal position. The stopper is marked with parallel lines 10° apart. The scribe marks were actually made on the waxed surfaces of the glass parts, and made permanent by etching with an HF solution and made more visible by inking. A line on the stopper can be matched with the long line traversing the short cross lines on the sphere.

The stopper with holder and specimen in place should be lowered slowly into the container part filled with liquid, having a refractive index preferably close to that of the crystal specimen. Entrapped air and superfluous liquid are removed, leaving the specimen in a completely filled sphere. The excess liquid is wiped away, and the glass surface should be cleaned with a suitable liquid solvent such as Xylene to leave the sphere surface clean and transparent.

A rubber pad used by chemists on evacuated filter flasks (Filtervac made by Alfred Bicknell Associates, Cambridge, Mass.) has a central hole of 3 cm. diameter lined on one side with a raised edge, forming a conically shaped rubber orifice, suitable for the support of the glass sphere on the microscope stage. The filled sphere converges the light from the concave mirror into the specimen held at the center, hence the sub-stage converging lens is not necessary. The objective needs to be of low power and preferably of long focal length. The polarizer, analyzer, and Bertrand lens are used in the normal manner.

The sphere can be rotated in many directions very quickly, and the interference figure can be followed very readily, and made to shift with change in crystal position. By holding the stopper firmly, the spherical part can be turned in the ground glass joint until the optical figure is located over the row of grid lines. The angle of tilt from the horizontal can be determined, and the corresponding line on the neck of the flask. By this means the location of the optical figure is oriented with respect to the position of the crystal in the sphere, and this location can be maintained after the stopper and specimen are removed from the sphere.

For beginners a very cheap combination can be made by using a boiling flask, with a metal holder held in a rubber or cork stopper. A clean capillary can be made by inserting a hypodermic needle in the stopper. The swelling of the rubber and the resulting discoloration of the liquids are draw-backs.

This spherical device should make a good learning tool for students before using the Universal Stage.

The help and interest of R. C. DeVries are gratefully appreciated.

After this idea was put into practice, it was learned that E. Leitz, Inc., has a "Waldermann Hollow glass sphere" for the examination of gem stones.

THE AMERICAN MINERALOGIST, VOL. 45, JULY–AUGUST 1960

A NEW MINERAL-PICKING APPARATUS

A. O. M. Savolanti and M. H. Tyni, *Institute of Geology, University of Helsinki, Helsinki, Finland.*

Two types of mineral-picking apparatus have been described by Murthy (1957) and Kauranne (1957). The present authors have made a new model which we believe is easier to build, and in certain respects is more serviceable.

Making the Apparatus

Figure 1 represents the mineral-picking apparatus. It was constructed out of a Penfield tube that had been used in making water determinations. A capillary (B) was drawn from the broken-off end of the tube. The capillary was given a suitable diameter for the collecting of mineral particles. The tip of the capillary was cut off at a slant, to make it horizontal during operations. A hole (A) was blown into one of the globes in the Penfield tube. The diameter of the hole is large compared to

Fig. 1. Photograph of mineral-picking apparatus in use.

the diameter of the tip of the capillary. The intact end of the Penfield tube was bent upward so as to be easy to handle and to make sure the grains would halt in the globes. A rubber hose connects this end of the tube to a vacuum pump.

There are binocular microscopes with a stationary stage in which the binocular eyepiece may be moved mechanically in two directions at right angles to each other. In working with high magnifications, it is useful to attach the mineral-picking apparatus firmly to the stereoscopic tube so that the tip of the capillary of the apparatus (B) is at the focal point of the microscope. In such cases the hole (A) is not made in the globe, instead the rubber hose is cut in two and a length of glass tubing with a hole is placed in between.

Procedure for Using the Apparatus

The mineral grains are spread out on a slide under a stereoscopic binocular microscope. The vacuum pump is set going and the suction

is regulated in such a way that the mineral grains will fly at a suitable speed into the globes and halt in them when the hole (A) is stopped by a finger. The suction is cut off immediately when the finger is lifted from the hole, whereupon it is possible to guide the mineral grains at will with the tip of the capillary. Only a slight motion of the finger is needed to start and to cut off the suction. It is easy to pour the mineral grains out of the apparatus through the hole (A).

If the mineral-picking apparatus is mounted on the stereoscopic tube, the tip of the capillary is guided to the mineral grain by means of the cross-stage.

Acknowledgments

The authors wish to express their appreciation to the Geological Institute of the University of Helsinki and to its head, Prof. Martti Saksela.

References

Murthy, M. V. N. (1957), An Apparatus for handpicking mineral grains: *Am. Mineral.*, **42**, 694–696.

Kauranne, L. K. (1957), Pikkuapua separatiolaboratorioon (A Little aid to the separation laboratory): *Geologi*, **1**, 3.

THE AMERICAN MINERALOGIST, VOL. 45, JULY AUGUST, 1960

METHOD OF MINIMIZING DAMAGE TO REFRACTOMETERS FROM THE USE OF ARSENIC TRIBROMIDE LIQUIDS[1]

By R. R. Coats, *U. S. Geological Survey, Menlo Park, California.*

If there be other users of high-index liquids containing arsenic tribromide who have overlooked Meyrowitz's (1955, p. 400) reference to Alexander's (1934, p. 181) caution against their use with refractometers having lead-glass prisms, or who have used them in ignorance of the composition (commonly undisclosed) of the prism, the following note may be useful.

The refractometer I used (a Zeiss instrument having a prism marked S-3 with an index above 1.83) promptly showed the same white film described by Alexander, when used with Meyrowitz's liquid of index 1.79. Within a few minutes, the film became so dense that the boundary line could not be seen.

[1] Publication authorized by the Director, U. S. Geological Survey.

Wiping with the soft absorptive paper furnished with the instrument did not suffice, as Alexander pointed out, to remove the film. However, when a drop of a slurry of fine tin oxide (available from dealers in lapidary supplies) was applied to a piece of the absorptive paper and the surface of the prism gently polished therewith, the film was quickly removed, and the refractometer restored to usable condition, if not to its pristine one. Examination of the surface of the prism after repolishing showed irregular, shallow, roughened areas, obviously not scratches, covering a small part of the surface. Both lead and bromine could be detected by *x*-ray spectrography on the paper used for polishing. Apparently, the arsenic bromide reacts with the lead glass to form lead bromide and arsenic oxide.

In view of the availability of the Morey lanthanum borate type glasses, with indices up to 1.88, that are "very stable" (Kingslake and DePaolis, 1949, p. 422), it is surprising that lead glass is still used in high-index refractometers. If refractometers using lanthanum borate glasses are available the fact does not seem to have been widely publicized. Possibly there are objections, not readily apparent, to their use.*

References

Alexander, A. E., 1934, Caution against the use of Borgströms liquids with lead-glass prisms: *Am. Mineral.* **19,** 181.

Kingslake, R., and DePaolis, P. F., 1949, New optical glasses: *Scientific Monthly*, **68,** 420–423.

Meyrowitz, Robert, 1955, A compilation and classification of immersion media of high index of refraction: *Am. Mineral.* **40,** 398–409.

* In commenting on this note, G. W. Morey (written communication, April 28, 1960) has kindly pointed out that, while the lanthanum borate glasses are hard and resistant to corrosion, dispersion is less in commonly available glasses than in the lead glasses of corresponding index. Dr. Morey has also suggested that it would not be difficult to produce a glass of the lanthanum borate type having a high enough dispersion but the market would be very small.

PITTSBURGH DIFFRACTION CONFERENCE

The annual Pittsburgh Diffraction Conference will be held November 9-11, 1960, at Mellon Institute, Pittsburgh, Pennsylvania. Sessions will be devoted to metals and alloys, instrumentation, structures, polymers and fibers, refractories, electron probe and electron diffraction. The evening meeting will be addressed by Professor I. Fankuchen of the Polytechnic Institute of Brooklyn. Further information can be obtained from L. F. Vassamillet, Mellon Institute, 4400 Fifth Avenue, Pittsburgh 13, Pennsylvania.

BOOK REVIEWS

THE STUDY OF ROCKS IN THIN SECTION, by W. W. Moorhouse. 514+xvii pages, 226 figures, 18 plates, 2 color plates. Harper and Brothers, New York, 1959. $8.00.

This is a notable and laudable effort by Professor Moorhouse of the University of Toronto to develop under one cover " . . . an adequate synopsis of the almost encyclopedic petrographic information presently available," The book may be considered as consisting of seven major parts. Following an introduction, Chapter 2 presents a summary of the methods of optical mineralogy. Chapter 3, 83 pages, is devoted to descriptions of individual minerals. Chapter 4 is made up of mineral identification tables. The petrography of igneous rocks is described in Chapters 5–17, by far the longest section of the book, (183 pages). The petrography of sedimentary rocks, 66 pages, is dealt with in Chapters 18–24. Metamorphic rocks are described in the 71 pages of Chapters 25–28. The last two chapters deal with the mineralogy of metasomatic rocks and ores.

The initial section dealing with the techniques of optical mineralogy, is, according to the preface, " . . . not intended as a substitute for the standard texts and references on this subject. Its object is to present as briefly and simply as possible the optical tests most frequently used in thin-section mineralogy." Certainly this section is inadequate for teaching purposes, and it might be questioned whether it would not have been better either to omit this part of the book entirely or to reduce it even further to a series of tables in which the arrangement of the optical tests might be more systematic and more readily accessible. This section concludes with a brief statement on the orientation procedure with the universal stage, yet the book contains no subsequent reference to the application of universal stage determinative methods. In this section there also appear the two colored plates, some figures of which seem to be of dubious value. For instance, Figure 5, which is a kyanite fragment under crossed nicols, states no thickness; the same is true for Figures 7 and 8. Figure 6, used to illustrate pleochroism, shows a mineral with a red color in one position and a blue color at right angles; the mineral is not identified. Similarly, Figures 17 and 18 seem to have little real application to the text.

The reviewer is puzzled as to the arrangement of species in the second section (Chapter 3). Here are described 149 minerals or varieties. The silicates are listed first, followed by the minerals of the various other groups. There is no attempt to arrange them in terms of optical complexity, a pattern which the beginning student often finds highly useful. Some of the species are in part inadequately described. For example, there is no mention of water in the composition of opal and its effect upon the refractive index, and certainly to say that the "optical character (of chalcedony) is unknown" is not in accord with data that have been available for some time. In addition, in the SiO_2 group, it should be pointed out that most natural tridynite and cristobalite are not pure SiO_2. The descriptions of the soda amphiboles seem to the reviewer to be inadequate. Furthermore, new data on cordierite and its polymorphism are not included. The formula of antigorite is given as $H_2Mg_3Si_2O_9$ whereas that of chrystotile is given as $H_4Mg_3Si_2O_9$. Dahllite and collophane are recorded as separate species, and their relationship to apatite is nowhere indicated. This section includes the 18 black and white plates, which are chiefly photomicrographs of minerals in thin section. These are clustered together between pages 44 and 45 , and it seems unfortunate that printing arrangements could not have been made so that pictures of the individual species appear with their descriptions.

The mineral identification tables, 13 in number, are likewise hidden in the front half of the book and thus difficult to use readily.

The section on igneous rocks, which is by far the best feature, is organized as follows: After a general chapter on igneous petrography, the author discusses volcanic and hypabyssal rocks, beginning with basalts and progressing to rhyolites, thence to trachytes and

phonolites. This is followed by a discussion of tuffs and pyroclastics. Next come the plutonic rocks, first the gabbros, then the alkali gabbros, and subsequently granodiorite, granite, followed by diorites, monzonites and syenites. Lastly are described the nepheline syenites, ultrabasic rocks and lamprophyres. Such an arrangement has two fundamental drawbacks: First, it results in a great deal of repetition in the discussion of compositionally allied rocks, some of which are extrusive and others of which are intrusive, and more important, it fails to indicate to the student affinities in composition, mineralogy, or occurrence.

Table 16, which is intended as a field classification of rocks, includes such varieties as quartz gabbro and quartz diabase, which are distinguishable megascopically only exceptionally. Table 17 uses "hybrid" apparently as an equivalent for "mela." The igneous rock classification presented by Moorhouse bases its initial subdivision on the presence or absence of olivine, which gives rise to numerous pigeonholes in which no common rocks are represented.

In general, discussions of the individual rock groups are excellent and complete. A particularly fine feature of the book, and a novel one, is that the alterations of the various rocks are discussed individually.

Readers might question the definition of an intersertal texture as being diabasic or ophitic and the inclusion of sanidinites as igneous rocks. Moorehouse further defends his ideas on the late paragenetic position of the common igneous accessory minerals; yet recent work by the U. S. Geological Survey (Bull. 1097-A, p. 26, 1959) has indicated that zircon may continue crystallizing throughout the consolidation period of the rock.

In that part of the book dealing with sedimentary rocks, it might be noted that there are no clays described, nor is there any reference whatsoever to bauxite. The taconite illustrated on page 391 is very likely of metamorphic derivation. This section has no documentation, whereas in that dealing with the igneous rocks there are a few references.

The description of metamorphic rocks do not present the same order of coverage as for the igneous rocks. Rather than the rocks being treated as mineralogical groups or subdivided on the basis of the facies principle, the categories are Dynamic Metamorphism, Thermal Metamorphism, and Regional Metamorphism. This renders difficult mineralogical descriptions of the various diverse chemical groups under each of the types of metamorphism.

There are a number of misspellings, e.g., aegirine and merwinite, and some of the abbreviations for the various states are not standard.

In general, the illustrations are good to excellent, except for a few of the line drawings in the first part of the book, which give evidence of having been prepared in haste. (e.g. figures 3, 35, 37, and 50a.) The author states "In most of the drawings a standard pattern has been used for each mineral or mineral group, so that labeling of the individual diagrams is not necessary." In some instances this is satisfactory, but in many of the drawings it is not, and species identification becomes difficult, particularly inasmuch as the drawings may not adequately emphasize differences in relief.

Apparently the book has been designed primarily for a year's course in petrography for students who previously have been exposed to some optical crystallography. If this is not the case, then certainly the section on optical mineralogical principles is inadequate. Professor Moorhouse has done a remarkable job in attempting to reduce such a large volume of material to a useful compilation in a highly usable form. It must certainly be concluded that his efforts to provide in a single book a combination of a short review of optical mineralogy, descriptions of rock-forming minerals, together with descriptions of the common rock types, have been in the main successful.

E. Wm. Heinrich
The University of Michigan
Ann Arbor, Michigan

THE LOVOZERO ALKALINE MASSIF (ROCKS, PEGMATITES, MINERALOGY, GEOCHEMISTRY, AND GENESIS), by K. A. Vlasov, M. V. Kuz'menko, and E. M. Es'kova, Akad. Nauk. S.S.S.R., Inst. mineralog., geokhim., i kristallokhim. redikikh elementor, 1959, 623 p. (in Russian). Izdatelstvo Akad. Nauk. S.S.S.R., Moscow, $11.50.

The Kola Peninsula has been famous for many years as a storehouse of new and rare minerals. The new volume is a comprehensive monograph on one of the famous massifs, of a size (623 pages, 201 tables, and 257 figures) that makes a detailed review impossible. The scope may be judged from an outline of the contents.

The rocks of the area are described thoroughly, with petrographic data and many chemical analyses. The earliest rocks of the massif are nepheline syenites, foyaites, and aegirine-bearing nepheline syenites; next came a complex of urtites, foyaites, and aegirine lujavrites, then a complex of eudialyte lujavrites and poikilitic sodalite syenites, and finally dikes of monchiquite, tinguaite, and similar rocks.

The section on mineralogy describes about 120 minerals. Emphasis is on paragenesis and mineral associations, but complete descriptions are given, including many previously unpublished analyses. The final section on geochemistry and genesis is very thorough and includes considerable unpublished data.

The book is nicely printed and the illustrations are excellent, but there is no index. It will be indispensable to anyone interested in alkalic rocks; for mineralogists trying to learn Russian, this is a good choice for practice and vocabulary.

Michael Fleischer
U. S. Geological Survey
Washington, D. C.

NEW MINERAL NAMES

Blixite

Olof Gabrielson, Alexander Parwel, and Frans E. Wickman. Blixite, a new lead-oxyhalide mineral from Långban. *Arkiv Mineralog. Geol.*, **2**, 411–415 (1960).

Analysis by A. P. gave $PbCl_2$ 30.16, PbO 69.50, CaO 0.30, H_2O 0.79, sum 100.75%. Spectrographic analysis also showed traces of As, Sb, Bi, Mg, Mn, Fe, and the alkali metals. No fluorine was detected (less than 0.02% F). The formula is probably $Pb_{16}Cl_8(O, OH)_{16-x}$ with x approximately 2.6, if the water is assumed to be essential; if it is not essential, the formula becomes $Pb_{16}Cl_8O_{12}$ or $Pb_4Cl_2O_3$. In either case, there is probably a defect oxygen lattice such as has been found for similar compounds such as nadorite. A study of dehydration showed losses of water (in %): 100° 0, 125° 0.04, 150° 0.04, 175° 0.07, 200° 0.15, total 0.29%. The material heated at 200° showed small but distinct changes in the x-ray pattern. The water is believed to be constitutional. The compound $Pb_4Cl_2O_3$ was synthesized by fusion of PbO and $PbCl_2$; its powder pattern differed from that of the mineral.

Blixite is soluble in dilute mineral acids.

No single crystals were found. The x-ray powder pattern (35 lines) was indexed by analogy with nadorite, which gives a similar pattern. This gives an orthorhombic unit cell a 5.832±0.003, b 5.694±0.005, c 25.47±0.02 Å. The space group could not be determined The strongest lines are 2.93 (10) (116, 200); 3.88 (8) (112); 1.660 (8) (308, 11.14, 136); 2.83 (6) (020); 2.12 (6) (00.12); 2.04 (6) (220). One distinct cleavage.

Blixite is pale yellow, streak pale yellow, luster vitreous, sometimes dull. H. about 3. G. 7.35. Not fluorescent with UV. radiation. Optically biaxial, positive, 2V 80°, *ns* $\alpha \sim 2.05$. $\gamma \sim 2.20$. The extinction is parallel to the distinct cleavage; the optic axial plane is perpendicular to this cleavage plane.

Blixite is a very rare mineral occurring in the "Amerika" stope, Långban, Sweden, as thin crystalline coatings on fissures in dolomite impregnated with hausmannite and sometimes associated with native copper. Also found as a coating of a fissure in manganophyllite skarn.

The name is for Ragnar Blix, 1898–——, chemist of the Department of Mineralogy, Swedish Museum of Natural History.

Discussion.—Presumably to be classed with the lead oxyhalides, Dana's System, 7th Ed., vol. 2, pp. 56–69.

Michael Fleischer

Batisite

S. M. Kravchenko and E. V. Vlasova. Rare-metal mineralization associated with nepheline syenites of the alkalic province of Central Aldan. *Doklady Akad. Nauk S.S.S.R.*, **128**, No. 5, 1046–1049 (1959) (in Russian).

Chemical analysis by A. V. Bykova gave SiO_2 39.00, TiO_2 22.00, Nb_2O_5 0.36, ZrO_2 1.90, Al_2O_3 0.9, Fe_2O_3 1.80, MgO trace, MnO 0.09, CaO 0.27, SrO 0.03, BaO 22.00, Na_2O 8.40, K_2O 2.60, H_2O^+ 0.50, loss on ignition 0.10, sum 99.95%. Separate photometric determinations gave Na_2O 9.03, K_2O 2.67%, and a separate sample had F 0.07%. The analysis corresponds to $Na_2BaTi_2(Si_2O_7)_2$. Melts at 1005° C.

The mineral occurs as elongated (up to 10 cm.) crystals showing (010), (001), (110), (031), (150), (011), and (310). Presumably orthorhombic. The axial ratio $a:b:c = 0.755:1:0.584$. Cleavage average on (100). Color dark brown, in powder rosy. Hardness 5.9, microhardness 764 kg/mm². Sp. gr. 3.432 (mean of 2 determinations by suspension). Optically biaxial, positive, *ns* α 1.727, β 1.732, γ 1.789, 2V 8°, $Z = c$, $Y = b$, $X = a$. Elongation

positive. Dispersion strong, r<v. Pleochroic with X colorless, Y yellow-brown, Z reddish-brown. The strongest *x*-ray lines are at 2.615, 4.009, 3.023, 1.947, and 1.482 Å.

Batisite occurs in the Inaglina nepheline syenite pegmatite with interstitial crystals of microcline; rarely with miaroles. Other minerals present are nepheline (zeolitized), aegirine, arfvedsonite, uranothorite, ramsayite, eudialyte, apatite containing more than 1% BaO, and adularia-like orthoclase containing 2.5% BaO.

The name is for the composition.

A fuller report will be published.

Discussion.—Similar in composition, but distinct from benitoite and shcherbakovite.

M. F.

Bergenite

Hans W. Bültemann and Günter H. Moh. Bergenit, ein neues Mineral der Phosphuranylit-Gruppe. *Neues Jahrb. Mineral., Monatsh.* **1959,** No. 10, 232–233.

The mineral was found on a dump at Streuberg near Bergen on the Trieb, Vogtland, Saxony, associated with much uranocircite, some torbernite, renardite, autunite, barium uranophane, and unidentified secondary U minerals. It is yellow, thin tabular, orthorhombic, biaxial negative, *ns* α 1.660, $\beta \sim 1.690$, $\gamma \sim 1.698$, $2V > 45°$, G>4.1 (Clerici soln.). Fluorescent weak orange-brown in short- and long-wave ultraviolet light. It is stated that *x*-ray fluorescence, spectrographic, and chemical data (not given) show it to be the barium analogue of phosphuranylite, $Ba(UO_2)_4(PO_4)_2(OH)_4 \cdot 8H_2O$. Indexed *x*-ray powder data are given (27 lines); the strongest are 7.78 st, 3.883 st, 3.076 st, 2.976 st-m, 3.437 m, 2.074 m, 1.974 m.

The compound was synthesized by Virginia Ross (*Am. Mineral.*, **41,** 818–920 (1956)), who called it barium-phosphuranylite. She found it to be orthorhombic, probable space group *Bmmb*, *a* 16.2, *b* 17.7, *c* 13.9 Å, biaxial, negative, *ns* α 1.660, β 1.690, γ 1.695.

The authors reject the name barium-phosphuranylite on the ground that this might be taken to mean not the barium-analogue, but a phosphoruranylite containing a little barium. The name bergenite is for the locality.

M. F.

Lead hydroxyapatite

A. K. Temple. The Leadhills-Wanlockhead lead and zinc deposits. *Trans. Roy. Soc. Edinburgh,* **63,** 85–114 (1955–56) (Publ. 1957).

$Pb_5(PO_4)_3(OH)$ occurs rarely at Whyte's Cleuch with polysphaerite (var. pyromorphite), pseudomorphous after galena. Identified by comparison with *x*-ray data of A.S.T.M. file. *X*-ray spacings or other data not given.

M. F.

Unnamed

A. K. Temple. The Leadhills-Wanlockhead lead and zinc deposits. *Trans. Roy. Soc. Edinburgh,* **63,** 85–114 (1955–56) (Publ. 1957).

The mineral occurs at the Hopeful Vein, Leadhills, as bright red elongated crystals. The *x*-ray pattern is similar to but not identical with that of lanarkite, $Pb_2(SO_4)O$, but with a larger unit cell. Spectrographic analysis showed Cr 6–15%; this may be a chromatian lanarkite. *X*-ray powder data (65 lines) are given; the strongest are 3.38 vs, 2.98 vs., 2.86 s., 1.87 s., 2.48 fs., 2.39 fs., 2.26 fs., 2.1 fs.

M. F.

Tangaite (new data on Redondite)

DUNCAN MCKIE. Notes on some minerals from Tanganyika. *Records Geol. Survey Tanganyika*, **5**, 81–94 (1955) (Publ. 1958).

Analysis by Bassett (*Records Geol. Survey Tanganyika*, **3**, 100–103 (1953) (Publ. 1956) of material from gneiss, Gerevi Hill, Tanga District, Tanganyika gave P_2O_5 42.50, Al_2O_3 29.25, Fe_2O_3 3.54, Cr_2O_3 1.11, CuO 0.93, H_2O^- 19.52, H_2O^+ 3.18, sum 100.03%, corresponding to (Al, Fe, Cr)$PO_4 \cdot 2H_2O$. McKie finds this material to have *ns* α 1.58, γ 1.60, birefringence 0.015, 2V neg., moderate. He gives an *x*-ray powder pattern which is stated to differ from those of the series variscite-strengite, but to correspond to that of type redondite (plus a few lines of turquoise). On this basis, redondite is not an intermediate member of that series; it is suggested that the Al end-member be named *tangaite* for the locality, "if the difference in structure between redondite and the variscite-strengite isomorphous series is substantiated by future single-crystal *x*-ray work."

DISCUSSION.—The evidence is unconvincing and the mineral should not have been named.

M. F.

NEW DATA

Bolivarite

R. VAN TASSEL. Bolivarite restudied. *Mineralog. Mag.*, **32**, 419–420 (1960).

Type bolivarite (Navarro and Barea, 1921; Dana's System, 7th Ed., **2**,, 872) was re-examined. It is amorphous to *x*-rays, optically very weakly birefringent, *n* 1.506±0.001, G. 2.04±0.01; strongly fluorescent bright green. Analysis give Al_2O_3 3.62, P_2O_5 24.9, loss on ignition 39.5, sum 100.6%. $H_2O^- = 25.5\%$. The water content is much higher than in the original analysis; the analysis gives $Al_2O_3 : P_2O_5 : H_2O = 2 : 1 : 12.5$. The material is compared with evansite and vashegyite.

M. F.

Scarbroite, Hydroscarbroite, Meta-scarbroite

W. J. DUFFIN AND J. GOODYEAR. A thermal and *x*-ray investigation of scarbroite. *Mineralog. Mag.*, **32**, 353–362 (1960).

G. W. BRINDLEY AND J. J. COMER. Electron-optical data for crystals of scarbroite. *Ibid.*, 363–365.

The preliminary report (see *Am. Mineral.*, **43**, 384–385 (1958)) that scarbroite is a valid mineral is confirmed. Analysis by R. A. Chalmers gave SiO_2 3.2, Al_2O_3 45.7, MgO 0.1, Na_2O 1.7, K_2O 0.2, H_2O 37.9, SO_3 1.8, CO_2 7.9, sum 98.5%. S. Melmore in 1930 found SiO_2 6.48, 5.69, 5.88%; Al_2O_3 44.19, 44.32 44.02%. If SiO_2 is deducted as quartz and minor constituents are considered to be due to impurities, the formula obtained is $Al_2(CO_3)_3 \cdot 12.9Al(OH)_3 \cdot 15.6H_2O$. A weight-loss curve shows a loss of nearly 17% up to 100° and a further loss of weight of about 23% up to 300°. On standing in air, or when heated to 40°, the material shows some changes in *x*-ray pattern; the fully hydrated mineral is called *hydroscarbroite;* the dehydrated material, perhaps ideally $Al_2(CO_3)_3 \cdot 12Al(OH)_3$ is called *scarbroite.* At 130°, the *x*-ray pattern changes completely; this material is called *meta-scarbroite.* Heating to higher temperatures causes shifts in lines and progressive diffuseness; above 230° no measureable lines remain. Infra-red absorption curves are in accord with loss of H_2O to 100°, loss of hydroxyl 100–245°, and loss of CO_2 below 490°.

Electron photographs show scarbroite to be thin plates about 1 μ in size, thickness about 0.01–0.05 μ. The edge angles are 66±1° and 113±1°. The *x*-ray data were indexed as corresponding to a triclinic cell with *a* 9.94, *b* 14.88, *c* 26.47, α 98.7°m β 96.5°, γ 89.0°. Assuming the formula $Al_2(CO_3)_3 \cdot 12Al(OH)_3$, Z=4, G. calcd. 2.03, measured after heating to 100° 2.17.

M. F.

SHALE'S

LISTING OF FINE MINERAL SPECIMENS

RUBIES IN CHROME DIOPSIDE MATRIX (Belgian Congo, Africa) Two 1" flat hexagonal crystals imbedded in matrix. Very showy—$50.00

BARITE CRYSTAL GROUP (Palos Verdes, Calif.) One of the largest ever found. 9x16 brown crystal group—$75.00

KYANITE GROUP (Minas Geraes, Brazil) 7x12 fine massive crystal group—$17.50

BERYL var AQUAMARINE CRYSTAL (Brazil) Fine 6x5 green-blue opaque crystal—$45.00

ZIRCON CRYSTALS IN MATRIX (Ontario, Canada) Two long crystals in 6x9 matrix. Very fine specimen—$40.00

AQUAMARINE CRYSTAL (Brazil) Green mostly gemmy 1½x2¼ crystal 172 grams—$165.00

FIRE OPAL (Virgin Valley, Nevada) 1½x2½ fire opal limb section—$75.00

CUPRITE AND SOME COPPER CRYSTALS. (Santa Rita, New Mexico) Bright 2x4 crystal specimen—$15.00

MINERALS FOR COLLECTIONS & STUDY

APATITES IN LIMESTONE MATRIX (Iron Mountain, Durango, Mexico) Fine yellow crystal specimens—$1.00, $1.50 and $2.00. Single crystals—25¢, 50¢ & 75¢

KYANITE CRYSTALS (Brazil) Blue crystal blades up to 3"—50¢, 75¢, $1.00 ea.

SAPPHIRE CRYSTALS (Mozambique, Africa) Blue opaque crystals. Up to 2x3" specimens—$1.50, $2.50 and $3.00 each

RUBY CRYSTALS (Ampanihy, Madagascar) Up to 1" flat hexagonal crystals—75¢, $1.00 and $2.00 each

QUARTZ CRYSTALS WITH INCLUSIONS OF PHANTOMS, ETC. (Brazil) 1" to 2½ crystals showing 1 or more phantoms and sometimes other inclusions—75¢, $1.00 & $2.00

"CHINESE JADE" JADEITE (Mogaung Upper Burma) Cores and cuttings from Hong Kong from Jade cutting factories—$5.00 per lb.; 3 lbs. $12.00

SPODUMENE var TRIPHANE (Brazil) up to 1" crystals partly clear—3 for $1.00

SEND FOR LISTINGS—WE ARE BUYERS OF COLLECTIONS

SHALE'S

9226 W. Pico Blvd. Los Angeles 35, Calif.

Phone CR-6-8222